

**DIPLOMA THESIS**

**DESIGN DEVELOPMENT AND  
PRODUCTION OF  
ELECTROMAGNETIC COILS FOR  
ATTITUDE CONTROL OF  
A PICO SATELLITE**

**Ali Aydinlioglu**

**Matr. Nr. 183875**

**Supervisors:**

**Prof. Dr.-Ing. W. Ley**

**Prof. Dr.-Ing. G. Schmitz**

**Dipl.-Ing. Jens Gieselmann**

**Aachen, February 2006**



I assure that I have composed the thesis autonomously with a support of the group and that I have only used references as mentioned. References are marked in the report and listed in a table.

This thesis is prepared to the best of my knowledge.

Aachen, February 2006

Ali Aydinlioglu



---

## **Abstract**

The Compass-1 CubeSat is an actively controlled picosatellite utilizing magnetic coils as only means of attitude control. The Attitude Determination and Control System (ADCS) provides the three-axis stabilizing capability. The ADCS was developed to stabilize the spacecraft against disturbances resulting from the spacecraft LEO environment. Magnetic coils are strapped to the satellite structure to generate the control torques.

This thesis presents the study carried out to establish three identical magnetorquer for an actively controlled picosatellite.

The design and development of the magnetorquer as well as the essential hardware for producing the magnetorquer, the coil winder, is elaborated.

### **Keywords**

CubeSat, picosatellite, Compass-1, ADCS Attitude Determination and Control System, three- axis stabilizing, magnetorquer

## Acknowledgements

I would like to acknowledge Prof. –Dr. –Ing. W. Ley, the head of Aeronautical and Astronautical Technology at the University of Applied Sciences Aachen in Germany, for his support during all the time of my studies.

Special thanks to Prof. Dr. rer. nat. H. J. Blome and Dipl.-Ing. E. Plescher for their efforts and support for me personally and the Compass-1 project in general.

I express my gratitude to Dipl.- Ing. J. Gießelmann, for sharing his knowledge, giving fruitful comments and for the time.

I also want to express my thanks to the head of the mechanical workshop Mr. Backhaus and his assistant Mr. Schnell for the precise and proper production results.

Furthermore I like to show appreciation to the members of the Compass-1 team, especially Rico Preisker, Georg Kinzy, Marco Hammer for the suggestions, the discussions and inspirations I received.

Aachen February 2006

## Table of Contents

<b>1</b>	<b>Introduction</b>	<b>1</b>
<b>2</b>	<b>ADCS System Overview</b>	<b>2</b>
<b>3</b>	<b>Magnetorquer</b>	<b>4</b>
3.1	Mathematical Background	4
3.2	Requirements	7
3.3	Design	9
3.4	Production	15
<b>4</b>	<b>Coil Winder</b>	<b>17</b>
4.1	Layout	17
4.2	Requirements	19
4.3	Hardware Design & Development	20
4.3.1	Base Plate	20
4.3.2	Wire Carrier / Wire Cover Brake	22
4.3.3	Pulley	24
4.3.4	Guidance	26
4.3.5	Winding Unit	31
4.3.6	Coil Mould	32
4.3.7	Force Measuring Unit	34
4.3.8	Electrical Drives and Measuring Unit	36
<b>5</b>	<b>Coil Winder Production</b>	<b>38</b>
5.1	Technical Drawings	38
5.2	Material and COTS Orders	38
<b>6</b>	<b>Control Unit Design</b>	<b>40</b>
6.1	Electrical Hardware Design	40
6.2	Circuit Design	41
6.3	PCB Layout	42

---

6.3	PCB Layout	42
6.4	Electrical Hardware Production	43
6.5	Software Design & Development	44
<b>7</b>	<b>Magnetorquer Production</b>	<b>45</b>
7.1	Prototype	45
7.2	Coil Connection	48
7.3	Results	49
<b>8</b>	<b>Modification</b>	<b>52</b>
8.1	Magnetorquer	52
8.2	Coil Winder	52
<b>9</b>	<b>Controlling Test</b>	<b>54</b>
9.1	Oscillation Test	54
9.1.1	Mathematical Concept	55
9.1.2	Setup	56
9.1.3	Preparation of Equipment	59
9.1.4	Conduction of Test	60
9.1.5	Results	61
9.1.6	Error Analysis	66
9.1.7	Gaussian Distribution	69
9.1.8	Test Summary	70
9.2	Demonstration Test	72
<b>10</b>	<b>Control Unit Development</b>	<b>73</b>
10.1	Cabling	73
10.2	Software Result	73
10.3	Calibration	74
10.4	Automatic Coil Winding	74
10.5	Results	75

---

<b>11 Outlook</b>	<b>77</b>
<b>12 Conclusion</b>	<b>78</b>
<b>References</b>	<b>79</b>
<b>Abbreviations</b>	<b>80</b>
<b>Nomenclature</b>	<b>81</b>
<b>List of Figures</b>	<b>82</b>
<b>List of Tables</b>	<b>85</b>
<b>Appendix</b>	<b>86</b>
<b>Appendix - A</b>	<b>87</b>
<b>Appendix - B</b>	<b>94</b>
<b>Appendix - C</b>	<b>97</b>
<b>Appendix - D</b>	<b>102</b>

## 1 Introduction

The Compass-1 satellite is the first picosatellite being developed at the University of Applied Sciences Aachen, Germany<sup>1</sup>. The project is managed and carried out by students of different engineering departments, with a majority being undergraduate students from the Astronautical Department.

The Compass-1 satellite is based on the CubeSat specification started by Stanford University and California Polytechnic State University (Cal Poly)<sup>2</sup> in the USA.

The primary goal of the CubeSat program is to provide students the opportunity to develop satellite systems at universities. Students are able to gain essential practical experience in realizing a research and development project from start to finish.

The goal of this thesis are the design, development and production of electromagnetic coils for the active Attitude Control System (ACS) of the Compass-1 satellite<sup>3</sup>.

The design and development activities for the electromagnetic coils were largely carried out in the constituted engineering laboratory at the University of Applied Sciences Aachen.

The outcome of this work is a crucial system component for the Attitude Determination and Control System of the Compass-1 satellite, which is being developed at the University of Applied Sciences Aachen & the Royal Melbourne Institute of Technology (RMIT)<sup>4</sup> Melbourne, Australia.

The expected results are the production of several developed and tested electromagnetic coils on engineering model (EM) level for testing of the integrated spacecraft.

The time frame was initially defined within three month, beforehand within a preparation time of about 8 months.

The software which was used for the required mechanical hardware was CATIA V5 R13 and Protel 2005 for the electrical hardware.

---

<sup>1</sup> <http://www.fh-aachen.de>

<sup>2</sup> <http://cubesat.calpoly.edu>

<sup>3</sup> <http://www.raumfahrt.fh-aachen.de>

<sup>4</sup> <http://www.rmit.edu.au>

## 2 ADCS System Overview

The Attitude Determination and Control System (ADCS) stabilizes the spacecraft against attitude disturbing influences resulting from the environment in the earth orbit within orient its payload, a VGA camera, into the desired nadir orientation.

The interaction with the local geomagnetic field is an important means of controlling the attitude or orientation of the spacecraft. A control torque to change the attitude of a satellite can be generated by a magnetic moment that interacts with the local geomagnetic field. These magnetic moments, a physical vector, can be produced by a coil or by a permanent magnet.

The permanent magnet has relatively large magnetic moments arising from the “intrinsic” moment of their atoms and can be used only with the decision of a passive control system. With a passive control system, the measurement of the geomagnetic field, for attitude control aspects is not necessary and in addition the satellite will “flip over” at the magnetic poles. This motion is repeated twice per orbit close to the Earth's magnetic poles.

In consideration of taking pictures of the surface of the Earth by downloading to different ground stations, only active control with actuators such as reaction wheels or magnetorquer fulfils these requirements. It should be pointed out that existing reaction wheels are set up for bigger satellites and this technology needs to be miniaturized so that it can fit into a CubeSat. The miniaturization of existing components is an enormous challenge, in contrast the production of magnetorquer seems a realizable challenge for Compass-1.

For the general design layout of the ADCS and its components, firstly, a mathematical concept was established, then, the hardware is been built around the mathematical equations. Finally the mathematical concepts needed to be revised by adapted test setups. The decision making process for the measurement and the actuator components can be consulted in the Phase B Documentation of the Attitude Determination and Control System of the Compass 1 project [1].

No other subsystem makes it more obvious than a dynamics related spacecraft system like the ADCS: the hardware carries the software, so the theoretical concept translated into a numerical and hardware solutions.

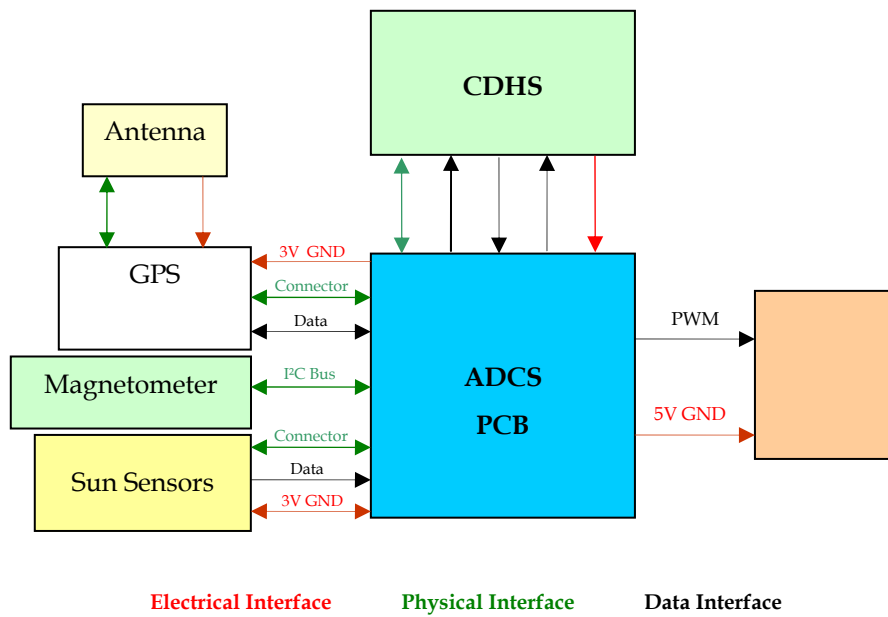


**Figure 2-1: ADCS hardware interface**

The upper Figure 2-1 reflects the interfaces between the ADCS Printed Circuit Board (PCB) and the adjacent components, subsystems and aids in obtaining an overall perspective on the ADCS hardware configuration.

The ADCS Hardware is separated mainly into two units:

- one unit determines the spacecraft attitude and position
- the second unit stabilizes the spacecraft.

The determination unit comprises the GPS system, the magnetometers and the Sun Sensors. The exposition of the operating modes of these hardware components are not a part of the thesis and would exceed its scope. Extensive documentation about the hardware definition can be gleaned in the Phase B Documentation of the ADCS. [1]

The stabilizing unit consists of magnetic coils (also referred to as magnetic torquer) as the only devices for actuation on board the Compass-1 picosatellite.

### 3 Magnetorquer

#### 3.1 Mathematical Background

Magnetorquers are actually nothing else than coils, whereas coils are nothing else than wires wound into “large” loops, generating a mechanical torque in an ambient magnetic field.

#### How do the coils generate the mechanical torque?

Magnetostatics fields are established by static electric current flows and therefore by moving charged particles. Observations show that force influences exist on an unloaded but current-carrying conducting lead, force influences exist. The magnetic field is described in terms of a vector and is denoted with  $\mathbf{B}$ .

The magnetic force also called “Lorentz force” on moving charge depends on its charge size, its velocity and the external magnetic field. [2]

It took a long time for physicists of the 19<sup>th</sup> century to discover what a current actually is, and the reinterpretation of it in terms of moving point charges didn't occur until about 1880. The force law is often called the “Lorentz force” after the physicist who worked out the theory.

$$\vec{F} = q \cdot (\vec{v} \times \vec{B}) \quad (1)$$

A current in a wire is the average of many moving charges, so the force on a wire can be determined by adding the forces on the individual charges.

Considering an infinitesimal section of wire as shown in Figure 3-1, with the current indicated by the direction of the current density. The number of charge carriers per unit volume is  $x$ , and each carrier has charge of  $q$ .

If the physical average velocity is  $v_d$ , then  $J = q \cdot v$ . In the volume  $A \cdot dl$  of the infinitesimal section, there are  $x \cdot A \cdot dl$  moving charges.

The total force on these charges is as follows:

$$dF = q \cdot (v \times B) \cdot (x \cdot A \cdot dl) = J \times B(Adl) \quad (2)$$

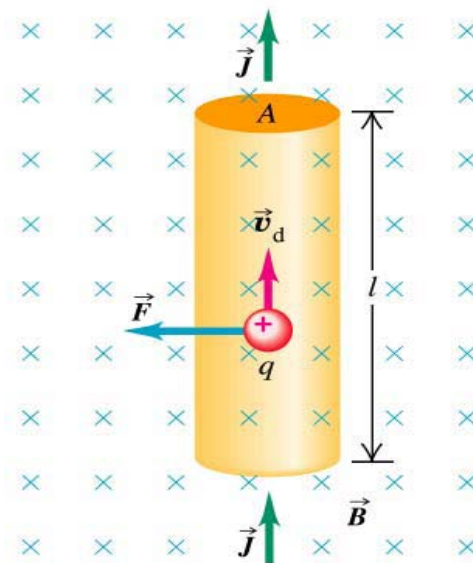


Figure 3-1: Lorentz force in a conductor

It is useful to write the equation (2) in terms of the total current in the wire, which is  $I = J \cdot A$ . The expression of a magnetic force on a current element in an external magnetic field is written as:

$$dF = (I \times B) \cdot dl \quad (3)$$

The total force on a finite piece of wire (or a whole circuit) is found by integrating this expression along the wires.

$$\vec{F} = (\vec{I} \times \vec{B}) \cdot l \quad (3.1)$$

A rectangular coil is in essence a long current carrying conductor wound into loops, for which the force on each side are given by the formula (3.1) which is shown in the following Figure 3-2.

The direction of the forces on each side can be visualized with the “right-hand-rule”, where the thumb indicates in direction of the current and the forefinger in direction of the magnetic field vector, resulting that the middle finger shows the force direction, if all three fingers are in the right angle. The Figure shows the four resulting Lorentz forces in a single turn loop and shows clearly the elimination of the forces on the y-axes, labelled with b, and the operating forces on the x-z axes, by the sides labelled with a. The forces on each side are determined by the formula 3.1 and are given as:

$$\vec{F} = (\vec{I} \times \vec{B}) \cdot l = (\vec{I} \times \vec{B}) \cdot a \quad (3.2)$$

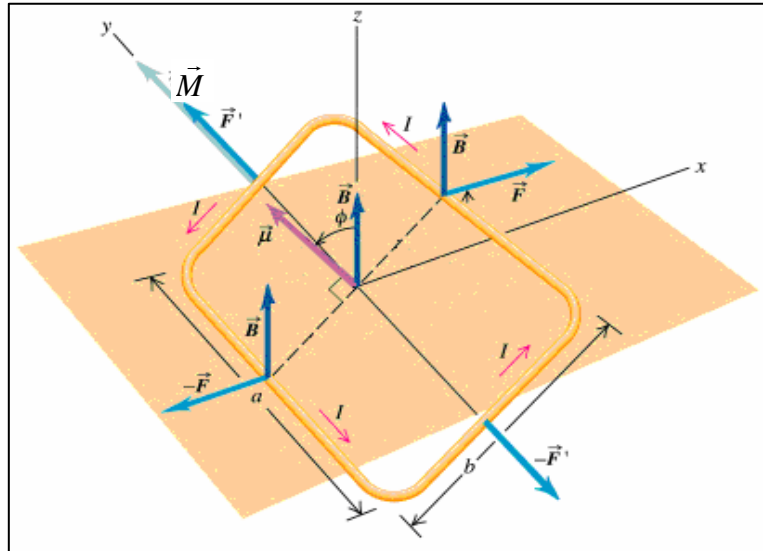


Figure 3-2: Lorentz force on coil sides

The resulting torque  $M$  of both forces is:

$$M = 2 \cdot F \cdot \frac{b}{2} = a \cdot (\vec{I} \times \vec{B}) \cdot b = a \cdot b \cdot I \cdot B \cdot \sin \phi \quad (4.0)$$

The determination of the Lorentz forces and the magnetic moment of the coil with  $N$  loops are generated simply by multiplication with  $N$ .

$$M = N \cdot A \cdot I \cdot B \cdot \sin \phi \quad (4.1)$$

The coil parameters  $a \cdot b$ , simplify to the area  $A$  and form with the current  $I$ , a vector property called magnetic moment, given by the vector  $m$  in Figure3-2.

$$m = I \cdot A \quad (4.2)$$

With the second “right-hand rule”, the direction of the magnetic moment  $m$  is also easily visualized:

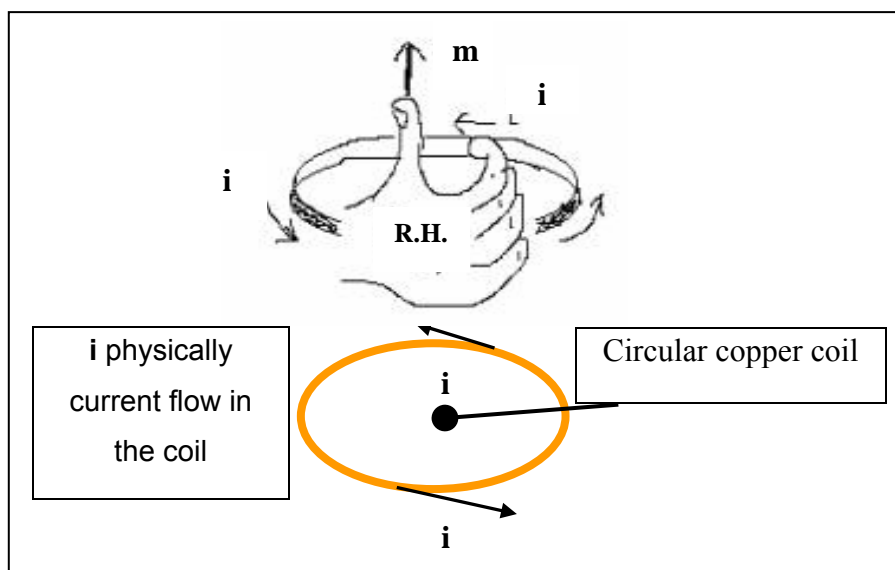


Figure 3-3: The second „Right-Hand-Rule“ used for a circular Coil

Palm curls in the direction of the current in the loop; the thumb indicates the magnetic field direction. This direction, perpendicular to the loop, is also the direction of the magnetic moment  $m$ . The magnetic moment  $m$  is resulting from the torque  $M$ , but is extended with the number of turns  $N$ .

$$m = N \cdot A \cdot I \quad (4.3)$$

Using the basic property of the Cartesian product the main equation is derived

$$|m| \cdot |B| \cdot \sin \phi = |m \times B| \quad (5)$$

$$N \cdot A \cdot I \cdot B \cdot \sin \phi = M \quad (6)$$

$$\vec{M} = \vec{m} \times \vec{B} \quad (7)$$

### 3.2 Requirements

The magnetorquer will be mounted on the inside of the side panels. Because the satellite is a three axis stabilized satellite it requires a minimum of three magnetorquer to dump magnetic moment  $m$  in every direction of the cube. An investigation about the practical use of “Helmholtz coil pairs” resulted in the fact that the use of this configuration has been rejected for Compass-1. The satellite will carry three magnetorquer, one coil for each axis. The magnetic dipole  $m$  is a basic unit of magnetism and is produced by a coil with  $N$  loops, the mathematical background was explained in the previous paragraph.

The magnetic moment of a coil can be pointed out only in combination with the resulting mechanical torque  $M$ , influenced from an external magnetic field, in our case the geomagnetic field.

$$\vec{M} = \vec{m} \times \vec{B}_{earth} \quad (7)$$

The magnitude of the required mechanical torque  $M$  to maneuver the satellite in every coordinate axis is determined by a simulation with the simulation tool MATLAB<sup>5</sup>. The simulations are conducted by the ADCS system supervisor Jens Gießelmann.

For this objective, the position and mass of all hardware components have been considered with their actual status.

This extensive calculation will not be a part of this thesis, therefore the size of the mechanical torque is defined by  $1\mu\text{Nm}$  in every axis and will be considered constant for further calculations.

The magnetorquer must generate this mechanical torque in the geomagnetic field.

---

<sup>5</sup> MATLAB / Simulink = mathematical simulation tool

The intensity of the geomagnetic field is a function of the altitude of the cube which again is depending on the launcher of Compass-1. The Cube Sat launchers usually go into a sun-synchronous orbit with an altitude of 500-800 km and an inclination of up to 98 degrees. The design altitude of Compass-1 was defined in the phase B study as 600 km. [1]

The cross product ( $\vec{M} = \vec{m} \times \vec{B}_{earth}$ ) in scalar solution denotes the angle between two vectors. With the knowledge of using three magnetorquer is the angle between the generated magnetic moment vector and the geomagnetic field intensity vector defined as  $\varphi = 90^\circ$ . The produced magnetic moment  $m$  is calculated with the multiplication of the current  $I$ , the number of turns  $N$  and the enclosed area  $A$  established in the previous paragraph:

$$m = N \cdot I \cdot A \quad (8)$$

A CubeSat has strict limitation on available power and maximum weight for all hardware components. Having in mind an average of 1 Watt that is constantly available for the total system, the coil has to be supplied with 250mW. The configuration of the coils allows an operation of two coils at the same time, but including a restriction that the coils are not in use constantly.

The mass budget is derived from the literature [3] and from the AAU CubeSat group. [4] The budget was defined during the development of the Phase B study of this student project with 20g for each coil.

The available space and size of the coils have been limited by the structure team; details are shown in the table 3-1.

Parameter	Symbol	Value	Unit
Max width	b	74	mm
Max height	h	83	mm
Max cross sectional width	d	2,1	mm
Max cross sectional height	s <sub>h</sub>	5	mm
Total mass limit	M <sub>ges</sub>	60	g
Coil mass limit	M <sub>c</sub>	20	g

**Table 3-1: Physical design dimensions**

The maximum width and this altitude define the physically available area. The cross sectional breath was defined in the early stage of the project. Other components e.g. the coil holder; have been designed under consideration of this definition. The cross sectional altitude can be designed in sizes between 1 and 6 mm.

The operational temperature was analyzed in another diploma thesis of the Compass-1 group member, who has determined the first thermal result considering the status of the hardware components in September 2004. [5] The analysis was executed with the thermal calculation tool ANSYS<sup>6</sup>. The results was a set of temperature distributions during earth orbits and temperature ranges for specific hardware components, e.g. camera, battery, solar cells, electronics and structure. Table 3-2 displays the defined operational temperatures, which consider the estimation about the self heating of the wire and the position of the coil inside the panels. They are results of the analysis performed:

Minimum temperature	T min	-50	°C
Nominal temperature	T Nominal	20	°C
Maximum temperature	T max	100	°C

**Table 3-2: Defined operation temperatures**

### 3.3 Design

The coils will require a significant portion of the critical mass and power budgets of the ADCS subsystem. The design of the magnetorquer is following the “as simple as possible” principle. As mentioned before the magnetorquer are nothing else than copper wire wound into large loops. The mass of every coil is calculated using the following expression:

$$M_c = N \cdot C \cdot a_w \cdot \rho_w \quad (9)$$

The total mass of a magnetorquer is depending on the number of turns  $N$ , its average circumference  $C$ , which is depending on the mechanical dimensions, the cross sectional area  $a_w$  of every single wire and the material density  $\rho_w$  of the used wire.

Parameter	Symbol	Value (Cu)	Value (Al)	Unit
Material density	$\rho$	8.93E-03	2.7E-03	g/mm <sup>3</sup>
Material resistivity	$\sigma$	1.55E-05	2.5E-05	$\Omega$ mm
Temperature coefficient of resistivity	$\alpha_0$	3.90E-03	3.90E-03	1/K

**Table 3-3: Wire data for copper and aluminium**

The wire will be operating under space conditions, relatively quick changes of working temperatures, which result in a design which considers the “worst case” scenarios. The resistance of the wire is a function of the operating temperature and the used wire dimensions.

<sup>6</sup> ANSYS / Thermal simulation tool

$$R = \frac{N \cdot C \cdot \sigma(T)}{a_w} \quad (10)$$

$$\sigma(T) = \sigma_0 \cdot (1 + \alpha_0 \cdot \Delta T) \quad (11)$$

A 5 V power supply is considered in the magnetorquer development.

The power stage (Coil Driver) used to control the magnetorquer will cause an additional power loss, this will be considered separately after being chosen and designed.

The power loss is considered with an additional function of about 200mV for these calculations. The dissipated electrical power is described by the following electrical equation:

$$P = U_c \cdot I = I^2 \cdot R \quad (12)$$

The produced magnetic moment  $m$  is calculated with the multiplication of the current  $I$ , the number of turns  $N$  and the enclosed area  $A$  affiliated in the chapters before:

$$m = N \cdot I \cdot A$$

With the equations (9) till (12), the power consumption of a single coil is expressed as:

$$P = \frac{\rho_w \sigma_T m^2}{M_c} \left( \frac{C}{A} \right)^2 \quad (13)$$

The ambition is to ensure the efficiency of the coil, with consideration of mass and power consumption. It becomes obvious at this stage that the design process will be a trade-off between mass and power consumption. It is possible to reduce the weight, by reducing the number of turns but the power consumption will increase, and vice versa.

Solving equation (13) for the achievable magnetic moment  $m$  yields

$$m = \frac{A}{C} \sqrt{\frac{M_c P}{\rho_w \sigma_T}} \quad (14)$$

The maximum of this equation is given with a minimized product of the material density ( $\rho$ ) and the material resistance  $\sigma_T$ . This product can be minimised by the choice of adequate wire material.

As wire material options we have the choice between copper and aluminium wire.

Copper has the lowest resistance, but aluminium has the lowest resistance-density product. Due to the fact that volume is expected to be more of a constraint than mass, copper seems the obvious choice.

It should be noted that the design of the coils does not only depend on the required mechanical torque and the selected number of turns. The commercial availability of the right wire with the qualified wire properties is becoming a more important argument.

The first research yielded a contact with the biggest wire supplier in Europe, Elektrisola<sup>7</sup>. The company is characterised by a diverse set of applications; many different wire variants are in use in many different engineering areas, e.g. in cars, computer, watches etc.

A large variety of available copper wire with a suitable insulation as well as the low cost outweighs the variety of the available aluminium wire.

After several discussions with the supplier about the available wire properties two wire types have been selected based on the European IEC 60317 standard [6] the copper wire type Polysol 180 and the ML 240 type copper wire. [7] The special copper wire ML 240 is qualified for military and space applications, whereas very high cost is linked to such a high quality wire type. In addition, the wire type ML 240 is produced in the U.S. and can be delivered only on special order. This has resulted in the fact that the only available wire type can be matched with the Polysol 180 type wire.

Polysol 180 is a self-bonding wire available from the diameter 0.1mm through 0.5mm.

For this reason of the right wire diameter, the environmental conditions need to be included into the mathematical design of the “rectangular” coil.

The intensity of the geomagnetic field is a function of the altitude of the orbit. For the determination of the geomagnetic field intensity is the radius considered from the geo centre with  $R = R_{earth} + h_{orbit}$ . With the constant sizes of the earth radius  $R_{earth} = 6371$  km the dipole moment of the earth as  $m_e = 7.96 \cdot 10^{22}$  Am<sup>2</sup> and the magnetic permeability  $\mu_0 = 4 \cdot \pi \cdot 10^{-7} \frac{Vs}{Am}$ .

$$B_{earth,min} = \frac{\mu_0 \cdot m_e}{4 \cdot \pi \cdot R^3} \quad (15)$$

Minimum geomagnetic intensity, at 600 km altitude is calculated as  $B_{earth} = 2.35 \cdot 10^{-5}$  T.

This magnetic moment needs to be generated at any scenario, with the limited amount of power. For the acceleration of the design task, an Excel programme was developed. The programme considers all requirements and delivers the necessary parameter, the wire diameter and the number of turns.

As explained before, the design process is a trade-off between mass and power consumption. Therefore the minimum required mass is determined first with the following expression.

---

<sup>7</sup> [www.elektrisola.com](http://www.elektrisola.com)

$$M_c = \left( \frac{mC}{A} \right)^2 \cdot \frac{\rho \sigma_{20}}{P} \quad (16)$$

The minimum required mass is determined at 20 °C, with the magnetic dipole moment  $m = 4.26 \times 10^{-2} \text{ Am}^2$ , the maximum available power  $P = 250 \text{ mW}$  and the mechanical dimensions  $C = 294 \text{ mm}$   $A = 6142 \text{ mm}^2$ .

The first calculations have resulted in a minimum required mass of 3,2 gram for each coil. With the knowledge about the minimum mass, the minimum wire cross section area is determined with the following expressions:

$$R_{\max} = \frac{U_{\text{coil},\min}^2}{P} \quad (17.0)$$

$$R_{\max} = \frac{U_{\text{coil},\min}^2}{P} = \frac{nC\sigma_{\max}}{a_{w,\min}} \quad (17.1)$$

$$a_{w,\min} = \frac{1}{U_{\text{coil},\min}} \sqrt{\frac{M_{c\min} P \sigma_{\max}}{\rho}} \quad (17.2)$$

The minimum cross section area  $a_{w,\min} = 0.00818 \text{ mm}^2$  of the wire delivers the minimum wire diameter as shown in the following matrix.

Wire Diameter [mm]	Cross Area [mm <sup>2</sup> ]	Diameter incl. Insulation [mm]	Area incl. Insulation [mm <sup>2</sup> ]	Filling Factor
0,100	0,007854	0,108	0,0091609	9124
0,106	0,008825	0,115	0,0103868	8154
0,110	0,009503	0,119	0,0111220	7571
0,112	0,009852	0,121	0,0114990	7331
0,118	0,010936	0,128	0,0128680	6627
0,120	0,01131	0,13	0,0132732	6431
0,125	0,012272	0,135	0,0143139	5934
0,130	0,013273	0,141	0,0156145	5454
0,132	0,013685	0,143	0,0160606	5307
0,140	0,015394	0,151	0,0179079	4775
0,150	0,017671	0,162	0,0206120	4165
0,160	0,020106	0,172	0,0233522	3686
0,170	0,022698	0,183	0,0263022	3250
0,180	0,025447	0,193	0,0292553	2931
0,190	0,028353	0,204	0,0326851	2618
0,200	0,031416	0,214	0,0359681	2386

Table 3-4: Datasheet of available Copper Wire IEC 60317 [6]

With the knowledge about the available wire displays that every wire diameter bigger than 0.106 mm can be used for the magnetorquer of Compass-1.

$$m = \frac{A}{C} \sqrt{\frac{N \cdot C \cdot a_w \cdot P}{\sigma_T}} \quad (17.3)$$

Equation (17.3) displays the direct proportionality of the magnetic moment to  $\sqrt{a_w}$  with constant number of turns  $N$ , constant circumference  $C$  and constant area  $A$ .

After selecting a suitable wire diameter, the new wire cross sectional area needs to be implemented for the number of turn calculations. Modulation of equation (17.2) delivers the required number of turns.

$$N = \frac{M_c}{C a_{w,avail} \rho} \quad (17.4)$$

The calculated minimum mass with  $M_c = 3.2g$  and the mass limit  $M_c = 20g$  determines the minimum and maximum number of turns. The highest power consumption of the wire occurs at the minimum operating temperature, when the resistance of the wire is lowest. The selection of the right number of turns in dependence of the power consumption is determined with the help of the following diagram.

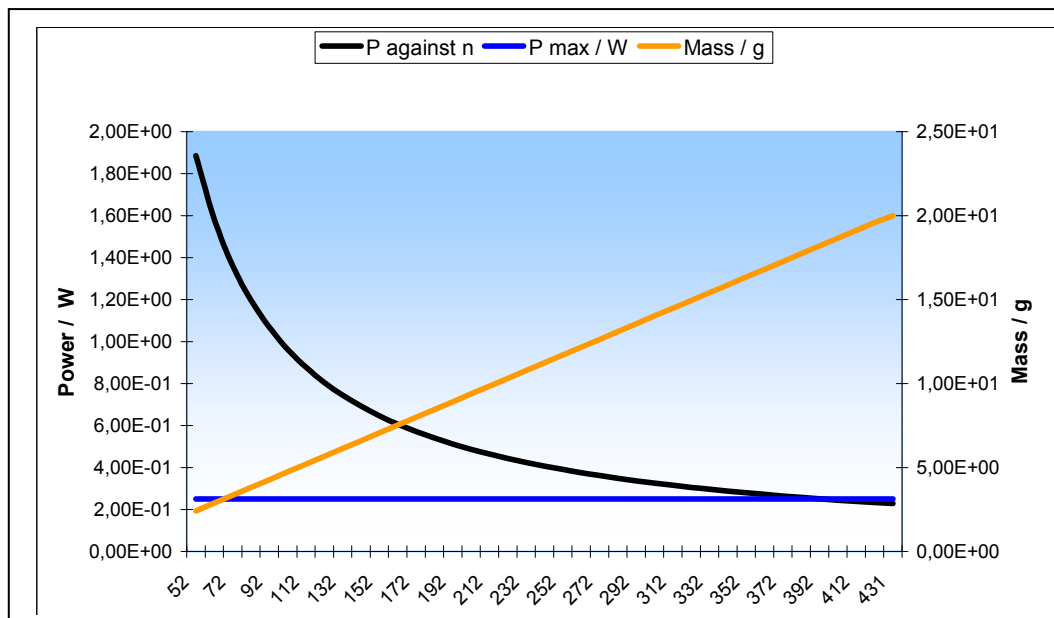


**Figure 3-4: Power and Mass Diagram**

Hence, sufficient analysis and optimization was spent on the coil design in the development phase to determine the suitable wire diameter. Many different variations have been tried during the design stage, so that coil designs with optimized numbers of turns and different wire diameters were the result.

## Design Results

Parameter	Symbol	Value 7	Value 8	Value 9	Unit
wire diameter	d	0,106	0,13	0,15	mm
number of turns	N	830	553	416	
mass of one coil	Mc	19,969	19,995	19,968	g
needed cross section area	Ac	10,179	10,139	9,988	mm <sup>2</sup>
nominal current	I (293K)	9,85	22,23	39,35	mA
supply voltage	U	5	5	5	V
Power consumption	P(223K)	65,95	148,87	263,46	mW
magnetic dipole moment	m	4,86E-02	7,07E-02	9,41E-02	Am <sup>2</sup>

Margin			
4.26 E-02 Am <sup>2</sup>	14.08 %	65.96%	120.89%

Figure 3-5: Design results

The design results shows the varieties of winded coils with constant mechanical size established by increasing the wire diameter by the smaller wire. An increase of the magnetic moment an increase of the power consumption and at the same time depending on the wire diameter is displayed.

The result shows a margin percentage of the generated magnetic moment, of up to 120%. Despite an overrun of the power consumption value 9 stands out compared to the other values, whereas the power consumption “change” to an adjustable function. The power consumption is drawn to the temperature limit at -50°C. The next matrix displays a possible coil design:

Parameter	Symbol	Value	Unit
Number of Turns	n	400	-
Bare wire diameter	d <sub>w</sub>	0.15	mm
Mass of one coil	Mc	19.20	g
Current through coil	I (20°C)	41.30	mA
Magnetic dipole moment	m	9.19E-02	A*m <sup>2</sup>
Needed cross section area	Ac	9.604	mm <sup>2</sup>
Power consumption (223K)	P	256.5	mW
Power consumption (293K)	P	202.3	mW
Coil resistance @ -50°C	R <sub>-50</sub>	93.55	Ω
Coil resistance @ 20°C	R <sub>20</sub>	116.21	Ω
Coil resistance @ 100°C	R <sub>100</sub>	161.53	Ω

Table 3-5: Coil design result

### 3.4 Production

For the production of magnetorquer at universities several possibilities exist.

Maybe some few universities have very good connections to their national space agencies so they can get the knowledge of producing space qualified magnetorquer, or even can get a installable magnetorquer for their cube.

Universities are able to cooperate with national space agencies and specialised companies, but not every university has existing connection to specialized companies.

A project like Compass-1 was initiated at the FH Aachen for the first time. It is financially supported by the DLR (German Aero Space Centre), the FH Aachen, the Ministry of NRW (Nordrhein-Westfalen) and ESA (European Space Agency).

About 4 weeks have been invested on research activities, which have resulted in contacts with diverse companies and universities, especially to CHK Wickeltechnik<sup>8</sup>.

This company is producing coils for any conceivable application. Several telephone calls and e-mails have resulted in the best offer of CHK Wickeltechnik. The company offered a production of six coils for a net cost of about 2000 – 3000 Euro. This contained the coil mould, the wire material and production costs, so that every new coil order will get charged with the wire and production expenses.

Considering the quality aspects, the development aspects in combination with the educational aspects and especially the financial aspects approves an in-house production of electromagnetic coils. The in-house production of coils will allow high flexibility; the production of magnetorquer can be converted into a relatively inexpensive procedure compared to a company production. Therefore an own automated coil winder needs to be designed, developed and produced. Prior to the design tasks, a feasibility study was accomplished. The study has shown that the coil winder can be designed with the same software tool used for the design of the satellite structure, CATIA. Afterwards, the production of the mechanical hardware can be accomplished at the own mechanical workshop. The in-house production of magnetorquer requires many different facilities and components. First of all the wire needs to be selected and ordered from the supplier, so that the available wire diameter can be taken into account throughout the coil winder design. Remembering that Compass-1 is a student project with very limited financial budget it was agreed upon with the company Elektrisola that two different diameters can be chosen.

---

<sup>8</sup> [www.chk-wickeltechnik.de](http://www.chk-wickeltechnik.de)



**Figure 3-6: Bonding wire type S180**

Elektrisola has spent surprisingly two 2 kg coils with special bonding wire of the wire type S180 with the chosen nominal diameter of 0.15mm and 0.16mm displayed in the picture. For further production aspects all available facilities will be used for the production of the magnetorquer. The electrical workshop in our own laboratory will be used for different electrical activities. Moreover a vacuum chamber, also a part of our own laboratory will be used for the space qualification of the coil.

But as a next challenge the design of a moderate-complexity coil winder will be presented in the next chapter.

## 4 Coil Winder

The following chapter describes the construction of the magnetorquers; which was theoretically designed in the chapter before.

To wind the coil manually with an easy mould; i.e. 4 screws mounted on a flat board, seems as the fastest and easiest way at first sight.

By considering the electrical specification, it might be right, but due to the fact that three identical coils with a very small wire diameter and a relatively high number of turns will be integrated are getting the mechanical dimensions even more attention.

It should be noted that the coils will operate under space conditions, for this aspect the coils need to pass all space qualification tests later on. Compass-1 space qualification tests include a vibration test of the whole cube, a thermal test and finally a vacuum test.

In the design status of the Coil shape it becomes obvious that the manufacturing of three coils which will produce a mechanical torque under space conditions requires a development of a customized coil winder.

The coil winder guarantees, a higher quality of produced coils compared to the manual wound coils.

### 4.1 Layout

To wind wire automated into a coil; different hardware components need to be designed.

First of all a coil mould is needed. The mould should be integratable into a winding unit with an integrated drive mechanism. To wind an accurate coil, a tracking package seems to be useful. For monitoring the wire tensions a force measuring unit need to be implemented, without integrating additional stress. Resulting from the not round coil architecture the wire will be under different stresses during the winding, to distribute these stresses; pulleys can be used. To finish the open cycle and in consideration of producing diverse coils a wire stock need to be generated and implemented.

The simplified layout which is shown in Figure 4-1 depicts the architectural concept of the main components of the winder.

The winder can be splinted into seven mechanical areas as follows a coil mould, a winding unit, a track package, a force measuring unit, the pulley's, the wire holder and the base plate.

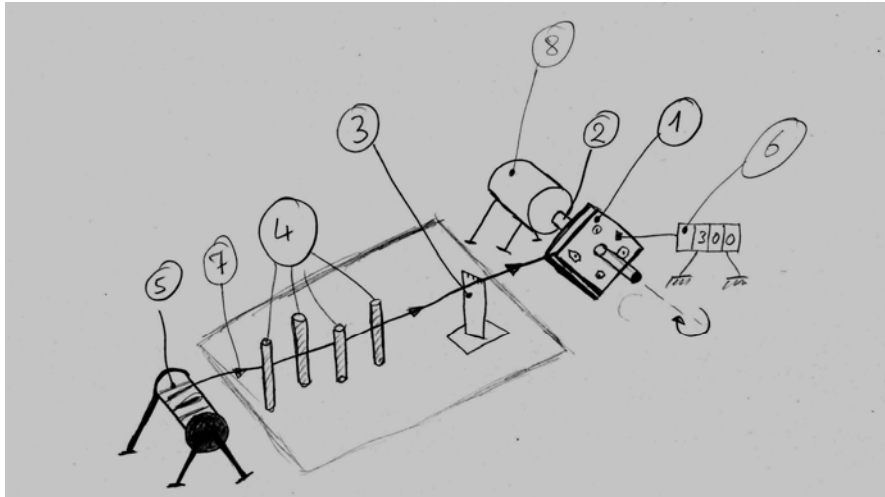


**Figure 4-1 Winder architecture concept**

The mechanical dimension of the coil mould is driven by the mechanical layout dimension of the magnetorquer. The maximum allowed dimension of the magnetorquer is given the available structural dimension of the cube; as  $83 \times 74 \text{ mm}^2$ . From the theoretical cross section altitude of the coil with 5mm results the dimension of the coil mould with  $73 \times 64 \text{ mm}^2$ .

The thickness of the coil was defined at 2,1mm. The shape of the coil mould needs to be rectangular and the mould needs to be hinged in the coil winding unit. The material and the mechanical dimension of the coil mould will be specifically discussed in an extra paragraph.

At this design stage the important aspects of the coil mould is expressed as:

- the mould has been integrable into the coil shape
- pivoted in any preferred way.

Next to the pivoted coil mould; the design of the other coil winder components must consider a constant stream of wire.

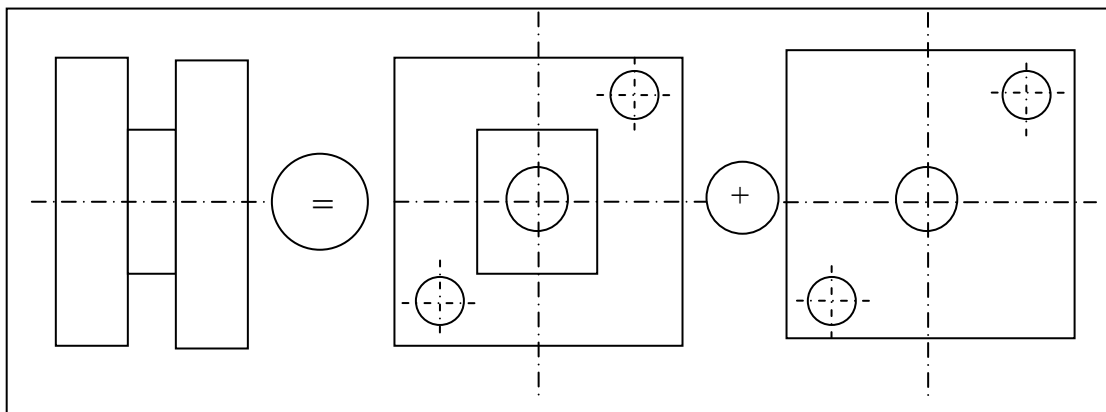


**Figure 4-2: Coil Mould Sketch**

The knowledge of the coil shape and the noted production setup (the rotation) need to be deferred at this stage of the design status.

Usually mechanical constructions are designed from the inside (main task) of the body to the outer surfaces, some winding subsystems are designed in consideration of this “construction Rule”.

To get more clearness about the function of the respective mechanical components the design of the winder is explained from one geometric sequence to another, starting from the fundamental hardware, the base plate.

All design and development activities are generated with 3D construction software CATIA V5 R13. The software CATIA V5 allows a full design and development of all mechanical parts including an assembly mode where all mechanical parts can packetize and assimilate with each other.

During the design and development phase and later on with the possible modifications phase; this software accelerate the different work packages for hardware production.

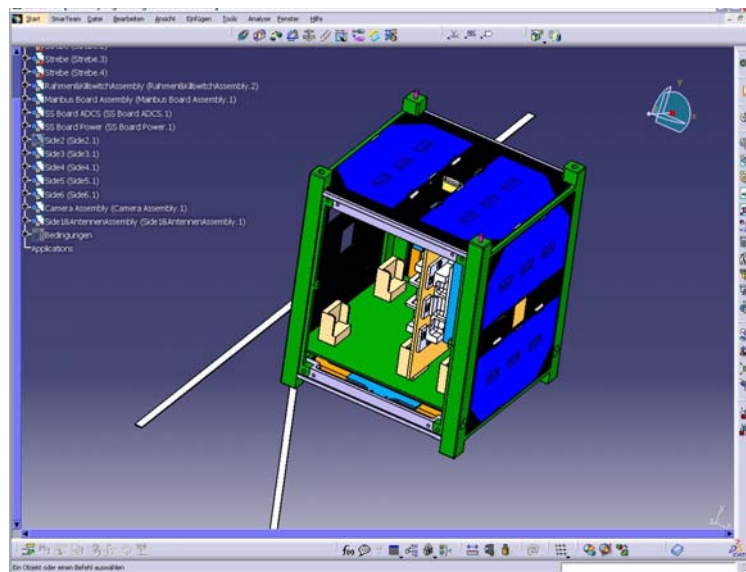


Figure 4-3: Catia V5 R13 screenshot of Compass-1 (EM)

## 4.2 Requirements

The design of the coil winder considers a modular mechanical body to provide a flexible configuration for any changes during the development phase.

The coil winder assumes in the whole design and development phase, in consideration of the production expenses and the financial budget, as simple as possible, without losing the focus for a sensitive winding tool an easy hardware construction.

The important recommended values for all hardware components is driven by the used copper wire. The maximum tension of the copper wire is appointed by the isolation characteristics of the copper wire. [6]

To manufacture high quality coils, the packing density of the coil needs to be as high as possible, so the wire needs to be wended as constant as possible. A high packing density is achievable with a combination of a relative high preliminary tension, in view of the coil volume and a good wire guidance.

The guidance needs to operate synchronously with the winding unit to appoint the required sensibility the increment of the guidance needs to be in the area of a quarter of the used wire diameter.

Next to all material limits the winder needs to be designed including as much as possible commercial of the self products (COTS). COTS products are performed on the basis of low cost, commercial availability and reliability hardware.

The material of the designed mechanical parts will be standard aluminium. Aluminium compared to steel has the advantage that the mechanical parts are not oxidizing and in the same time aluminium is easier and faster to handle at the FH mechanical workshop.

## 4.3 Hardware Design & Development

### 4.3.1 Base Plate

The base plate should offer a flexible modular platform, which allows less restraint for a general design. For the layout of the base plate different opportunities are given:

A base plate could be manufactured at the FH mechanical workshop, therefore all hardware interfaces including the base plate itself need to be defined from the beginning of this design task. The same base plate can also be machined also from time to time, depending on the improvement of the winder. Nevertheless this kind of manufacturing will take much more production time and furthermore the accuracy of all hardware interfaces could be imprecise. The base plate should offer a relative flexible design of the coil winder parts. A modular and at the same time a relative flexible base plate is in use at usual CNC milling machines, a so called T groove profile plate. This kind of base plate will be the best solution, and in addition the T groove plates are offered very cheap by the company ISEL<sup>9</sup>.

---

<sup>9</sup> [www.isel.com](http://www.isel.com)

At the home page of the provider several aluminium profiles are displayed, which are actually differentiated from the mechanical sizes and their application area.

A good solution for the required coil winder modularity is given with aluminium PT-Profiles. [8]

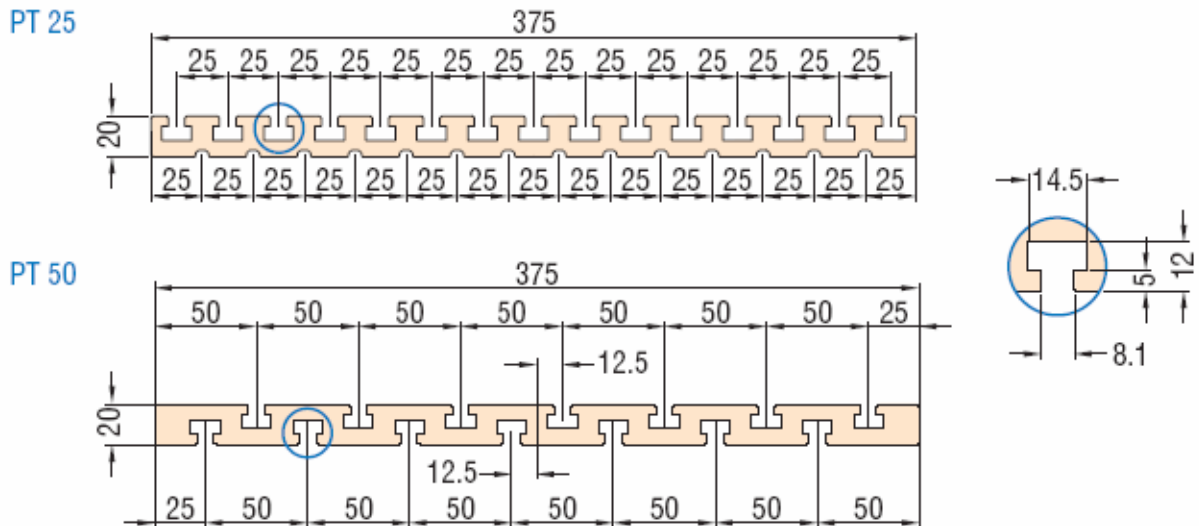


Figure 4-4: Different PT-Aluminium-Profiles

The PT-Profiles require universal surfaces which are naturally anodized, thick walled, without distortions, dimensionally stable and double sided mill cut.

The PT 25 Profile offers an middle flute distance of 25 mm with a constant height of 20 mm and is in its width available in 125mm steps.



PT 25 Profile Catia Model (front view)

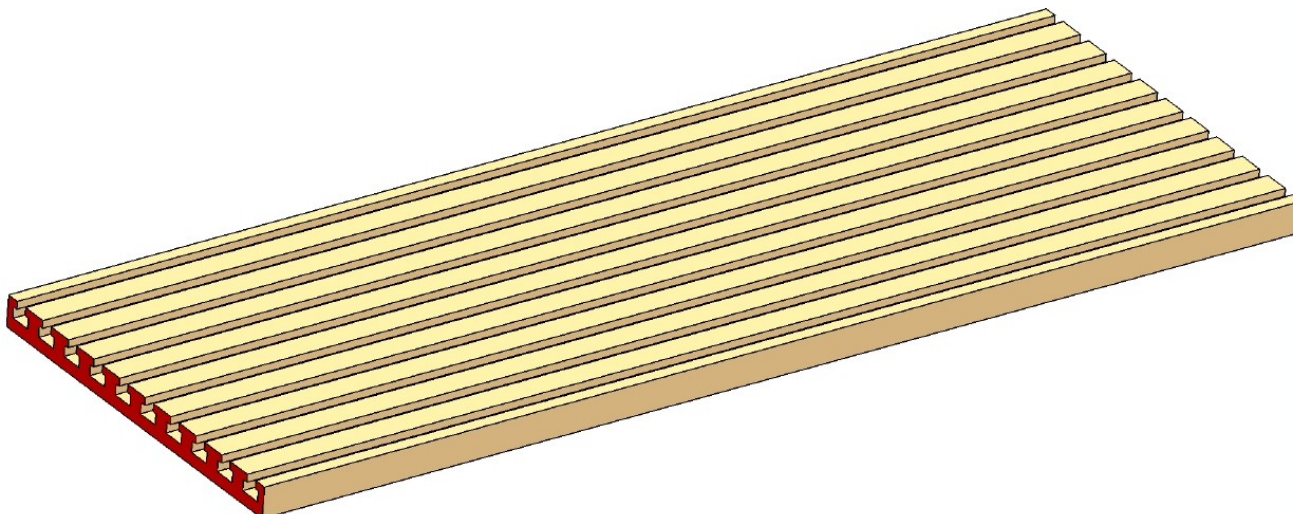


Figure 4-5: PT 25 Profile 3 D Catia Model

T-Groove blocks show a good opportunity for the interface between the T groove plate and the different hardware parts. The T-Groove blocks allow a flexible interface with only one condition, that all interfaces need to be established with M 6 screws, therefore all trough hole drills need to be laid out for M6 screws DIN EN 20273 with the fine diameter of 6,4mm or middle diameter of 6,6mm.

This T groove screw nuts are offered relatively cheap from the supplier Maedler<sup>10</sup>. In consideration of the hardware accuracy the DIN EN 20273 middle norm was chosen for further model layouts.



Figure 4-6: T Groove Screw Nut M6 DIN 650

### 4.3.2 Wire Carrier / Wire Cover Brake

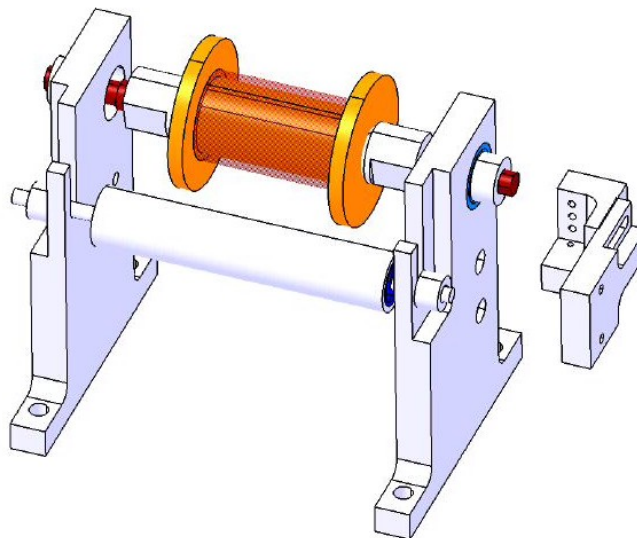


Figure 4-7: Wire Stock as 3 D Model

The main function of the wire stock coil is to deliver constant wire for more than only one coil. This body is build up with two sidewalls with integrated FAG bearings with a thread bolt (spindle) where the wire stock cover can mount on. The cover is fixed with a

---

<sup>10</sup> [www.maedler.de](http://www.maedler.de)

customized screw nut, which helps to centre the wire cover compared to the thread bolt. This sanction guarantees the concentricity of the system. Both ends of the “M 10” threaded bolt are reduced to a size of 8 mm and are secured against horizontal movements with usual retaining rings. The wire at the wire stock transacts the wire constantly so it decreases its circumference constantly, therefore a relative flexible transaction level (high) is implemented into the system. The limiter is constructed with a standard aluminium rod with integrated FAG bearings and a small standard spindle with a diameter of 5 mm. This spindle is also secured with retaining rings against vertical movements.

To avoid an uncontrolled unwinding of the wire, a friction brake needs to be implemented. The wire brake has the function to hold an initial load of the wire at a constant level. With the consideration of the small wire diameter and its allowed forces, it was decided to design a wire brake, which allows a small friction force resulting in a low brake momentum at the wire stock coil. All commercial available brakes, i.e. drum brakes, are either not proper for this force area or show the problem that the brake is not adjustable very fine for this use. Therefore a mobile unit was designed where easily a spring steel rod is integrated. Usual screws are used for folding the spring steel rod and transforming a frictional force to the wire carrier.

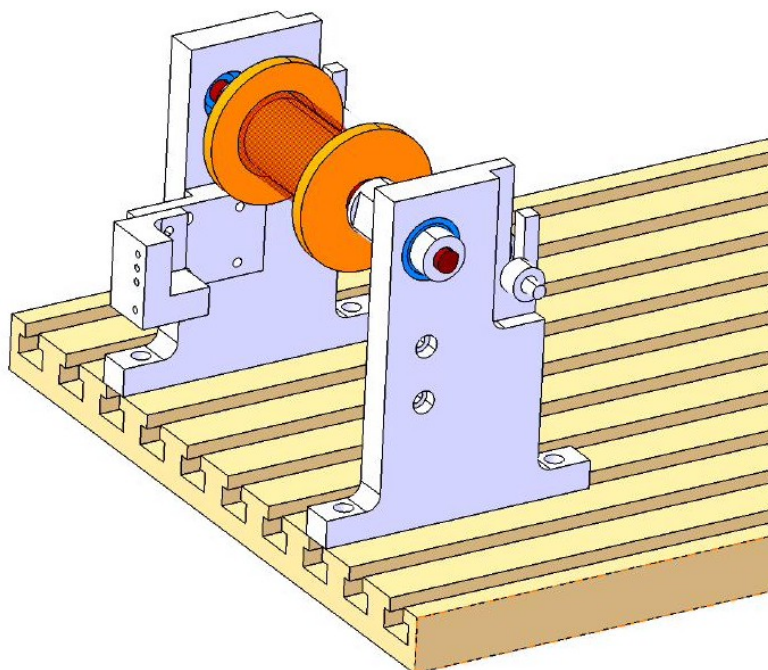


**Figure 4-8: Wire Carrier & Wire Brake mounted on the base plate**

After construction of the wire carrier part, the wire needs to appease during the recoil movements. A reassurance of the system can be managed by deflection pulleys in special configurations.

### 4.3.3 Pulley

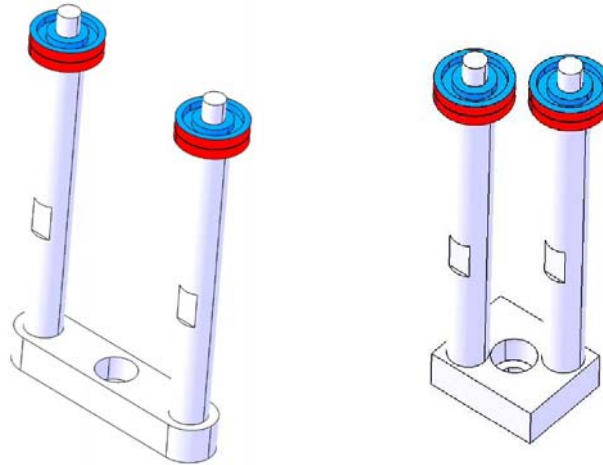


**Figure 4-9: Deflection pulleys mounted on an aluminium rod with different offsets**

Relative big buffers with different configurations are needed so that all wire movements can be distributed and controlled. The first movement which needs to be under control is the recoil movement of the wire which is moving from one side to another.

The second movement is caused by the rectangular coil mould, which affects the wire with different pull forces. The deflection pulleys have the function to turn round the wire and therefore generate a buffer for the agent forces. The same pulleys, but with a “smaller” offset of the rods (Figure 4-9) in a different configuration are used to appease the recoil movement of the wire. The pulleys are mounted on standard aluminium rods and these again are screwed on a socket.

The deflection rollers are deliverable in four different variations. [9]

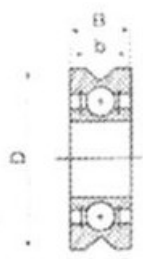
The variations differentiate only in the milled groove. The deflection roller are deliverable with edged groove, V-grooved, round groove and without any groove. This groove enables a safe wire stream at a defined height. The next figure shows the offered pulleys from the bearing provider GedeHemer<sup>11</sup>.

---

<sup>11</sup> [www.gedehemer.com](http://www.gedehemer.com)

**Richtrollen einreihig, beidseitig abgedichtet**  
**Straightening rollers, single row, sealed from both sides**

Art.-No.	d	D	B	Draht/wire Ø	
R 150 ZZ...	1,5	4	2	- 0,2	
R 623 ZZ...	3	10	4	- 0,4	
R 624 ZZ...	4	13	5	- 0,5	
R 634 ZZ...	4	16	5	- 0,8	
R 625 ZZ...	5	16	5	- 0,8	
R 635 ZZ...	5	19	6	- 0,9	
R 626 ZZ...	6	19	6	- 0,9	
R 62621 ZZ...	6	21	6	- 1,4	
R 608 ZZ...	8	22	7	- 1,5	
R 60826 ZZ...	8	26	7	- 2,5	
R 609 ZZ...	9	24	7	- 1,5	
R 600030 ZZ...	10	30	8	- 3,0	
R 361200 ZZ...	10	32	9	- 4,0	
R 620035 ZZ...	10	35	9	- 3,5	
R 361201 ZZ...	12	35	10	- 4,5	
R 620247 ZZ...	15	47	11	- 7,0	
R 361203 ZZ...	17	47	12	- 7,5	
R 361204 ZZ...	20	52	14	- 8,5	
R 361205 ZZ...	25	62	15	- 10,0	
R 361206 ZZ...	30	72	16	- 11,0	
R 361207 ZZ...	35	80	17	- 15,0	

  
 Profil V  
  
 Profil F ①  
  
 Profil R ①

*Bitte max. Draht-Ø angeben  
 please indicate required wire Ø*

Figure 4-10: Deflection pulleys

The size of the groove is depending on the size of the wire and the wish of the customers. In order that the guided wire is not getting extra punctual stress, the pulley with an outer diameter of 12 mm with a round groove of 0.25 mm was selected.

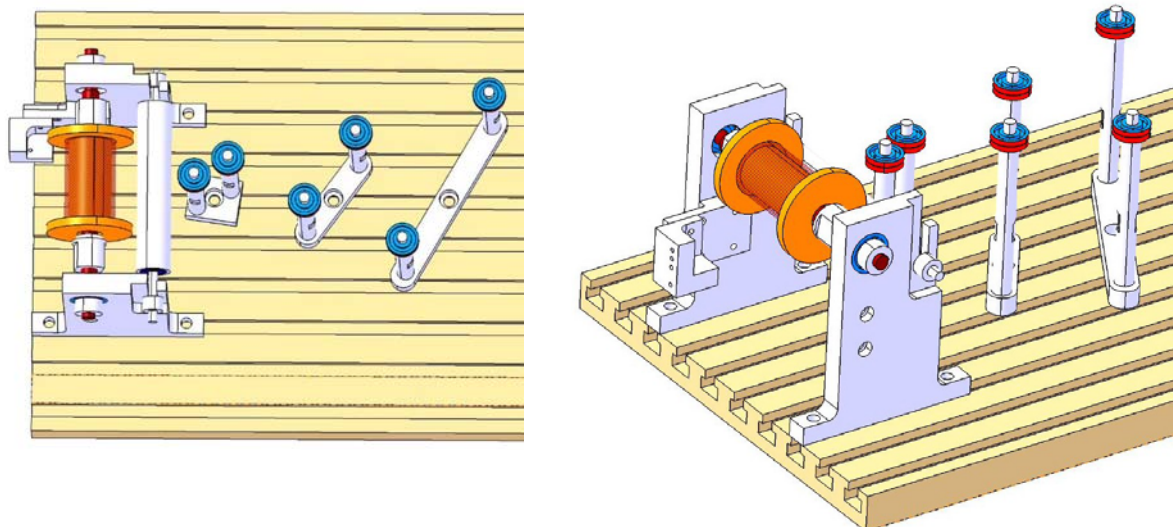


Figure 4-11: Pulleys placed on the base plate

### 4.3.4 Guidance

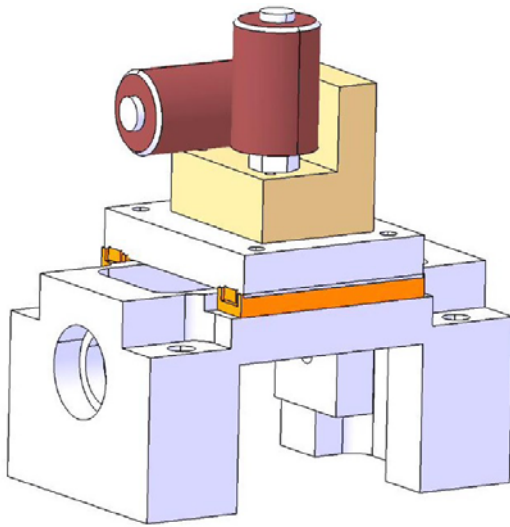


Figure 4-12: Redesigned guidance unit

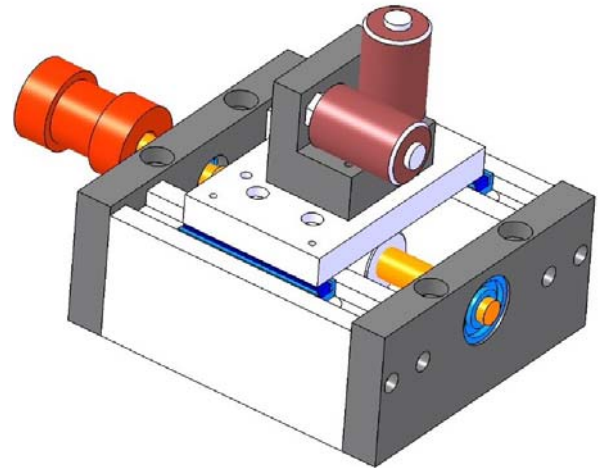


Figure 4-13: First design of the guidance

The manufacturing of high quality coils with a high packing density requires guidance of the wire during the winding process. The guidance needs to be very accurate, because of the very thin copper wire with a nominal diameter of 0.15mm. This means that the guidance accuracy needs to be at least the wire diameter, better a quarter of the wire diameter. To guarantee such guidance special units, possibly COTS products, needs to be implemented into the guiding unit. The unit needs to reciprocate the wire “only” in the horizontal axis but with a very high accuracy. A good solution for a reciprocate movement is given with a threat rod with an integrated interface, which transform the rotation into an accurate horizontal reciprocate flow.

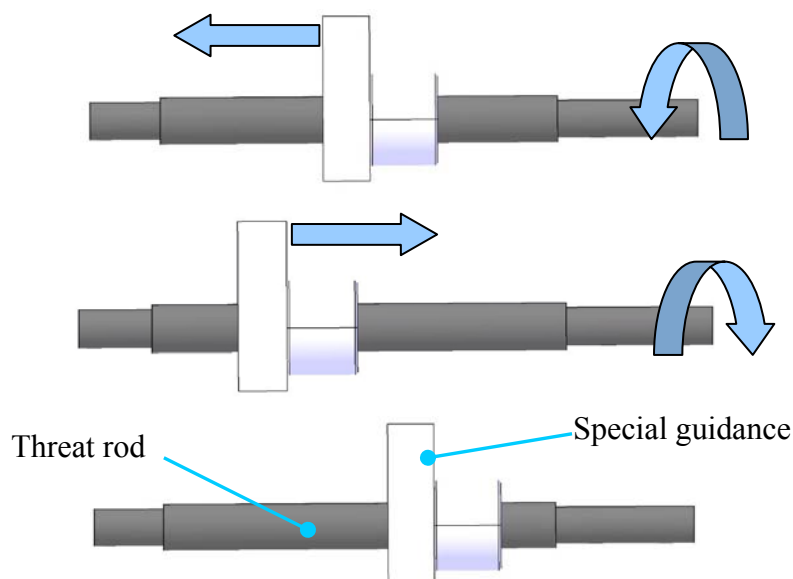
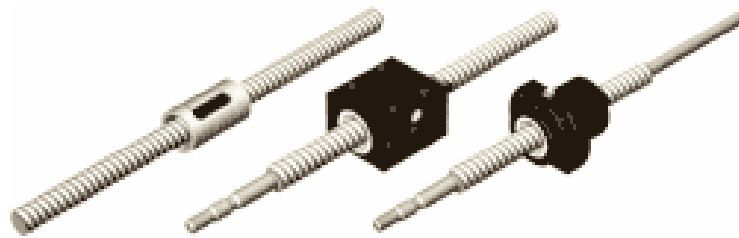


Figure 4-14: Moved threat rod with interface

The guidance needs high precision, therefore the unit needs to be best with  $\pm$  zero tolerance. The practice shows that high quality COTS products are also relative high in cost. For this reason some companies have student discounts up to 20%. Not infrequent the companies offer their different possibilities to support student activities as best with a complete sponsoring of the hardware product.

Anyway, a very fine guidance is established in every CNC milling cutter with special ball screw spindles [10].



**Figure 4-15: Several spindles with different guide interfaces**

The special ball screw spindles offer high tracking precision which are not depending only on the spindle itself, but rather on the quality of interfaced units.

The spindles are usually delivered in combination with the adequate bearings and every supplier offers also variations of guide blocks, gear units and drive mechanisms. The only limit for *ready* units is set actually with the financial budget. Ready units can costs up to 1000 Euro and more therefore this unit is setup with cheaper COTS products but with similar functions.

Stepping motors as the drive mechanism offer compared to the usual electric motors (DC motors) the possibility of linear guide by dividing a whole circle of a rotation into steps. The drive mechanism could be designed also with a DC motor but in combination with a very expensive measurement technology, e.g. Exposed Linear Encoders from the supplier HEIDENHEIN<sup>12</sup>.

The “Body” of the guidance is designed around the special spindle. The body is constructed with two main blocks and two sidewalls. The special screw spindle bearings (blue) are integrated into both sidewalls for an easy integration of the spindle. The main block offers the integration of special guide rails, which are needed in consideration of the horizontal movement.

---

<sup>12</sup> [www.heidenhain.de](http://www.heidenhain.de)

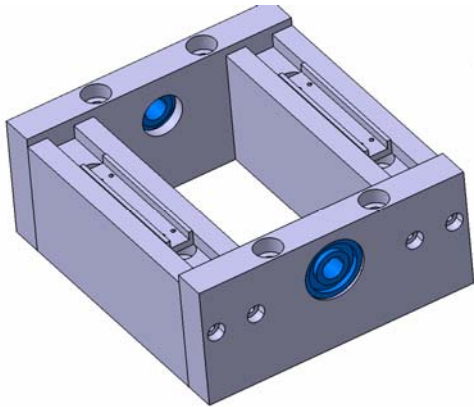


**Figure 4-16: Base construction with guide rails**

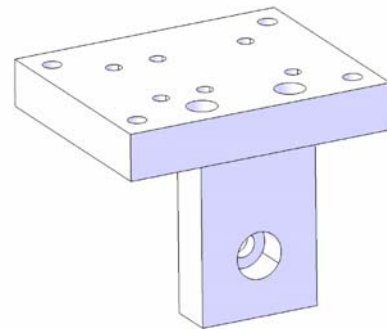


**Figure 4-17: Interface unit**

To transfer the spindle movement to a guidance movement an extra interface is designed. The interface is built-on with two perpendicular screwed plates, one plate interfaces with the spindle and the other plate interfaces with the “roll board”.

The “roll board” enables easy integration of two perpendicular guidance rolls and creates the interface between the guidance unit and the guided wire.

Before the “roll board” can be designed into a final version, the kind of usable rolls needs to be identified, while every roll offers different surface properties.

A research about guidance rolls has resulted that different “rolls” exist. Just to name a few: Guide rolls, cone rolls, straightening rollers, roller crosses, guide units and so on.

[9]

The last two expressions are actually ready build units, where different rolls are in use.

Considering the financial budget of the winding unit and the view of a new design possibility, the ready units will require too much of the available budget, therefore the different rolls should help to solve the guidance design. The next figure shows the offered rolls from the bearing provider GedeHemer<sup>13</sup>

---

<sup>13</sup> [www.gede-hemer.de](http://www.gede-hemer.de)

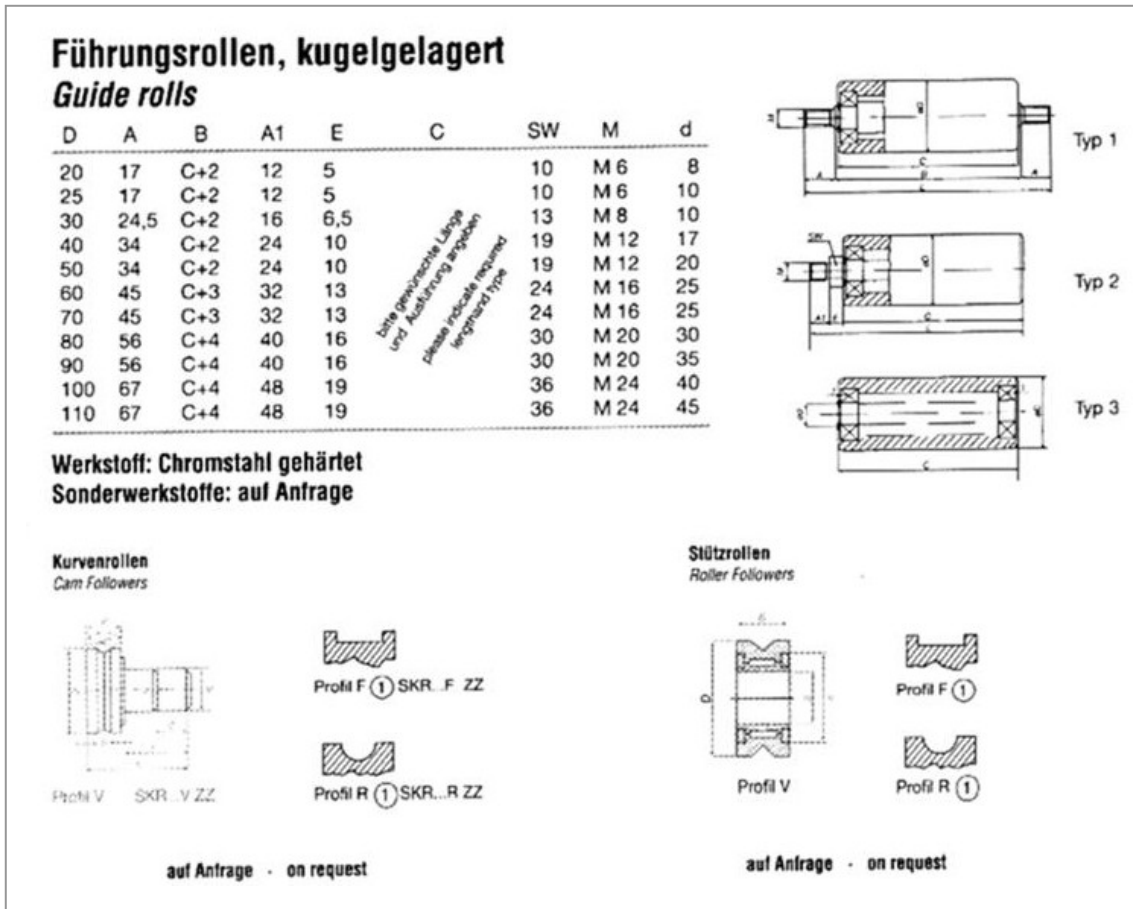


Figure 4-18: Guide rolls, Cam Followers, Roller Followers

A good solution is given with the guide rolls Type 2, these rolls are screw-mountable from one side, which is advantageous for integration aspects and in addition these rolls are in use for similar uses in production lines of big winding companies.

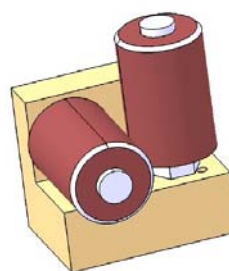


Figure 4-19: Roll board

During the development phase of this unit, the Linear Actuator [11] have been referenced by a Compass-1 team member. The institute which he is working for is using this actuator for “hexapod” applications.

The linear actuators compromise actually a stepping motor with a small increment, a high tracking guidance with an easy assembly possibility.



Figure 4-20: Linear Actuator LC 15

This unit is the smallest commercially available linear actuator in the world, with a step accuracy of 0.02mm per step. The drive mechanism of this unit comprises a stepping motor with also 200 steps per revolution.

The unit is used for medical instrumentation, optics, machinery automation and many more automated devices which require precise remote controlled linear movements in a very small package size. [11] This unit combines, compared to the other solution, the thread rod with the special interface, the FAG bearings and a clutch with a corresponding stepping motor. These huge advantages will increase the quality of this unit by reducing the costs in the same time.

Hence these facts drove this unit to a redesign. At the redesign of the guidance unit all designed parts, except the basic unit, have been transferred to the new required unit.

The huge advantages of this COTS product caused a redesign of the guidance unit.

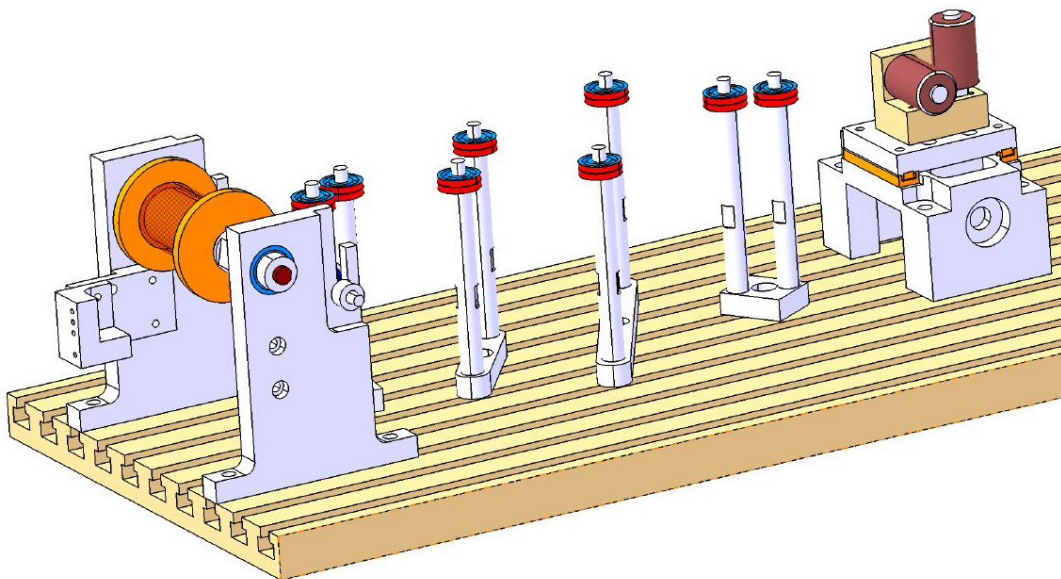
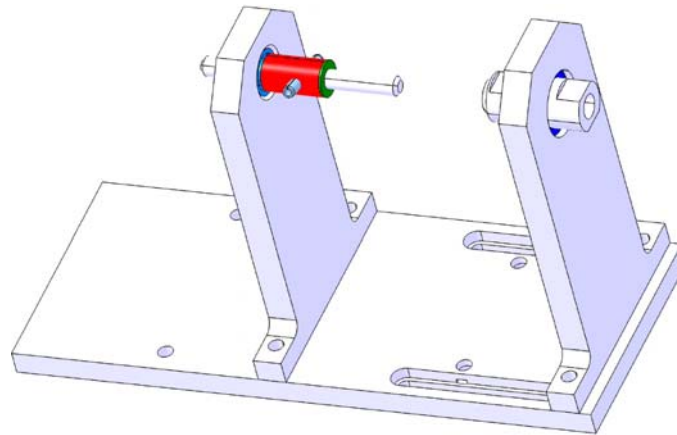


Figure 4-21: Coil winder model with additional the guidance unit

### 4.3.5 Winding Unit

The main design idea of this unit considers the easy integration and later an easy demounting of the coil mould for further activities. An easy unit can be established e.g. with an easy construction where every part fits into only one position. The winding unit is built around the coil mould and is built-on a flat base plate. The hardware offers a static defined Holder (figure left) where the coil mould can easily installed.



**Figure 4-22: Winding unit mounted on a flat plate**

The holder itself is actually nothing else than a sidewall with an integrated FAG bearing, with a spindle which is secured against the vertical movement with a retaining ring. To get a mechanical contact for rotation aspects, between the coil mould and the shaft; an easy solution is to impose a brass sleeve over the shaft, which is locked with a pin. It should be noted that the rotation frequency will not be so high compared to long run production.

To avert a handicap between the shaft and the bearing, the shaft diameter (red) must be smaller than the diameter of the inner ring of the FAG bearing.

The coil mould and the shaft are made up of different materials to block the internal wear out. The shaft is made up of brass material and the coil mould of standard aluminium.

Next to the locking devices the pin has an additional function. It is helping to create an interface between the coil mould and the mechanical drive (Stepping motor).

To accomplish the interface a slotted hole needs to be milled into the coil mould where the pin is fitting in. In addition the interface will be greased with standard machine oil, lubrication grease, for a better integration and removal of the adequate coil mould.

The design of the spindle considers the bending loads causing from the weight of the coil mould.

After the assembly of the coil mould on the “holder”, the coil mould needs to be matched for rotation aspects with a mobile sidewall. The sidewall secures a counter pressure onto the coil mould, which guarantees a pivot rotation. The horizontal guidance of the sidewall is realized with two parallel slotted holes at the base plate, where the screw nuts fit on the underside of the plate which enables to screw the sidewall tightly.

The mobile sidewall is built up in the same way as the “Holder” side plate, with the only difference that the secure against horizontal movements is not realized with retaining rings. The locking device secures itself automatically while the two fixing parts are mutually screwed tightly, so they secure themselves automatically.

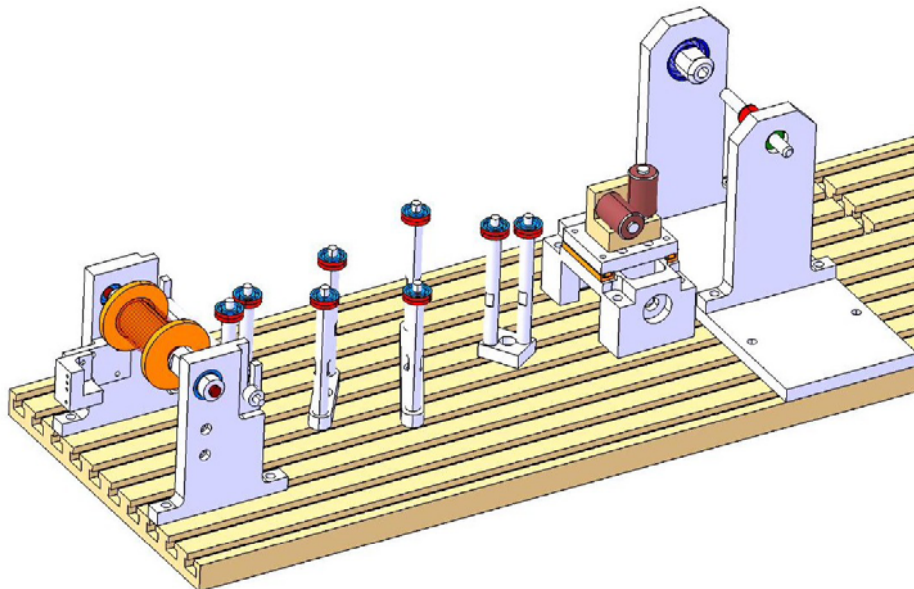


Figure 4-23: Design of the winding unit without the coil mould

### 4.3.6 Coil Mould

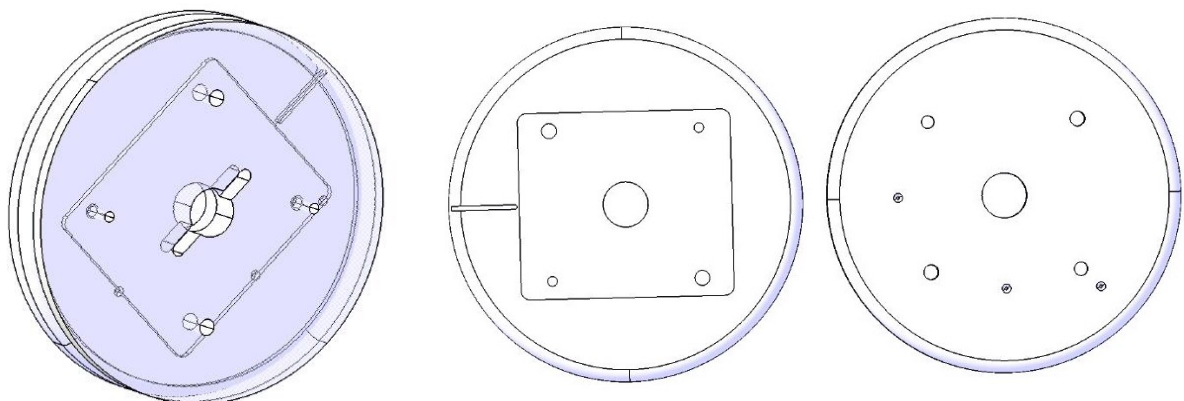


Figure 4-24: Coil mould

The mould simply consists of two round plates, one plate to wrap up the wire and a second plate to generate the counter plate, with three small drills to thread the wire to the desired position. These two plates are fixed with two converse oriented dowel pins and are also screwed with two converse oriented hexagon socket screws.

In order not to destroy the wire during the winding a round winding mould with rounded edges with an integrated rectangular coil mould was designed. The edges of the rectangular coil mould, at the inside, are also rounded with a minimum size of 3 mm. The rectangular coil mould with  $73 \times 64 \text{ mm}^2$  is resulting from the theoretical coil thickness of 5 mm.

The coil mould is built up with standard round aluminium which is relative easy to manufacture and in addition aluminium shows a relatively good thermal character. This thermal character will be important for further connection activities, whereas the bonding will be established by heating up the wire.

The coil will have a thickness of 2,1mm which results from 2 mm winding place, which was available at the cube, plus a safety margin of 5 %. The margin will upgrade the connection quality of the coil on the panels, due the fact that the coil holder will have only 2.0 mm space. The small difference will cause a small squeeze effect at the coil itself but without any mechanical deformations.

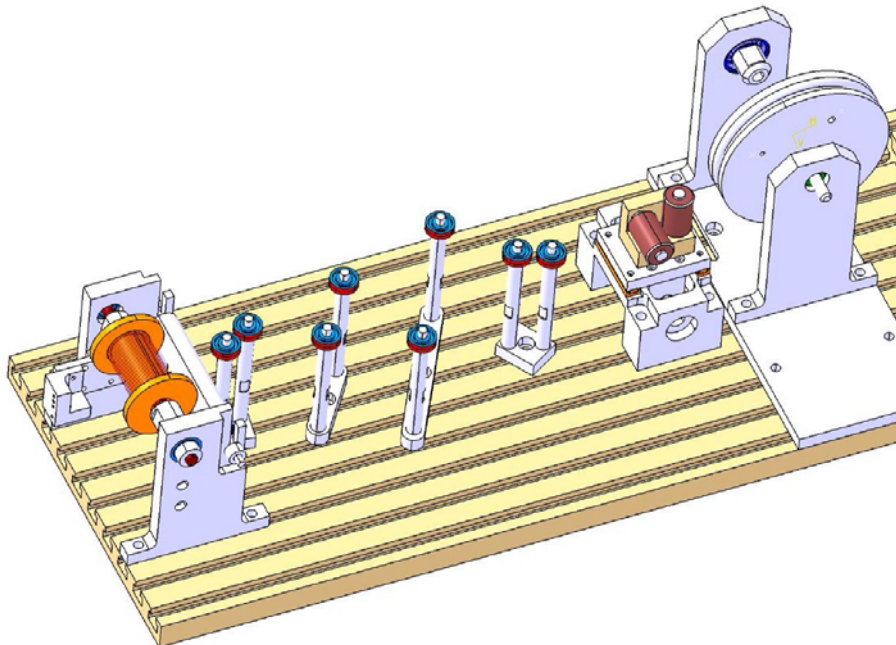


**Figure 4-25: Design result of the coil winder**

### 4.3.7 Force Measuring Unit

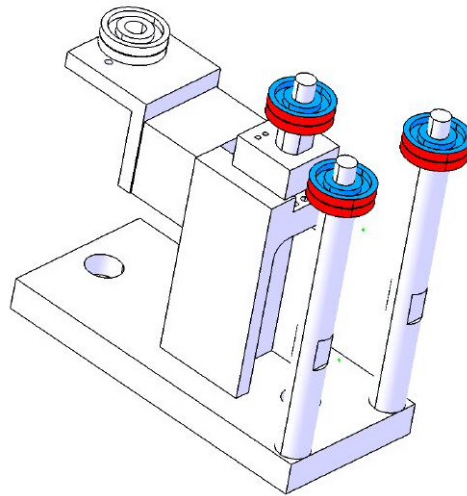


**Figure 4-26: Force measuring unit**

The force measuring unit is an additive unit which is designed to monitor and record the wire forces during the winding. The tension of the wire has in the calculation no direct influence to the electrical characteristics, but to the mechanical dimensions. Low tensions cause an unconstant dimension of winded coils; the result of the first prototypes will confirm this proposition.

The maximum force limit is governed by the wire isolation, which is around 1.5N. The force measuring is challenging the design task with a transferring of the horizontal wire stream forces into a digital signal, without temper the measuring. Electrical units i.e. potentiometers can help to transfer mechanical movement to a digital signal, but the friction of the potentiometer transforms this solution to an inoperative solution.

The measuring unit should introduce a very small error into the measurement otherwise it makes no sense, especially at this small measurement range, to record the wire tensions. The recording of the wire tensions at big cable companies are measured with special instruments. This instruments use the measuring principle of a tackle which creates the basis for the design of this unit.

The wire needs to be positioned and controlled before and after the force measuring unit, in order to carry out the measurement inside the tackle.

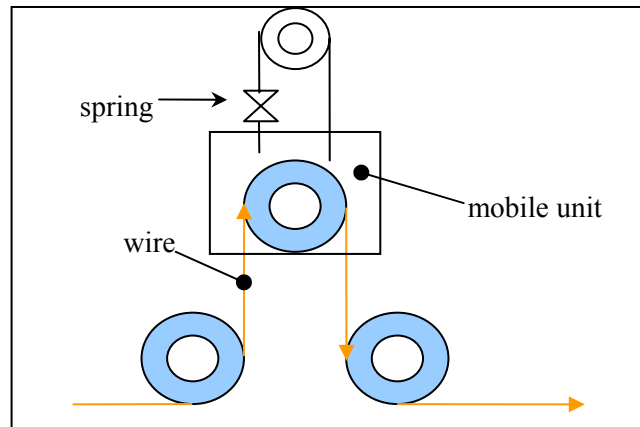


**Figure 4-27: Tackle principia**

The wire stream forces are transformed with the tackle design into a horizontal movement, where the middle pulley is mounted on a fine guide rail with a low self locking. With the aid of this mobile pivoted roll, the wire force changes are visible, assumed that this pivoted roll is “fixed” to another system. A fix and in the same time mobile roll is established by the integration of a spring into the fastener cable. This arrangement enables the transformation of the horizontal drive into a rotation, assuming that the referenced system is also pivoted.

A pivoted measuring unit, an incremental driver from the model making have been recommended for this special feeding. With the known spring stiffness the wire forces are recordable from the proportion between the rotation-angles enabled from the expansion of the spring. The incremental driver has in case of an angle measurement a unique resolution up to a half degree. The compound between the pivoted roll and the incremental driver is designed flexible, so that during the manufacturing the right spring can be chosen and integrated easily.

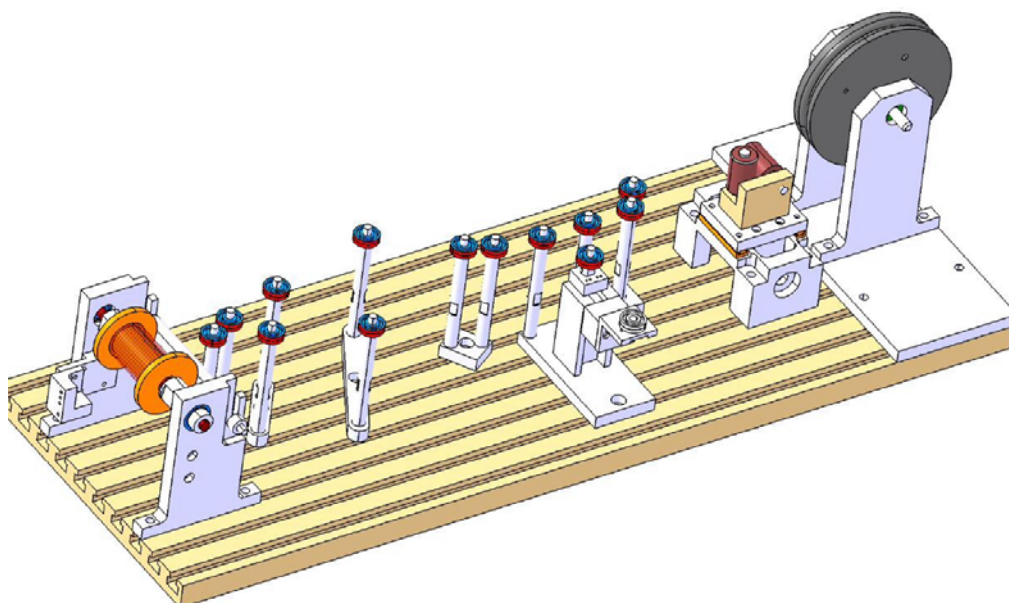


**Figure 4-28: Coil winder with force measuring unit**

### 4.3.8 Electrical Drives and Measuring Unit

During the design task of the coil winder the electrical drives have been considered. The electro-mechanical units are stepping motors; stepping motors fill a unique niche in the motion control world. These motors are commonly used for measurement and control applications. Sample applications include CNC machines and volumetric pumps. Several features common to all stepper motors make them ideally suited for these types of applications. These features are as follows:

1. **Open Loop Positioning** - Stepper motors move in quantified increments or steps. As long as the motor runs within its torque specification, the position of the shaft is known at all times without the need for a feedback mechanism.
2. **Holding Torque** - Stepper motors are able to hold the shaft stationary.
3. **Excellent Response** - to start-up, stopping and reverse movements.

There are three basic types of stepping motors: permanent magnet, variable reluctance and hybrid. Permanent magnet motors have a magnetized rotor, while variable reluctance motors have toothed soft-iron rotors. The stator or stationary part of the stepping motor holds multiple windings. The arrangement of these windings is the primary factor that distinguishes different types of stepping motors from an electrical point of view. From the electrical and control system perspective, variable reluctance motors are distant from the other types. Variable Reluctance Motors have three to five windings connected to a common terminal.

Unipolar stepping motors are composed of two windings, each with a center tap. The center taps are brought outside the motor as two separate wires as a result unipolar motors have five or six wires. The center tap wires are tied to a power supply and the ends of the coils are alternately grounded.

Bipolar stepping motors are composed of two windings and have four wires. Unlike unipolar motors, bipolar motors have no center taps. The advantages of not having center taps is that current runs through an entire winding at a time instead of just half of the winding. As result, bipolar motors produce more torque than unipolar motors of the same size. The draw back of bipolar motors, compared to unipolar motors, is that more complex control circuitry is required by bipolar motors.

The selected stepping motor for the drive mechanism of the coil winder offer the possibility to share a whole revolution into 200 steps ore more.

The used stepping motor is a unipolar motor but used as a bipolar stepping motor, which increase the rotation torque of the stepping motor.

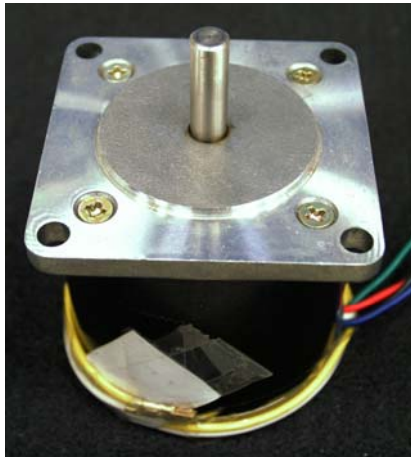


Figure 4-29: Bipolar stepping motor



Figure 4-30: Incremental driver, rotary encoder

The drive mechanism of the guidance unit is realized with the Linear Actor LC 15 which is actually also a stepping motor with the respective electrical supply.

The gauge of the force measuring unit is the MATSUSHITA Rotary Encoder. The datasheets of the used unit have not been found from at the supplier, this could result from the fusion of the producer MATSUSHITA Electric Works LTD<sup>14</sup> by Panasonic<sup>15</sup>.

Nevertheless this encoder allows a determination of the rotation angle with a resolution up to  $0.5^\circ$ , depending on the electrical supply. The important features of the encoder are as follows:

- electrical supply 5 V
- contact less angle determination with a integrated optical encoder
- open collector measurement
- resolution: 360 pulses per rotation

<sup>14</sup> <http://www.mew.co.jp/e/corp/>

<sup>15</sup> <http://www.mew.com.br/>

## 5 Coil Winder Production

### 5.1 Technical Drawings

Diverse commercial off-the-shelf (COTS) are implemented into the coil winder, to guarantee a given amount of quality. The remaining units of the coil winder have been custom-designed and developed at the FH Aachen. Following the coil winder design and development all unit parts have been drawn as technical drawings which were required for the production tasks at the own FH mechanical workshop. The technical drawings are constructed with the same software used for the model design and development of the coil winder, with CATIA V5 R13.

All drawings are coordinated, so that the required accuracy can be manufactured.

After the drawings of different hardware parts, all drawings have been checked from an assistant of the FH mechanical workshop. For this project the head of the FH mechanical workshop has checked all drawings and in addition he was contact person in charge for manufacturing problems.

After the checks some technical drawings needed to be modified. These small modifications which are usual at the development of specific parts will be not discussed in details. The final drawings of the coil winder units are ready for access at the Appendix –A.

### 5.2 Material and COTS Orders

After the technical drawings were finished, the needed material has been ordered from diverse suppliers, depending on the cost. The majority of the coil winder unit parts are milled from standard 10mm or 12mm aluminium plates, ordered from Olimex<sup>16</sup>. The thickness resulted from the column width of the PT25 base plate and the particular functions. The PT 25 T-groove plate was ordered from the supplier ISEL<sup>17</sup>. The FAG bearings the majority of the screws and diverse accessories have been ordered from the supplier KSA<sup>18</sup> in Aachen.

---

<sup>16</sup> [www.olimex.de/](http://www.olimex.de/)

<sup>17</sup> [www.isel.com](http://www.isel.com)

<sup>18</sup> [www.ksa-aachen.de](http://www.ksa-aachen.de)

The different pulleys, except of the long roll at the wire carrier are chosen and ordered from the supplier GEDE Hemer<sup>19</sup>. The standard 10 mm aluminium sticks and the round aluminium for the coil mould have also been ordered with the aluminium plates from Olimex. As written in the production part of this thesis Elektrisola has spent the special bonding copper wire type S180 in two different types.

The stepping motor of the winding unit, the incremental driver of the force measuring unit and the three guidance rails were sponsored by a Compass-1 group member. The Linear Actuator LC 15 of the guidance unit was ordered from the European supplier A-drive<sup>20</sup>.

The manufacturing of the coil winder has been carried out at our own mechanical workshop. The diverse unit parts were constructed and produced with different dimension limits depending on the function. Details of the manufacturing activities are displayed by the Appendix-B.

---

<sup>19</sup> [www.gede-hemer.de](http://www.gede-hemer.de)

<sup>20</sup> [www.a-drive.de](http://www.a-drive.de)

## 6 Control Unit Design

This part describes the needed electrical hardware interfaces and their software programming. The adjustments like the synchronicity of the driving mechanisms are integrated into the software. The different automated tasks of the coil winder are split into the electrical and the corresponding software design tasks. Hardware and software design (and development) generally goes hand in hand.

However, the software is by nature the more flexible part that can be modified more easily. Therefore it is very advisable to finish the hardware design first but wait with the development until the software has advanced far enough, so that modifications can still be integrated in the hardware design.

The electrical hardware components and the software for this control unit are designed and developed with the layout software Protel 2005.

The transaction of these activities was actually not part of this thesis but different tasks e.g. layout, selection, ordering activities have been accomplished in a work group.

The documentation of the generated hardware will be limited in this thesis.

The required functions and the interfaces to the different electrical units have been layout and defined together.

### 6.1 Electrical Hardware Design

The design process shall derive a physical architecture from the functional analysis and requirement allocations. The electrical design of the coil winder is affected by the used drive mechanisms and the used measurement hardware. The principal design of these electrical components is shown as follows:

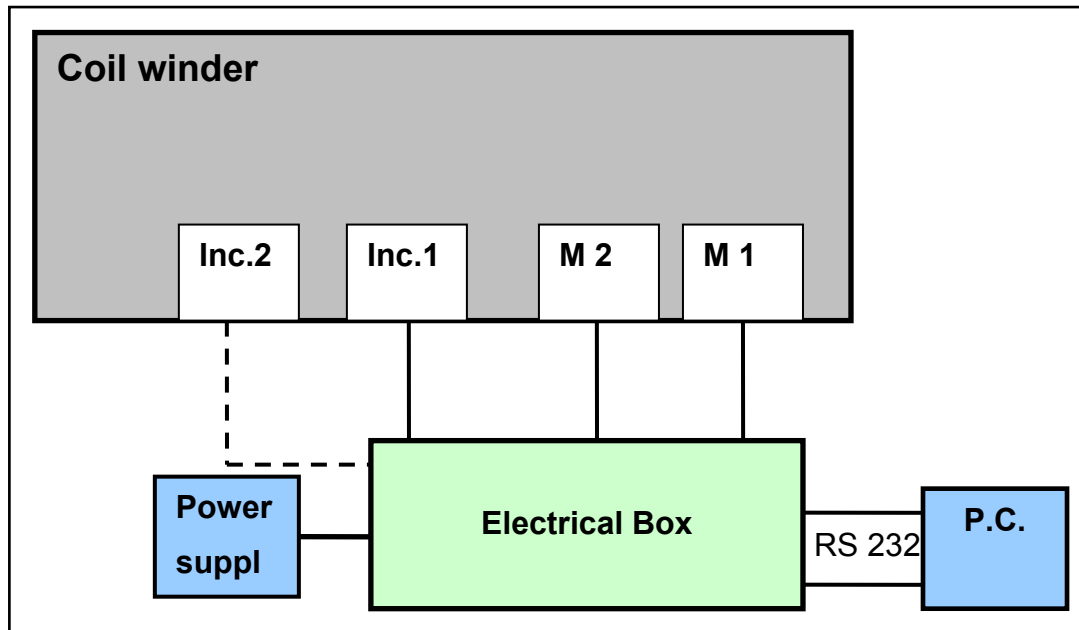


Figure 6-1: Electrical interfaces of the coil winder

The M1 & M2 in Figure 6-1 represent the stepping motors, M1 embodies the drive mechanism of the winding unit and M2 the stepping motor, Linear Actuator of the guidance. The Inc.1 represents the incremental unit used in the force measuring unit, the second incremental unit was considered for the determination of the total coil length. The unit was planned for the case that the length needs to be determined, while the main aspect of the coil is described with its resistance.

The electrical box represents a PCB where different hardware components, e.g. the MCU, power amplifier or voltage regulator and much more components are soldered on.

At this stage the decision about the integration of a COTS controller unit for the stepping motor drive seems to be the best and easiest way. But the consideration of the gauge an incremental, rotary encoder with a high resolution and the financial budget have resulted in the decision of the design development and production of the own controller unit, which combines the control of the used different electrical components.

## 6.2 Circuit Design

The circuit design includes the selection and implementation of necessary parts in order to adjust the main devices in a proper form, e.g. capacitors, resistors, power amplifier, reset buttons. It should be underlined that the circuit design activities are the most time consuming parts of the electrical hardware design.

For the selection of the main electrical hardware, the microcontroller unit (MCU), the required digital pins have been determined.

The triggering of both stepping motors is established by using two stepper driver types IMT 901 from the supplier Nanotec<sup>21</sup>, which require seven digital I/O pin per driver.

The incremental drivers or rotary encoders require three digital I/O pins each.

It was decided to configure the board for a stand alone function, therefore an interface for a LCD and a keyboard is provided. The standard LCD is characterised with 4 lines x 20 symbols. The I<sup>2</sup>C Bus will be used for the connection of the keyboard.

Summarizing all I/O pins results in more than 30 necessary I/O pins for the MCU. The selected MCU for this control application is the AVR ATmega 128<sup>22</sup>. The ATmega 128 combines an easy software development with the debug interface called JTAG and a free available Integrated Development Environment (IDE) AVR Studio.

Circuit design details of the coil winder PCB are displayed in the Appendix-C.

After the circuit has been proven the PCB layout has been started as next.

### 6.3 PCB Layout

The PCB layout consists of the definition of the physical board layout which is displayed in Figure 6-3. The layout activities comprise the definition of the board layout combining with the part placement and manual routings.

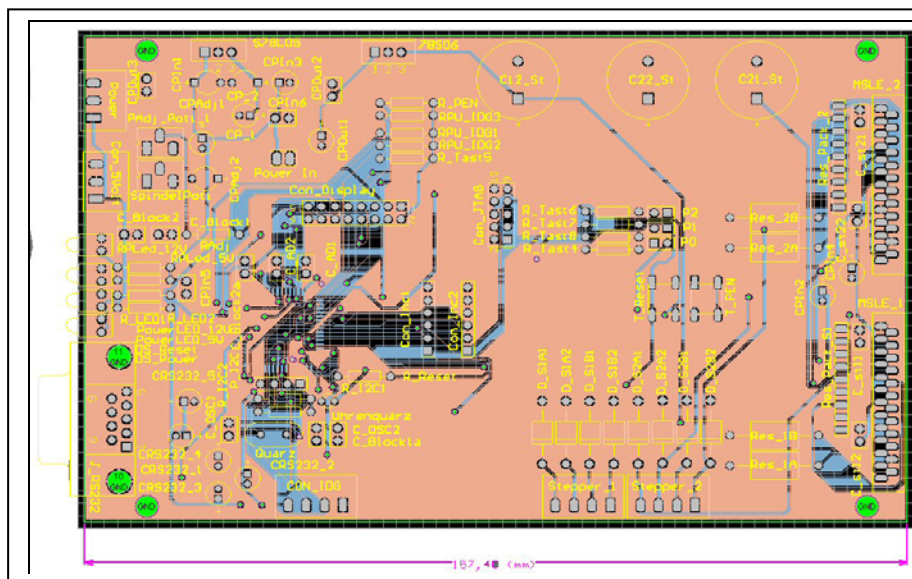
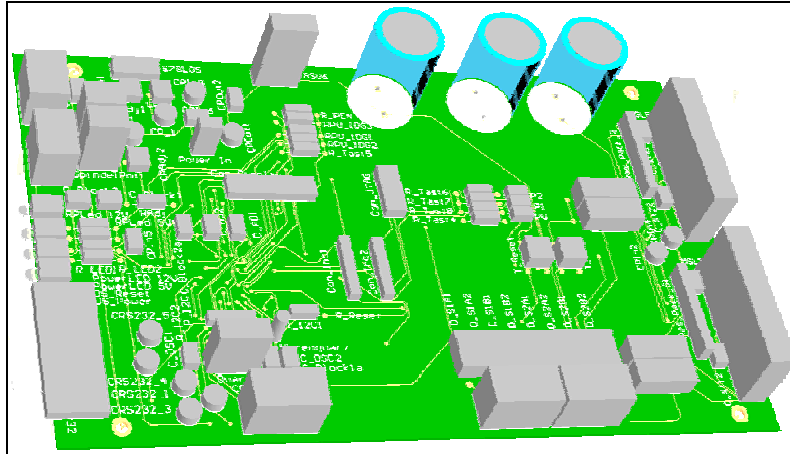


Figure 6-2: PCB layout without electrical parts

<sup>21</sup> [http://nanotec.de/page\\_steuerungen\\_imt901\\_de.html](http://nanotec.de/page_steuerungen_imt901_de.html)

<sup>22</sup> [www.atmel.com](http://www.atmel.com)



**Figure 6-3: PCB layout with electrical parts**

All required electrical parts have been ordered and delivered. It is sometimes possible, that some parts are not deliverable in general or in the small quantity. The required electrical components are ordered from different suppliers, e.g. Reichelt<sup>23</sup>, Farnell<sup>24</sup>, Conrad Elektronik<sup>25</sup>, RS components<sup>26</sup>.

## 6.4 Electrical Hardware Production

After the software had an advanced status, the fabrication of the PCB has been accomplished. Therefore the designed PCB has been handed over to the manufacturer Multi PCB<sup>27</sup> through the internet in form of Gerber files.

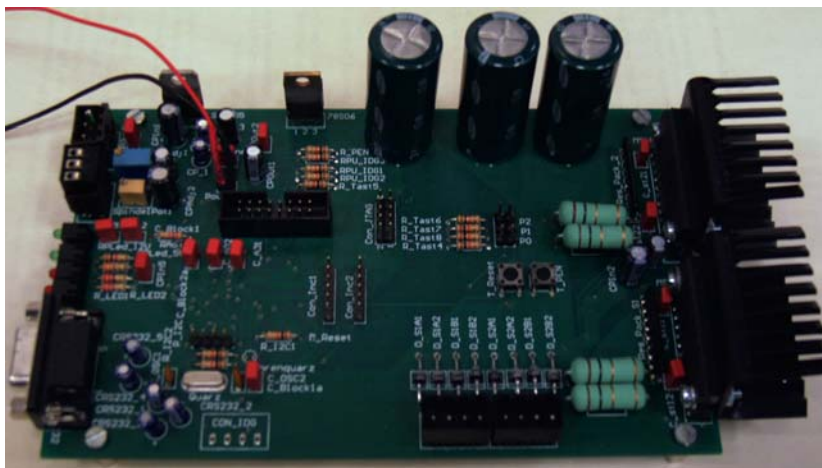


**Figure 6-4: Soldered PCB**

<sup>23</sup> [www.reichelt.de](http://www.reichelt.de)

<sup>24</sup> [www.farnell.de](http://www.farnell.de)

<sup>25</sup> [www.conrad.de](http://www.conrad.de)

<sup>26</sup> [www.rsonline.de](http://www.rsonline.de)

<sup>27</sup> [www.multipcb.de](http://www.multipcb.de)

The manufacturer produces the tracks by chemically removing of the conduction copper and drills the holes and Vias (connection between layers) including all system checks.

The soldering of the components onto the board has been undertaken by a very experienced Compass-1 group member. Thereby the soldering activities have been shortened to some hours.

### **6.5 Software Design & Development**

The software coding is a big activity which can take much more energy from the coder as imagined. The software has the function to order the movements of the electrical hardware. By each turn of the coil mould the guidance should move a “step”. The drive mechanism of the winder is acting only to one side, whereas the stepping motor of the guidance is changing the direction for every layer. Such setups are defined with the software.

The software also needs to perform a record function of the wire forces during the winding. The record of these data needs some memory capacity, which influences the electrical design of the required hardware. Plenty choices represent the software languages: C, assembler or even Pascal can be used as software language. The most practical language is given with C and Assembler, depending on the software compiler.

The software for the coil winder is written completely in the computer language C with the AVR Studio whereas the software for the visualization and configuration of the board is running on a PC and is developed with Borland Delphi 7.0. The communication between the two software modules (ATMEL and PC) is realized by a RS232 serial interface.

The software development of the control unit took more time as scheduled concerning the complexity of this task. Different challenges e.g. the communication between the two software modules or the fine synchronization of the steppers needed more attention as expected.

The whole teamwork was a learning process with different errors, reasonable on the one hand from the understandings and on the other hand from the new experiences.

Anyway the software delay caused that the first experience of producing coils have been accomplished with manual winded coils.

The hand winding gave the opportunity for functionality tests of the coil winder for further modification activities.

## 7 Magnetorquer Production

The manual production of the coil will save general development time, so that other activities like the connection to the ADCS PCB are possible to analyse.

The coil winder has been modified with a crank arm for the manual fabrication of the coils.

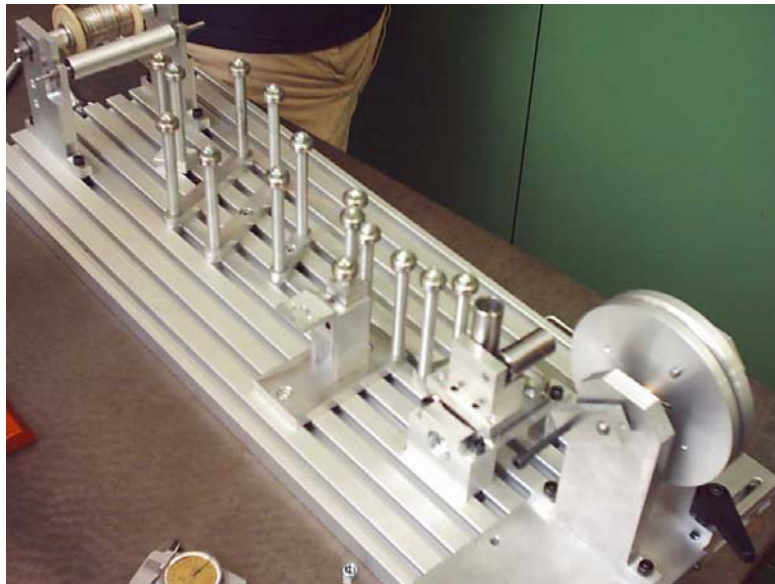


**Figure 7-1: Assembled coil winder without sensors**

After the assembly of the coil winder the coil material, the wire has been winded on the wire cover. With the manufacturing of the first manually wound coils, the analyses of the sensible fabrication has started.

### 7.1 Prototype

The first prototype of the coils was made by hand indeed with an accent that except of the guidance and the drive mechanism all units were used. The wire tensions have been increased by every new produced coil so that the wire-string-fixing possibilities are analysed in the beginning. The wire of the produced coils is made of bonding wire. This wire is able to connect every wire string with each other through the self bonding methods [7]. The self bonding of the coil is possible with two different methods. The first method requires solvent for the self bonding which increases the complexity of this feeding, where in contrast the second method requires the heating of the wire. The heating of the wire is established with the resistive self bonding method. The required subjects of this method are only an electrical supply unit and a thermal control unit. The prototype production has been analysed in the same time the increasing tension and the bonding dependencies. Therefore several coils have been winded with different winding tensions for the bonding analysis.



**Figure 7-2: Manual winded coil inside the coil mould**

This analysis describes the dependency of the needed power consumption for an inseparable connection of every wire. An inseparable connection of every wire is achieved by a bonding temperature, ranging from 160 °C to 190°C. Hence two target temperatures, firstly 110°C and later 160°C were investigated. A power supply unit with a working voltage of 115 V was in use. The next matrix displays the bonding results of seven manual winded coils, where the cooling down process was analysed also.



**Figure 7-3: Coil prototype Nr. I**

Winding character	Manual I	manual II	manual III	Unit
wire diameter	0,15	0,15	0,15	mm
number of turns	406	506	402	
mass	18,5	22,5	17,7	g
bonding voltage	78	78,8	78	V
bonding current	0,56	0,47	0,56	A
resistance	123,4	161,5	131,56	Ω
Room temp.	27,4	24,7	29,4	°C
max bonding temp	118,7	107,1	109,1	°C
bonding time	35	40	30	min
cool down time	60	40	35	min
cooling method	Freezer, -5	Freezer, -6	Freezer, -6	°C
bonding power	43,68	37,04	43,68	W
surface quality	<b>bad</b>	<b>o.k.</b>	<b>o.k.</b>	

**Table 7-1: Boning test result with low voltage supply**

Winding character	manual IV	manual V	manual VI	manual VII	Unit
wire diameter	0,15	0,15	0,15	0,15	mm
number of turns	400	405	400	400	
Mass	17,6	18,2	17,6	17,6	g
bonding voltage	110	95	110	110	V
bonding current	0,78	0,71	0,80	0,82	A
Resistance	124,72	122,67	124,43	122,52	$\Omega$
Room temp.	26,9	26,8	29,1	28,4	$^{\circ}\text{C}$
max bonding temp	163,4	134,4	160,7	161,4	$^{\circ}\text{C}$
bonding time	25	240 <sup>28</sup>	30	50 <sup>29</sup> 3	min
cool down time	45	40	50	30	min
cooling method	Air	Air	Air	MCU	$^{\circ}\text{C}$
bonding power	85,8	67,45	88	90,2	W
surface quality	good	good	good	very good	

Table 7-2: Bonding test results with high voltage supply

The matrix shows the dependency between the needed power and the different achievable bonding temperatures. The results show that the resistive self bonding method is working very well by high voltage supply and results at the recommended bonding temperature a high quality of bonded coils.



Figure 7-4: Cooling with MCU cooler

The cooling down method with two MCU cooler was efficient and very comfortable at the same time.

<sup>28</sup> =the coil mould was not placed correctly

<sup>29</sup> =bonding time included a constant bonding period of 30 minutes at 160 $^{\circ}\text{C}$

## 7.2 Coil Connection

Next to the production of coils, the electrical interface to the ADCS subsystem PCB has been designed. Many different connection types exist to connect the coils with the ADCS PCB. It gives the impression that the easiest and the fastest connection method should be the soldering of the copper wire directly onto the ADCS Board.

The technical feasibility of the connection extracts some requirements as follows:

- small connection size
- easy assembly
- one way polarization
- mechanically and electrically stable connection

The connection is solved in a satisfied way with plug-and-socket connection. The ADCS require a lot of electrical hardware on PCB with very limited space, therefore all electrical hardware has been selected as small as possible.

The contact between the cable and the ADCS PCB is established with special two-core SMT connectors [12], available from the supplier Farnell<sup>30</sup>.

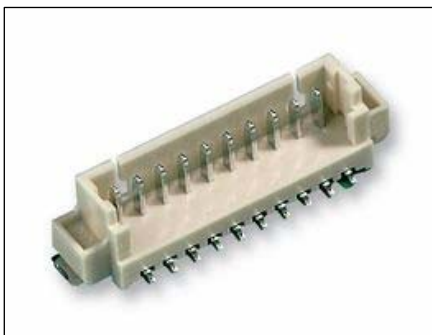


**Figure 7-5: Micro SMT multiway**

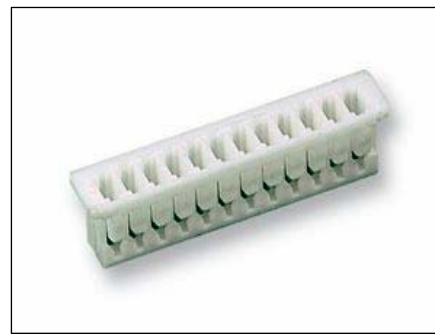


**Figure 7-6: SMT crimp connector housing**

This connector configuration requires crimped cable ends for a smooth required connection. It is not possible to crimp the sleeves directly with the copper wire therefore thicker cables are required. In consideration of the operating conditions Teflon cable is creating the best solution. Teflon or Polytetrafluoroethylene (PTFE) has the lowest coefficient of friction of any known solid material. The PTFE is non-reacting, have a non-stick surface and a melting point of about 327 °C[13] so that out gassing possibilities in vacuum conditions will be prevented. The Crimp contact guarantees on one hand that the isolation of the cable conducted in a mechanical robust way and in the other hand a simple and safe electrical interface. For the crimping of the wire connection a Crimp nipper is needed.

<sup>30</sup> <http://de.farnell.com>

Nevertheless varieties of crimped cable are available with an advisable price but not with Teflon isolation. The crimped cables from the producer Molex<sup>31</sup> are proper for the chosen SMT crimp connector housings and have been ordered from the supplier Farnell. The isolation of the cable is Nylon but with an operating temperature range of -40°C to 85°C, which is compatible for this operation. Independent from the isolation material the cable needs to be fixed with the copper wire. The twist of the copper wire around the bared cable provides a mechanical stabile connection next to the electrical connection. A soldering of both units combines the connection. The mechanical security against a wire break, caused from any traction is established with Kapton tape. This special tape is actually in the implementation similar to sellotape, which a huge contrast that sellotape is not properly for space application. Concerning the fixing method is the solder point coated with a Teflon tube

### 7.3 Results

The winding tensions have been increased by every new manual winded coil, resulting in a improvement of the quality. The differences are visible at the pictures of the winded coils in Figure 7-3 and figure 7-7. The best result was achieved with the last produced coil no. VII, which had a the highest winding tension and a bonding time of 50 minutes included a constant bonding period of 30 minutes at 160°C. The winding with high tension in combination with the long bonding time results in an upgrade of the stiffness which is advantageous in two ways. A stable produced coil will generate a more accurate magnetic field resulting in a better activation and will cause less problems at the general scheduled tests of the satellite specially the vibration tests.



**Figure 7-7: Produced coil Nr. VII**

---

<sup>31</sup> [www.molex.com](http://www.molex.com)

After the production of the coils the inductance and the resistance have been measured for the electrical specification. The inductances have been determined with an LCR Meter type Agilent 4284 A at different frequencies. The LCR Meter allows the determination of the inductance between 20 kHz and 1.0 MHz. The gage delivers also a measurement of the quality of the coil Q which is not decisive for the configuration of the coils. Where against the size of the inductance need to be determined precisely and implemented into the coil driver software, which is part of the ADCS main software.



Figure 7-8: LCR meter Agilent 4284

Winding character	manual I	manual II	manual III	Unit
wire diameter	0,15	0,15	0,15	mm
number of turns	406	506	402	--
Inductance Ls at 10 kHz	27,73	42,80	27,77	mH
Q	14,0	16,8	11,0	--
Inductance Ls at 100 kHz	39,72	71,79	31,99	mH
Q	39,5	39,4	38,4	--

Winding character	manual IV	manual V	manual VI	manual VII	Unit
wire diameter	0,15	0,15	0,15	0,15	mm
number of turns	400	405	400	400	--
Inductance Ls at 10 kHz	28,15	28,23	27,58	26,25	mH
Q	14,0	14,3	13,9	13,8	--
Inductance Ls at 100 kHz	35,64	34,24	34,18	31,78	mH
Q	59,1	66,8	62,5	63,7	--

Table 7-3: Inductance measurement results

The LCR Meter features the possibility to measure and record the inductance depending on the frequencies, so that also the eigenfrequency of the coil can be displayed. Such a record action has not been accomplished for these prototypes considering a drive of the coils with a Pulse-width modulation (PWM) signal of 10 kHz. The inductances of the

coils in this measurement area around 27mH. In spite of increasing the winding tensions shows the mechanical dimension of the coil an overrun of the limits.

Parameter	Symbol	Value	Limit	overflow
width	b [mm]	78	74	5.41 %
height	h [mm]	87	83	4.82 %
cross sectional width	d [mm]	2.1	2.1	0.00 %
cross sectional height	sh [mm]	7	5	40.0 %
mass of coils	Mc [g]	17.6	20.0	-12.0 %

Table 7-4: Prototype Nr. VII dimension

The cross sectional height overflow is forcing a modification of the coil mould which is explained in the next chapter.

## 8 Modification

### 8.1 Magnetorquer

The mechanical overload of the coil is justified from the manual winding of the magnetorquer. The space for the coil at the side plate of the cube is strictly limited, so that for a proper solution a meeting with the structure team for available space have been accomplished. This meeting had the function to determine the available space for imminent modifications. It has resulted that at the outer dimensions no changes can be managed but a change at the inside area with a total of 3 mm space for each side could be realizable. With the knowledge of manual produced coil it is assumed that the automated guidance will manage a better winding of the coils resulting in proper dimensions, but it is not possible to eliminate an overload of total 4 mm only with the proper guidance. The coil moulds have been modified within the scope of the manageable dimensions at the inside area of the side plate into a rectangular mould of 71 x 62 mm<sup>2</sup> which had a dimension of 73 x 64 mm<sup>2</sup> before.

This modification could delete 2 mm of the total overload where the rest will be eliminated with a very accurate guidance.

### 8.2 Coil Winder

The small modifications of the coil winder have resulted from the manual winding activities. The less modification of the coil winder shows that the design and production activities have been performed very well. Nevertheless the implemented transaction level could not be fixed precisely with the retaining rings. The integration of a screw thread at one side of the rod have able a precise and in the same time an easy calibration possibility of the transaction level, with a usual nut. The brake at the wire carrier unit could not fulfil the right function, therefore an adapter for a better torque transference has been integrated. The adapter allows a higher brake torque compared to the bare spring steel. The general winding activities show that the winding tensions for proper produced coils need to be as high as possible, which challenges the basic necessity of the force measuring unit. At this point it is to underline that alternating loads caused from the rectangular coil are existent. The force(s) measuring unit has been designed for additional verification of the tensions where the record about the high tension would display an interesting outcome and inspection. The measurement system of the force-measuring unit has been modified with the integration of an adapter onto the incremental driver for a smooth rotation. The used conventional spring was replaced by

a tension spring with the adequate stiffness. The modification of the coil winder comprised also the fabrication of the rack for the used stepping motor, which needs to be designed, drawn and produced, too.



**Figure 8-1: Modified Coil Winder**

## 9 Controlling Test

During the development time of the magnetorquer, the question about the right inspection method of the designed magnetorquer has been initialised. The verification of the produced mechanical torque of the coils has required an external magnetic field. The geomagnetic field on the earth surface shows a very low value for this kind of measuring.

At the physic laboratory Helmholtz coils in different sizes with adequate Tesla-Meter are available for this function. The gage allows the measurement of the generated (almost) homogeneous magnetic field.

### 9.1 Oscillation Test

Measuring the mechanical torque of the magnetorquers is a time-consuming/intricate procedure. Hence, instead of applying this method, a phenomenon related to the mechanical torque is experimentally investigated. This mechanical torque results in an oscillating motion of a coil suspended in an external homogeneous magnetic field generated by a Helmholtz coil pair, which will be analysed in the following oscillation test.

The coil is adjusted in order to achieve a low mounting stiffness of the oscillating system, whereas the oscillation period is measured by a photoelectric barrier.

The primary function of the oscillation test is the analysis of the generated magnetic moment depending on the number of turns and the current flow in the magnetorquer.

The accuracy of the test results obtained by an experimentally appointed, physical dimension of the generated magnetic moment is extraordinary. To generate such accuracy in an experiment, the mathematical concept needs to be set up first of all.

### 9.1.1 Mathematical Concept

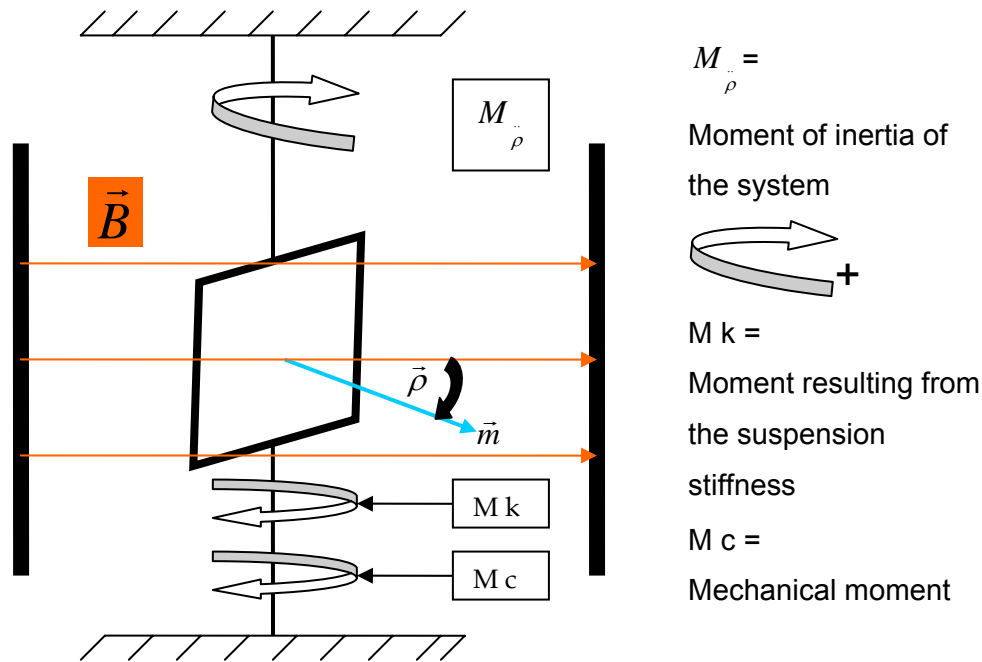


Figure 9-1: Dynamical test setup with current flow in the coil

The relationship between the external torque and the angular acceleration is of the same kind as Newton's second law. This is why it is sometimes called Newton's second law for rotation. They differentiate by a less linear relationship than usual because the moment of inertia is not strictly a scalar quantity. The moment of inertia ( $I_{x,y}$ ) is the name given to rotational inertia, the rotational analogy of mass for linear motion. They are related in the same way as the dynamics of rotational motion. The moment of inertia must be specified with respect to a chosen axis of rotation.[14]

$$\sum M = I_{x,y} \cdot \ddot{\rho} \tag{1}$$

The external torque in the dynamical test is the result of the sum of the mechanical torque arising from the current flow within the copper coil and the mechanical torque resulting from suspension stiffness.

$$\vec{M}_c + \vec{M}_k = \vec{M}_{\rho} \tag{2}$$

The strained wire at both ends of the coil becomes twisted in the activated system and reacts with a reverse torque. (Inside the area of validity) Within the range of Hook's law this reverse torque shows proportionality to the twisting angle.

$$M_k = -k_{\rho} \cdot \rho \tag{3}$$

The constant dimension  $k_\rho$  describing the stiffness of the strained wire is mostly called “Direktionsmoment”. The mechanical torque  $\vec{M}_c$  resulting from the Cartesian product of the magnetic moment of the copper coil together with the external magnetic field is shown in Figure 9-1.

$$\vec{M}_c = \vec{m} \times \vec{B} \rightarrow M_c = -m \cdot B \cdot \sin \rho \quad (4)$$

The depicted equation is described as:

$$-m \cdot B \cdot \sin \rho - k\rho \cdot \rho = I_{x,y} \cdot \ddot{\rho} \quad (5)$$

For harmonic oscillation the *move* angle needs to average out  $5^\circ$ , therefore the expression  $\sin \rho$  is reduced to  $\rho$ .

$$\sin \rho \approx \rho \quad (\rho < 5^\circ ; 15^\circ) \quad (5.1)$$

$$-(m \cdot B + k\rho) \cdot \rho = I_{x,y} \cdot \ddot{\rho} \quad (5.2)$$

Harmonic oscillation can be expressed as:

$$\rho_{(t)} = A \cdot \sin(\varpi \cdot t + \rho_0)$$

The cycle starting conditions of the oscillation test is integrated with the dimension  $\rho_0$ , in this test defined by  $\rho_0 = 0$ . The angular acceleration of harmonic oscillation is shown in the following formula:

$$\ddot{\rho}_{(t)} = -\omega^2 \cdot \rho_{(t)}$$

When inserted into the torque equation (5.2) the *move angle* is eliminated.

$$-(m \cdot B + k\rho) \cdot \rho = -I_{x,y} \cdot \omega^2 \cdot \rho \quad (5.3)$$

The measured magnetic moment is calculated with the following expression.

$$m = \frac{(I_{x,y} \cdot \omega^2 - k\rho)}{B} \quad (5.4)$$

### 9.1.2 Setup

Before the magnetorquer oscillation test is accomplished, the four coils are set up for the test. First of all, every test coil is weighed and all physical measures are documented for further analyzing aspects. The coils are suspended in their center of gravity and are positioned in the suspension frame shown in Figure 9-2 & Figure 9-3.

The external magnetic field is simulated by Helmholtz coils, which generates a magnetic flux density the size of up to 40 times of the earth's magnetic field at sea level (Figure9-8).

In order to get an oscillation the coil are activated from its basic position. The oscillation periods are influenced by coils suspension and air friction [14]. In order to achieve a low mounting stiffness the coil is positioned very tightly in the suspension framework. However, the suspension stiffness has to be determined experimentally and separately for every coil. The air friction can be reasonably neglected owing to its very small size.

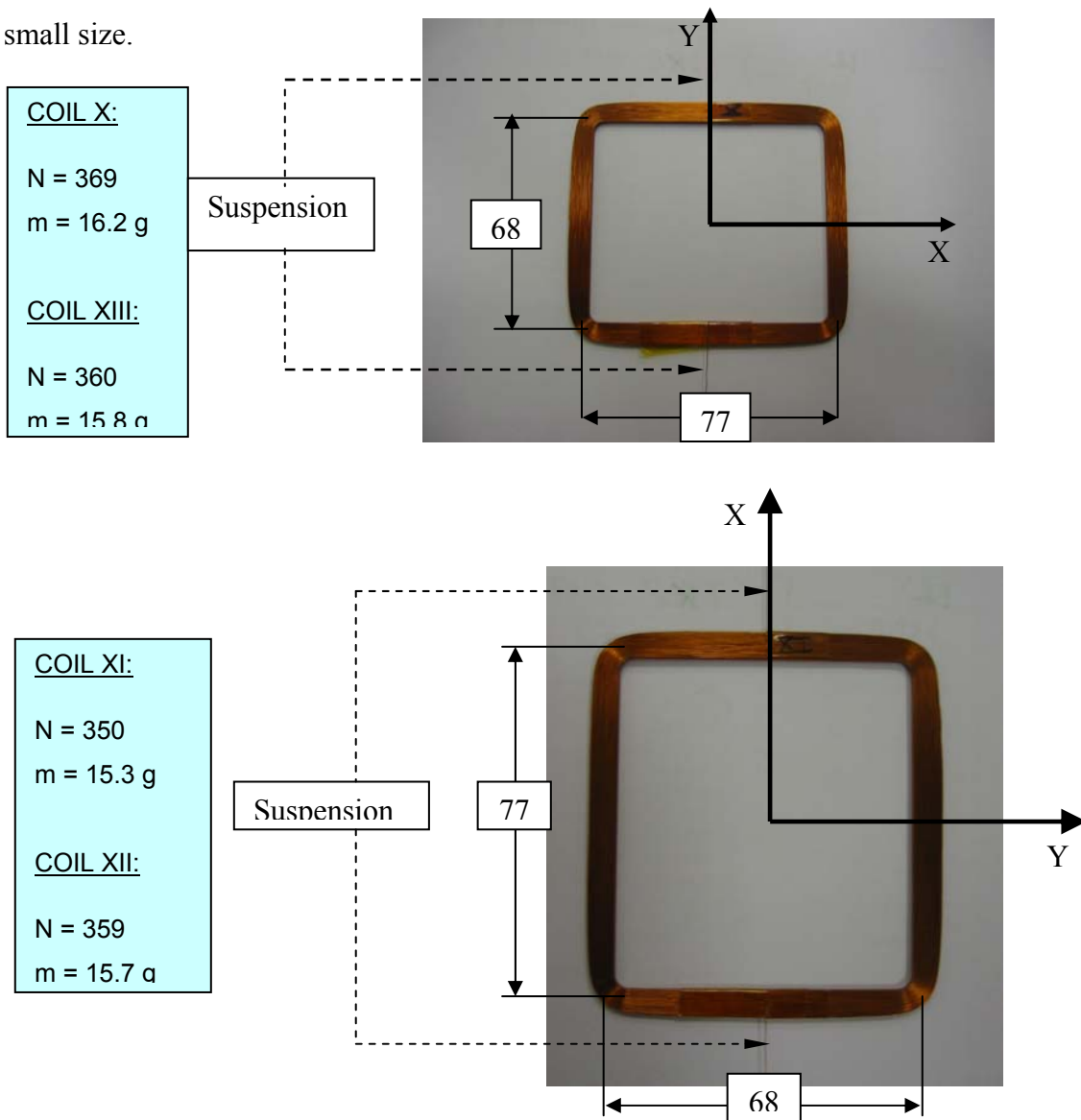


Figure 9-2: Suspension disposition of coils

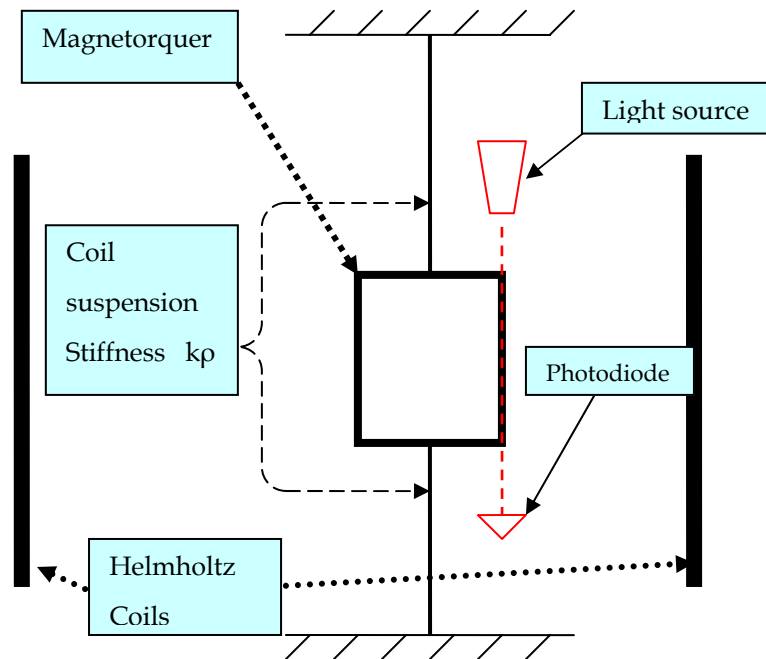
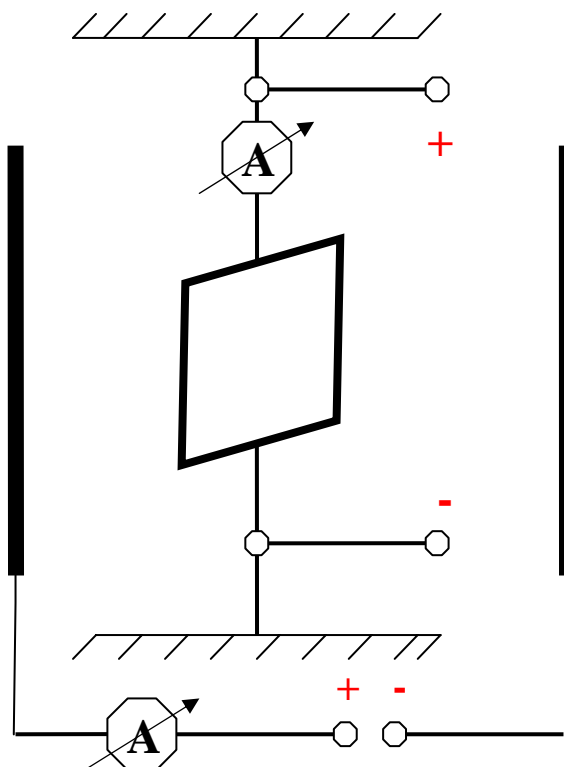


Figure 9-3: Schematic suspension setup

### Electrical Setup

In order to enable the electrical supply both ends of the coil are soldered on a connector which is interfaced with the test frame. The external magnetic field is generated by a constant current supply of 3.5A; this results in a field intensity of up to 40 times compared to the Earth's magnetic field intensity.



Magnetorquer  
current = 0 - 60 mA

Helmholtz coils  
current = 3.50 A

Figure 9-4: Electrical setup

### 9.1.3 Preparation of Equipment

After the test installation is set up the measurement instruments need to be added.

For the purpose of measuring the oscillation period a light barrier are implemented into the coil suspension frame. The light barrier is divided into two main hardware components: a laser source and a photodiode connected to a timer.

Two power supply units are in use, one for the magnetorquer supply and one for the external Helmholtz coils supply. In addition two multimeter (Voltcraft, VC 120 & VC 880) for the corresponding current flow measurements are arranged in serial connection.

Before starting the test, the suspended coil is balanced in an equilibrium position

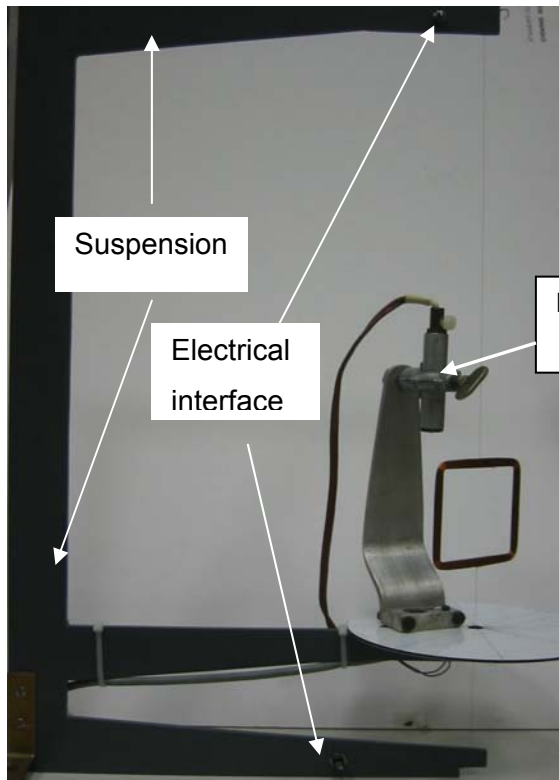


Figure 9-5: Frame position setup

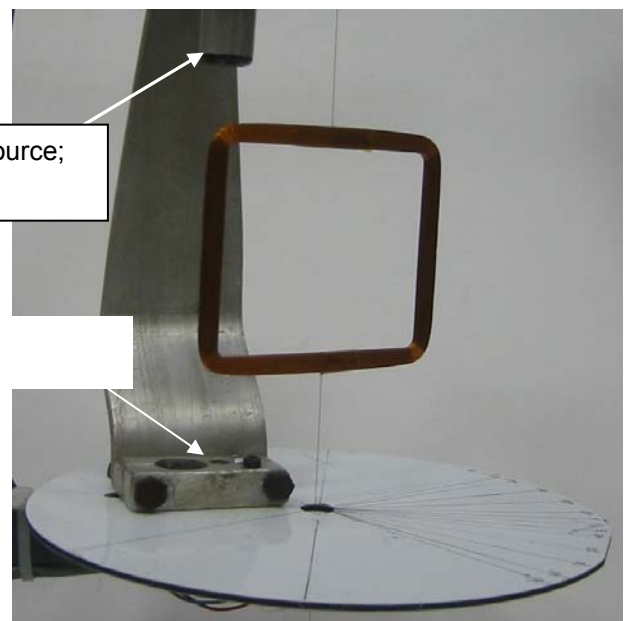
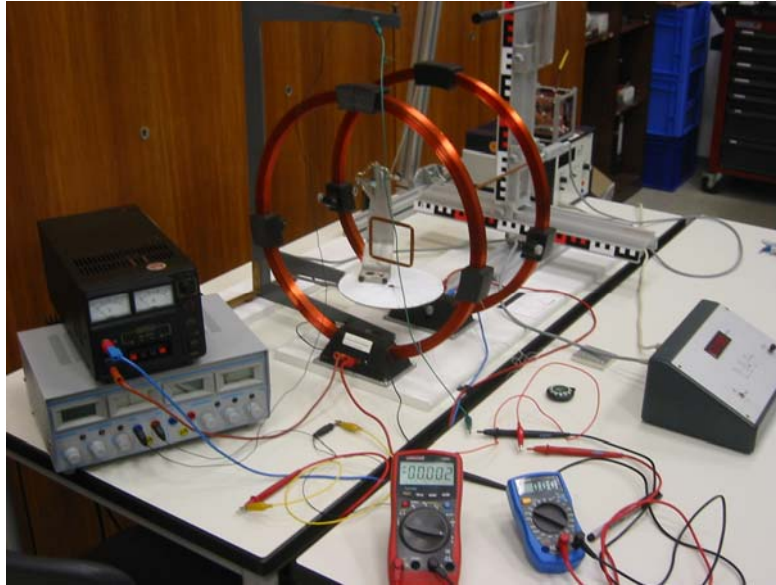


Figure 9-6: Suspended coil



Figure 9-7: Oscillation dial gauge



**Figure 9-8: Test setup**

To minimize the error modes of the oscillation test several requirements need to be in focus during the test. The external Helmholtz coils are getting warm during the operation, therefore the current flow need to be matched to a constant 3.5 A. The resulting magnetic field intensity of the Helmholtz coils is approximately 2.49 mT – 2.56 mT. The heating of the magnetorquer can be neglected because of the very low current flow, and the relative short operation time. The test conditions of every coil oscillation measurement should be constant.

#### **9.1.4 Conduction of Test**

Once the single coil is in rest position, the measurement, which is divided into 2 stages, can be started. The first stage of the measurement describes the influences of the coil suspension stiffness and the second measurement describes the oscillation of the magnetorquer with constant current supplies. To further analyze the second dependency of the magnetic moment, the test coils are wound with different number of turns.

The first oscillation period is measured without electrical supply of the coils, therefore to obtain the stiffness of the suspended coil. The amplitude of this oscillation can be selected arbitrarily within practical limits, but the amplitude of the oscillation with current supply should be in the area of about  $15^\circ$ , actually less than  $5^\circ$  when considering the mathematical simplification of  $\sin \rho = \rho$ . To minimize the error of the light barrier, the oscillation period is given as an average period resulting from ten separate oscillation periods.

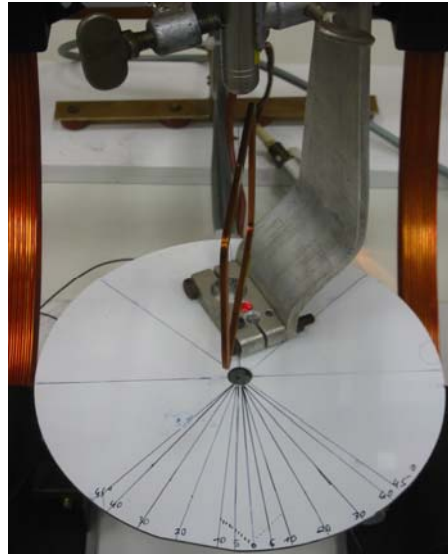


Figure 9-9: Excited coil during oscillation

### 9.1.5 Results

The test coils are labeled with increasing roman numbers, starting with the produced coils from the beginning of the coil production for this project.

The moment of inertia is determined separately for every coil with the CAD software Catia V5. For these determinations the average exterior area and the volume of every coil is held constant as  $A = 5205 \text{ mm}^2$  or  $3524 \text{ mm}^3$ . Four magnetorquers are tested, each with a different number of turns. Considered a constant volume for each magnetorquer, the different number of turns results in different volume densities, which are considered in the moment of inertia determinations with the CAD software. The results are explained in detail in coil X. The remaining results are analyzed in an analogous manner. At the end of this chapter the results of all coils are presented.

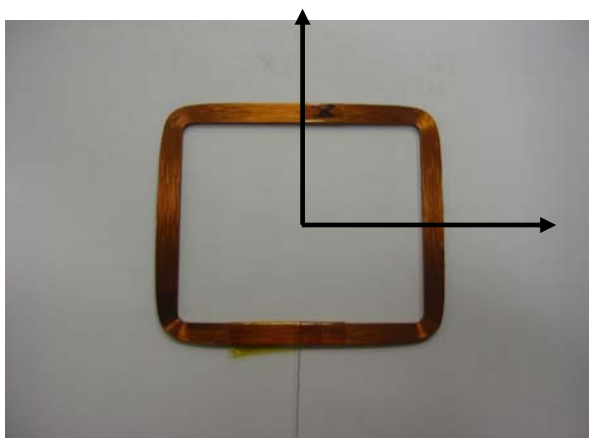


Figure 9-10: Magnetorquer



Figure 9-11: Average exterior area

Coil Nr.:	X				
moment of inertia	$I_x$ [E-05 kgm <sup>2</sup> ]	1,26955			
	$I_y$ [E-05 kgm <sup>2</sup> ]	1,52352			
number of turns	N	369			
current	I [mA]	free oscillation	20	40	60
	oscillation period				
	T1 [msec.]	5443,7	2249,3	1640,6	1394,2
	T2 [msec.]	5421,7	2251,6	1640	1394,4
	T3 [msec.]	5442	2245,9	1649,2	1397
	T4 [msec.]	5427,2	2250,3	1645,1	1396,6
	T5 [msec.]	5424,8	2239,4	1647,1	1392,1
	T6 [msec.]	5432,7	2239,1	1647	1394,7
	T7 [msec.]	5417,7	2234,6	1644,4	1396,1
	T8 [msec.]	5428,2	2238,8	1642,1	1395,7
	T9 [msec.]	5431,4	2238,1	1642,7	1394
	T10 [msec.]	5421,7	2239,5	1644	1393,6
	T average [sec]	5,429	2,243	1,644	1,395
ext.magnetic field intensity	B [E-03T]	0	2,55	2,55	2,55
suspension stiffness	k [E-05 Nm]	2,0406			
determined magn. moment	$m^*$	0	3,889	7,924	11,323
$m=NIA$	$m$	0	3,841	7,683	11,524
(relative) error	$ \Delta m $	0,00%	1,25%	3,15%	1,74%

Table 9-1: Oscillation results coil X

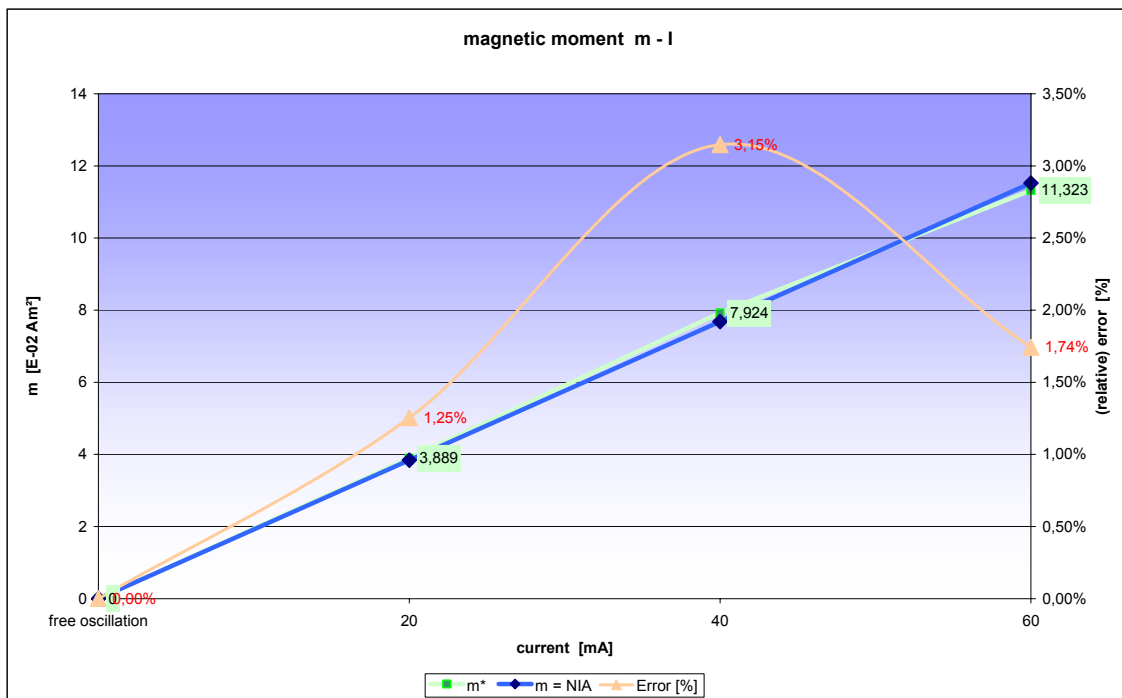


Figure 9-12: Magnetic moment analogy of coil X

Coil Nr.:		XI			
moment of inertia	lx [E-05 kgm <sup>2</sup> ]	1,19896			
	ly [E-05 kgm <sup>2</sup> ]	1,43881			
number of turns	N	350			
current oscillation period	I [mA]	free oscillation	20	40	60
	T1 [msec.]	4350	2007,3	1486,1	1280,3
	T2 [msec.]	4343	2005,4	1484	1285,9
	T3 [msec.]	4335,7	2001,7	1484,5	1283,5
	T4 [msec.]	4332,3	2003,8	1484,6	1281,5
	T5 [msec.]	4332,3	2002,6	1483,3	1280,3
	T6 [msec.]	4331,1	2004,5	1483,1	1279,8
	T7 [msec.]	4334,8	2004,5	1481,8	1278,6
	T8 [msec.]	4327,4	2004,9	1482	1278,1
	T9 [msec.]	4328,5	2003,6	1482,3	1277,3
	T10 [msec.]	4327,1	2003,7	1483	1276
T average [sec]	4,3342	2,0042	1,4835	1,2801	
ext.magnetic field intensity	B [E-03T]	0	2,55	2,55	2,55
suspension stiffness	k [E-05 Nm]	2,5197			
determined magn. moment	m*	0	3,633	7,447	10,339
m=NIA	m	0	3,6435	7,2870	10,9305
(relative) error	$ \Delta m^*/m  / 100\%$	0,00%	0,29%	2,19%	5,41%

Table 9-2: Oscillation results coil XI

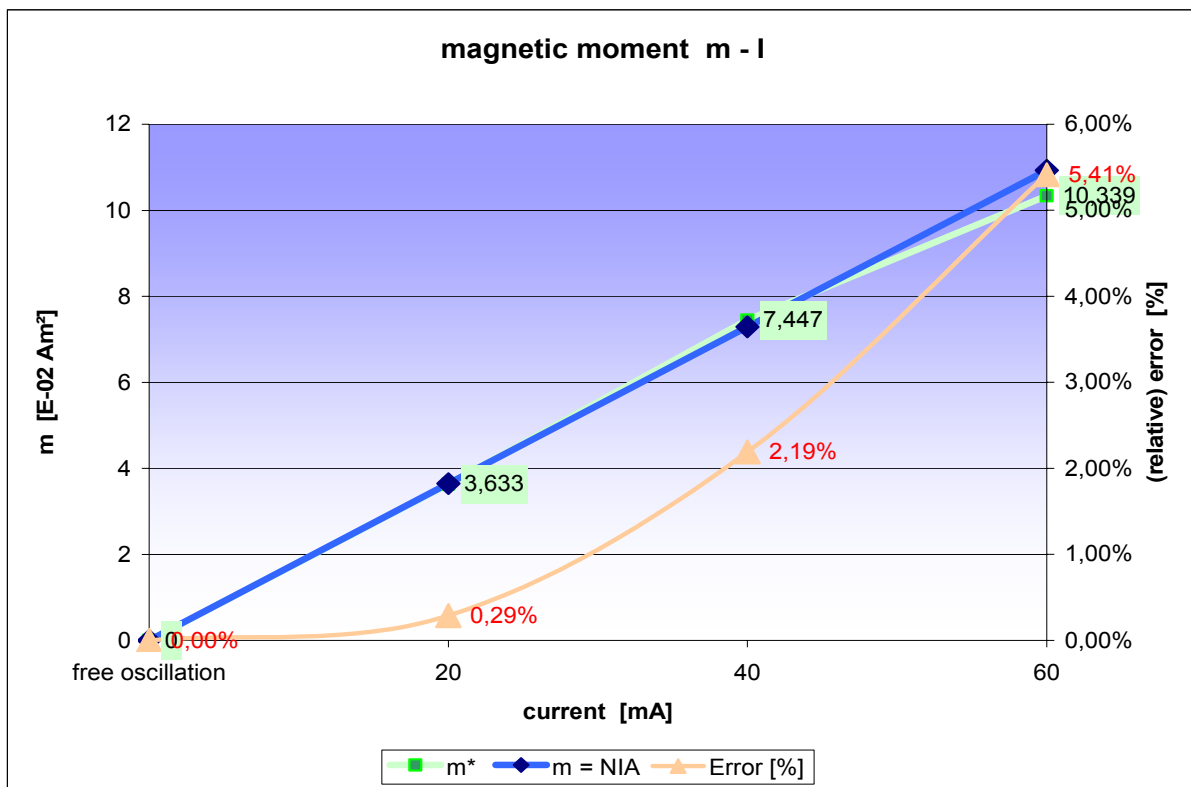


Figure 9-13: Magnetic moment analogy of coil XI

Coil Nr.:	XII				
moment of inertia	lx [E-05 kgm <sup>2</sup> ]	1,23031			
	ly [E-05 kgm <sup>2</sup> ]	1,47643			
number of turns	N	359			
current oscillation period	I [mA]	free oscillation	20	40	60
	T1 [msec.]	5535,5	2092,7	1525,3	1280,6
	T2 [msec.]	5538,5	2088,6	1524,5	1280,1
	T3 [msec.]	5542,2	2092,4	1522,3	1279,8
	T4 [msec.]	5542,9	2085,5	1522,7	1281,8
	T5 [msec.]	5534,6	2086,3	1523,3	1279,1
	T6 [msec.]	5537,8	2086,7	1524,1	1280,9
	T7 [msec.]	5540,9	2084,5	1524,8	1281,6
	T8 [msec.]	5539,7	2085,9	1523,6	1281,9
	T9 [msec.]	5537,5	2083,8	1521,8	1280,6
	T10 [msec.]	5535,9	2084,4	1522,3	1280,1
	T average [sec]	5,5386	2,0871	1,5235	1,2807
ext.magnetic field intensity	B [E-03T]	0	2,55	2,55	2,55
suspension stiffness	k [E-05 Nm]	1,5834			
determined magn. moment	m*	0	3,752	7,586	10,993
m=NIA	m	0	3,7372	7,4744	11,2116
(relative) error	$ \Delta m^*/m /100\%$	0,00%	0,39%	1,49%	1,95%

Table 9-3: Oscillation results coil XII

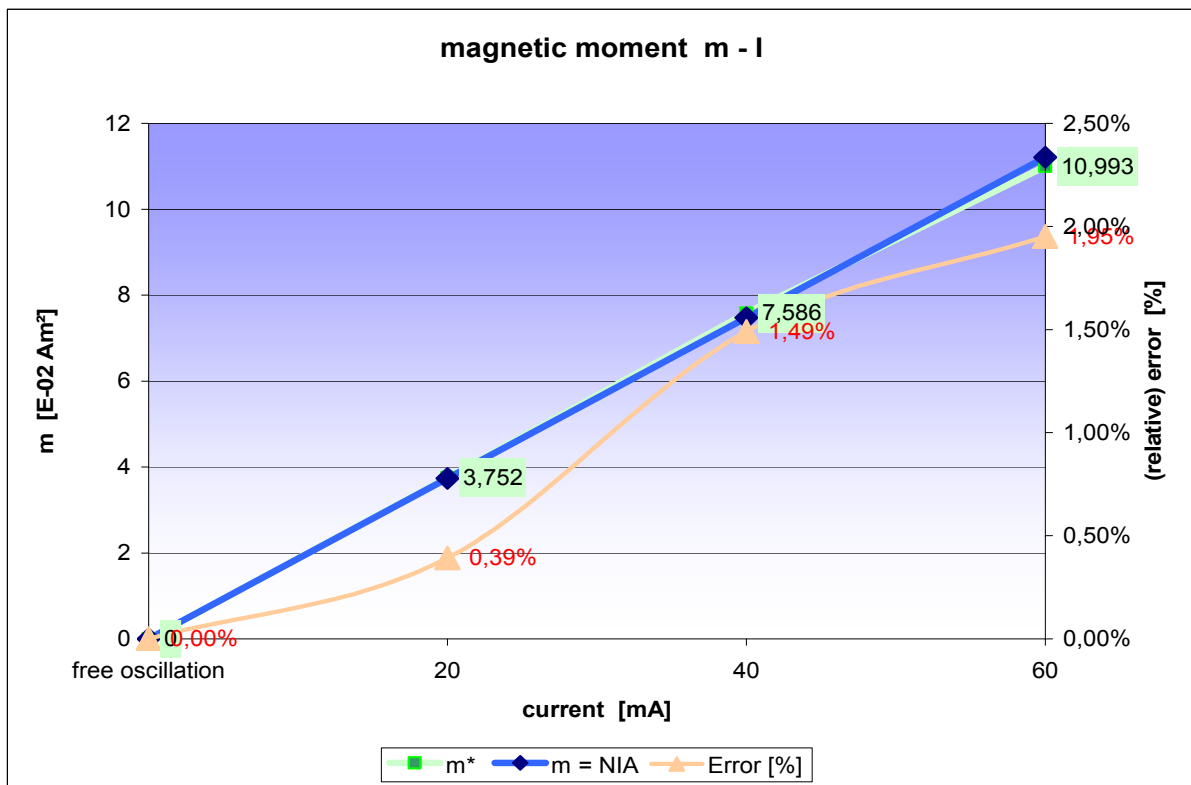


Figure 9-14: Magnetic moment analogy of coil XII

Coil Nr.:	XIII				
moment of inertia	$I_x$ [E-05 kgm <sup>2</sup> ]	1,23815			
	$I_y$ [E-05 kgm <sup>2</sup> ]	1,48584			
number of turns	N	360			
current oscillation period	I [mA]	free oscillation	20	40	60
	T1 [msec.]	5310,9	2219,9	1677,2	1402,9
	T2 [msec.]	5301,7	2218,9	1678,7	1404,7
	T3 [msec.]	5298,9	2216,9	1677,8	1402,7
	T4 [msec.]	5296,6	2218,3	1677,9	1403,4
	T5 [msec.]	5298,3	2218,5	1678,7	1401,7
	T6 [msec.]	5299,1	2218,2	1678	1403,1
	T7 [msec.]	5289,1	2218,2	1678,2	1401,9
	T8 [msec.]	5294,1	2217,9	1678,9	1403,3
	T9 [msec.]	5289,5	2218,5	1678,3	1401,5
	T10 [msec.]	5274,2	2218,1	1678,9	1403,2
T average [sec]	5,2952	2,2183	1,6783	1,4028	
ext.magnetic field intensity	B [E-03T]	0	2,5	2,5	2,5
suspension stiffness	k [E-05 Nm]	2,0920			
determined magn. moment	$m^*$	0	3,931	7,494	11,086
$m=NIA$	$m$	0	3,7476	7,4952	11,2428
(relative) error	$ \Delta m^*/m /100\%$	0,00%	4,90%	0,02%	1,40%

Table 9-4: Oscillation results coil XIII

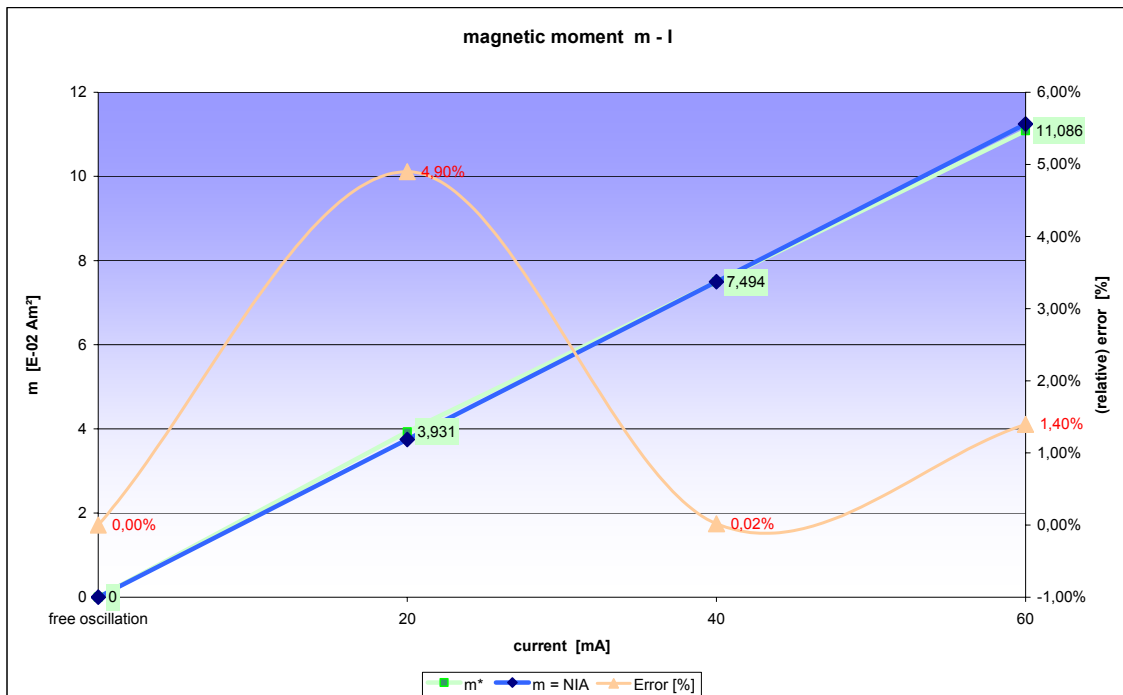


Figure 9-15: Magnetic moment analogy of coil XIII

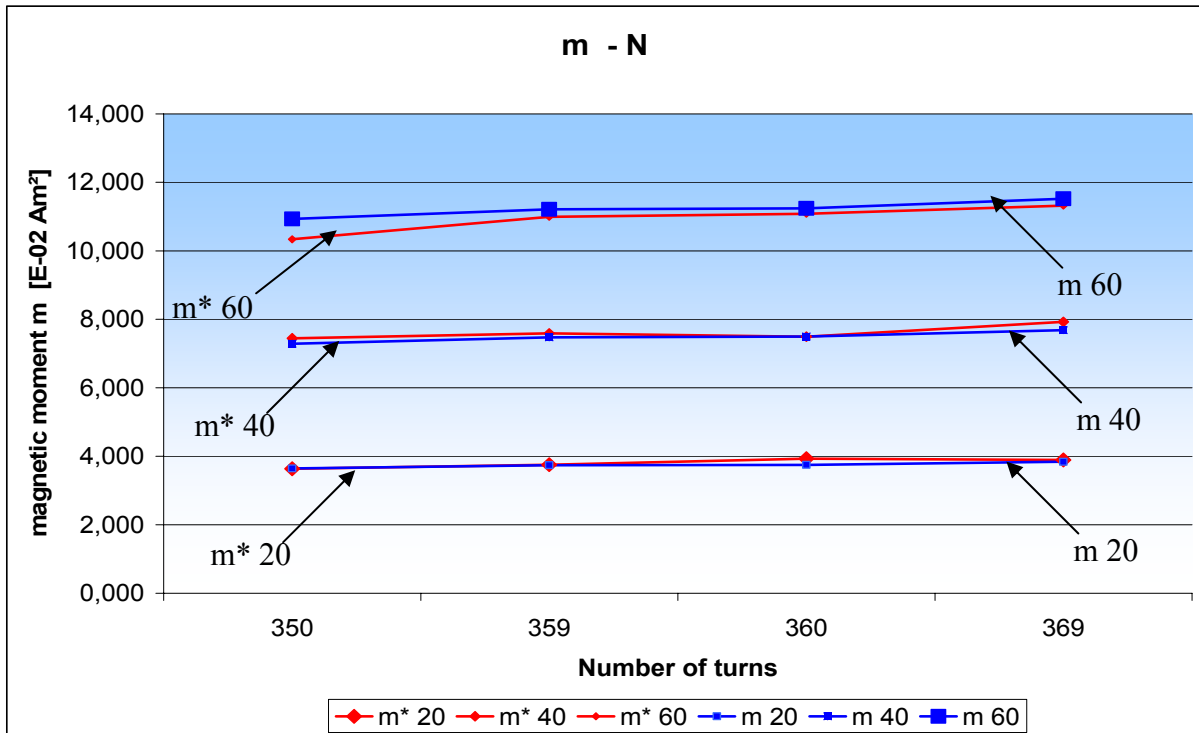


Figure 9-16: Magnetic moment depending on number of turns

### 9.1.6 Error Analysis

The measurements contain a number of error sources, as usual for physical tests.

Random errors occurring during the test series, e.g. static errors and system errors are caused by the used measurement hardware and their exactness. The error analysis is based on the equation describing the magnetic moment.

$$m = \frac{(I_{x,y} \cdot \omega^2 - k\rho)}{B}$$

The total maximum error of each influence has been calculated and is shown in details in tables five, six and seven. In the end a detailed error analysis of the determined magnetic moment of the coil X will be given.

#### Measuring Hardware:

- Voltcraft VC 120 used for the current supply of the Helmholtz coils
- Voltcraft VC 860 used for the current supply of the magnetorquer
- Period timer

#### Accuracies of the hardware:

- Voltcraft VC 120 for DC current supply in the measurement range  
10 A ±(2.0%+5dgt) [15]
- Voltcraft VC 860 for DC current supply in the measurement area  
400mA ±(0.80%+10dgt) [16]
- Tesla Digital Multimeter error  
 $\frac{\Delta B}{B} = \pm 2.0\%$  [17]
- Period time clock deviation determined by the average period time

- Suspension stiffness deviation determined by the average stiffness
- Moment of inertia deviation determined mainly by the weight error

	$\Delta T \times 0$	$\Delta T \times 20$	$\Delta T \times 40$	$\Delta T \times 60$	Unit
$(T_{\text{mittel}} - T_1)^2$	212.87	44.09	13.10	0.41	msec <sup>2</sup>
$(T_{\text{mittel}} - T_2)^2$	54.91	79.92	17.81	0.19	msec <sup>2</sup>
$(T_{\text{mittel}} - T_3)^2$	166.15	10.50	24.80	4.67	msec <sup>2</sup>
$(T_{\text{mittel}} - T_4)^2$	3.65	58.37	0.77	3.10	msec <sup>2</sup>
$(T_{\text{mittel}} - T_5)^2$	18.58	10.63	8.29	7.51	msec <sup>2</sup>
$(T_{\text{mittel}} - T_6)^2$	12.89	12.67	7.73	0.02	msec <sup>2</sup>
$(T_{\text{mittel}} - T_7)^2$	130.19	64.96	0.03	1.59	msec <sup>2</sup>
$(T_{\text{mittel}} - T_8)^2$	0.83	14.90	4.49	0.74	msec <sup>2</sup>
$(T_{\text{mittel}} - T_9)^2$	5.24	20.79	2.31	0.71	msec <sup>2</sup>
$(T_{\text{mittel}} - T_{10})^2$	54.91	9.99	0.05	1.54	msec <sup>2</sup>
$\Sigma 1/n (T_{\text{mittel}} - T_i)^2$	66.02	32.68	7.94	2.05	msec <sup>2</sup>
$\pm \Delta T = (\Sigma)^{1/2}$	8.13	5.72	2.82	1.43	msec
$3 \Delta T$	24.38	17.15	8.45	4.29	msec
$\Delta T / T$	0.15 %	0.25 %	0.17 %	0.10 %	

**Table 9-5: Period time clock deviation**

$\omega$	2.80	3.82	4.50	1/sec.
$\Delta \omega_1^2$	6.84 E-05	7.11 E-05	4.28 E-06	(1/sec.) <sup>2</sup>
$\Delta \omega_2^2$	1.24 E-04	9.67 E-05	2.02 E-06	(1/sec.) <sup>2</sup>
$\Delta \omega_3^2$	1.63 E-05	1.33 E-04	4.85 E-05	(1/sec.) <sup>2</sup>
$\Delta \omega_4^2$	9.05 E-05	4.18 E-06	3.22 E-05	(1/sec.) <sup>2</sup>
$\Delta \omega_5^2$	1.66 E-05	4.46 E-05	7.86 E-05	(1/sec.) <sup>2</sup>
$\Delta \omega_6^2$	1.98 E-05	4.16 E-05	2.04 E-07	(1/sec.) <sup>2</sup>
$\Delta \omega_7^2$	1.02 E-04	1.75 E-07	1.65 E-05	(1/sec.) <sup>2</sup>
$\Delta \omega_8^2$	2.33 E-05	2.43 E-05	7.70 E-06	(1/sec.) <sup>2</sup>
$\Delta \omega_9^2$	3.26 E-05	1.25 E-05	7.37 E-06	(1/sec.) <sup>2</sup>
$\Delta \omega_{10}^2$	1.56 E-05	2.62 E-07	1.61 E-05	(1/sec.) <sup>2</sup>
$\Sigma 1/n (\omega_{\text{mittel}} - \omega_i)^2$	5.09 E-05	4.29 E-05	2.14 E-05	(1/sec.) <sup>2</sup>
$\Delta \omega = (\Sigma)^{1/2}$	7.14 E-03	6.55 E-03	4.62 E-03	1/sec.
$\Delta \omega / \omega$	0.25 %	0.17 %	0.10 %	

**Table 9-6: Angular velocity deviation**

$k_1$	2.0296	E-05 Nm	$(k_{\text{mittel}} - k_1)^2$	1.20 E-04
$k_2$	2.0461	E-05 Nm	$(k_{\text{mittel}} - k_2)^2$	3.10 E-05
$k_3$	2.0309	E-05 Nm	$(k_{\text{mittel}} - k_3)^2$	9.35 E-05
$k_4$	2.0420	E-05 Nm	$(k_{\text{mittel}} - k_4)^2$	2.02 E-06
$k_5$	2.0438	E-05 Nm	$(k_{\text{mittel}} - k_5)^2$	1.04 E-05
$k_6$	2.0379	E-05 Nm	$(k_{\text{mittel}} - k_6)^2$	7.34 E-06
$k_7$	2.0492	E-05 Nm	$(k_{\text{mittel}} - k_7)^2$	7.38 E-05
$k_8$	2.0413	E-05 Nm	$(k_{\text{mittel}} - k_8)^2$	4.50 E-07
$k_9$	2.0338	E-05 Nm	$(k_{\text{mittel}} - k_9)^2$	3.01 E-06
$k_{10}$	2.0461	E-05 Nm	$(k_{\text{mittel}} - k_{10})^2$	3.10 E-05
$k_{\text{mittel}} = (\sum 1/n k_i)$	2.0406	E-05 Nm	$\Delta k^2$	3.72 E-05
$\pm \Delta k = (\sum 1/n \Delta k^2)^{1/2}$	0.00610	E-05 Nm		
$\Delta k / k$	0.30 %			

**Table 9-7: Stiffness deviation**

The error analysis is based on equation 5.4, affiliated in chapter “mathematical concept”

$$m = \frac{(I_{x,y} \cdot \omega^2 - k\rho)}{B} \quad (6.0)$$

The equation is replaced by two terms in order to simplify the analysis

$$a = \frac{(I_{x,y} \cdot \omega^2)}{B} \quad \& \quad b = \frac{-k\rho}{B} \quad (6.1) \ \&$$

$$(6.2)$$

The absolute error of the substituted term “a” is determined with the partially differentiation of each influence.

$$\Delta a = \pm \left( \left| \frac{\partial m}{\partial I_{x,y}} \cdot \Delta I_{x,y} \right| + \left| \frac{\partial m}{\partial B} \cdot \Delta B \right| + \left| \frac{\partial m}{\partial \omega} \cdot \Delta \omega \right| \right) \quad (6.1.1)$$

Application of the equation 6.1

$$\Delta a = \pm \left| \frac{\omega^2}{B} \cdot \Delta I_{x,y} \right| + \left| \frac{I_{x,y} \cdot 2 \cdot \omega}{B} \cdot \Delta \omega \right| + \left| -\frac{(I_{x,y} \cdot \omega^2)}{B^2} \cdot \Delta B \right| \quad (6.1.2)$$

The absolute error of the substituted term **b** is determined in the same way as before.

$$\Delta b = \pm \left| \frac{\partial m}{\partial k_\rho} \cdot \Delta k_\rho \right| + \left| \frac{\partial m}{\partial B} \cdot \Delta B \right| \quad (6.2.1)$$

$$b = \frac{-k\rho}{B} \quad (6.2)$$

Application of the equation 6.2

$$\Delta b = \pm \left| -\frac{1}{B} \cdot \Delta k_{\rho} \right| + \left| \frac{k_{\rho}}{B^2} \cdot \Delta B \right| \tag{6.2.2}$$

Addition of both substituted terms “a” and “b”, results in the absolute maximum error of m.

$$m = a + b \quad ; \quad \text{absolute maximum error } \Delta m = \Delta a + \Delta b$$

$$\text{Relative maximum error } \frac{\Delta m}{m} = \frac{(\Delta a + \Delta b)}{m} \tag{6.3}$$

$$\Delta m = \left| \frac{\omega^2}{B} \cdot \Delta I_{x,y} \right| + \left| \frac{I_{x,y} \cdot 2 \cdot \omega}{B} \cdot \Delta \omega \right| + \left| -\frac{(I_{x,y} \cdot \omega^2)}{B^2} \cdot \Delta B \right| + \left| -\frac{1}{B} \cdot \Delta k_{\rho} \right| + \left| \frac{k_{\rho}}{B^2} \cdot \Delta B \right| \tag{6.3.1}$$

The term 6.3.1 is transferred into a excel sheet in order to simplify the analysis of the remaining coils.

$$\Delta m \quad \pm (\omega^2/B)\Delta I \quad + \quad ((2 I \omega)/B) \Delta \omega \quad + \quad I^2 \omega^2 \cdot (\Delta B/B^2) \quad + \quad (1/B) \Delta k \quad + \quad (k/B) \cdot (\Delta B/B)$$

$$\pm (4 \cdot \pi^2 / T^2 B) \Delta I \quad + \quad (4 \cdot \pi \cdot I / T \cdot B) \Delta \omega \quad + \quad (I^2 \omega^2 / B) \cdot (\Delta B/B) \quad + \quad (1/B) \Delta k \quad + \quad (k/B) \cdot (\Delta B/B)$$

						$\Delta m$		$\Delta m/m \cdot 100\%$
$\Delta m$ 20	0,0469	+	0,0239	+	0,0938	+	0,0024	+ 0,0160 = 0,1830 E-02 Am <sup>2</sup> 4,70%
$\Delta m$ 40	0,0872	+	0,0299	+	0,1745	+	0,0024	+ 0,0160 = 0,3100 E-02 Am <sup>2</sup> 3,91%
$\Delta m$ 60	0,1212	+	0,0249	+	0,2425	+	0,0024	+ 0,0160 = 0,4070 E-02 Am <sup>2</sup> 3,59%

Table 9-8: Maximum absolute and relative error coil X

						$\Delta m$		$(\Delta m / m) \cdot 100\%$
$\Delta m$ 20	4,62E-02	+	6,73E-03	+	9,24E-02	+	3,14E-03	+ 1,98E-02 = 0,1683 E-02 Am <sup>2</sup> 4,63%
$\Delta m$ 40	8,43E-02	+	1,45E-02	+	1,69E-01	+	3,14E-03	+ 1,98E-02 = 0,2904 E-02 Am <sup>2</sup> 3,90%
$\Delta m$ 60	1,13E-01	+	4,27E-02	+	2,27E-01	+	3,14E-03	+ 1,98E-02 = 0,4054 E-02 Am <sup>2</sup> 3,92%

Table 9-9: Maximum absolute and relative error Coil XI I

						$\Delta m$		$(\Delta m / m) \cdot 100\%$
$\Delta m$ 20	4,37E-02	+	1,27E-02	+	8,75E-02	+	6,04E-04	+ 1,24E-02 = 0,1569 E-02 Am <sup>2</sup> 4,18%
$\Delta m$ 40	8,21E-02	+	1,22E-02	+	1,64E-01	+	6,04E-04	+ 1,24E-02 = 0,2714 E-02 Am <sup>2</sup> 3,58%
$\Delta m$ 60	1,16E-01	+	1,58E-02	+	2,32E-01	+	6,04E-04	+ 1,24E-02 = 0,3772 E-02 Am <sup>2</sup> 3,43%

Table 9-10: Maximum absolute and relative error Coil XII

						$\Delta m$		$(\Delta m / m) \cdot 100\%$
$\Delta m$ 20	4,77E-02	+	5,66E-03	+	9,54E-02	+	2,90E-03	+ 1,67E-02 = 0,1683 E-02 Am <sup>2</sup> 4,49%
$\Delta m$ 40	8,33E-02	+	9,53E-03	+	1,67E-01	+	2,90E-03	+ 1,67E-02 = 0,2791 E-02 Am <sup>2</sup> 3,72%
$\Delta m$ 60	1,19E-01	+	2,82E-02	+	2,38E-01	+	2,90E-03	+ 1,67E-02 = 0,4055 E-02 Am <sup>2</sup> 3,61%

Table 9-11: Maximum absolute and relative error Coil XIII

### 9.1.7 Gaussian Distribution

The occurrence of a maximum error is very unlikely in reality. The average error is determined by applying the Gaussian distribution of the magnetic moment [18], as can be seen in the following:

Relative Gauß error: 
$$\frac{\Delta m}{m} = \pm \sqrt{\left| \frac{\Delta a}{a} \right| + \left| \frac{\Delta b}{b} \right|} \quad (6.4)$$

$$\frac{\Delta a}{a} = \pm \sqrt{\left| \frac{\Delta I_{x,y}}{I_{x,y}} \right|^2 + \left| \frac{2 \cdot \Delta \omega}{\omega} \right|^2 + \left| \frac{\Delta B}{B} \right|^2} \quad (6.4.1)$$

$\Delta a/a$	$(\Delta I / I)^2 + (2 \Delta \omega / \omega)^2 + (\Delta B / B)^2$
$\Delta a/a$ 20	1,00E-04 + 2,59E-05 + 4,00E-04

$\sum \Delta a/a$	= 5,29E-04
$\sum \Delta a/a$	= 5,13E-04
$\sum \Delta a/a$	= 5,05E-04

**Table 9-12: Relative error ratio of term “a”**

$$\frac{\Delta b}{b} = \pm \sqrt{\left| \frac{\Delta k_{\rho}}{k_{\rho}} \right|^2 + \left| \frac{\Delta B}{B} \right|^2} \quad (6.4.2)$$

$\Delta b/b$	$(\Delta k / k)^2 + (\Delta B / B)^2$
$\Delta b/b$	9,93E-06 + 4,00E-04

$\sum \Delta b/b$	4,10E-04 = $\Delta b/b$ const at all measurements
-------------------	---

**Table 9-13: Relative error ratio of term “b”**

$$\frac{\Delta m}{m} = \pm \sqrt{\left| \frac{\Delta a}{a} \right| + \left| \frac{\Delta b}{b} \right|}$$

$\Delta m/m$ 20	$\Delta a/a$	+	$\Delta b/b$	=	3,06E-02
$\Delta m/m$ 40	$\Delta a/a$	+	$\Delta b/b$	=	3,04E-02
$\Delta m/m$ 60	$\Delta a/a$	+	$\Delta b/b$	=	3,02E-02

$\Delta m/m$ 20*100%	=	3,06%
$\Delta m/m$ 40*100%	=	3,04%
$\Delta m/m$ 60*100%	=	3,02%

**Table 9-14: Relative error of coil X**

### 9.1.8 Test Summary

After this experimental oscillation test, the generated magnetic moment in an external magnetic field shows a direct proportionality to the number of turns (Figure 9-16) and the size of the current flow (Figure 9-12 to Figure 9-15).

The analysis of the dependency on the number of turns is actually not proven 100 %, because a narrow range of the number of turns has been considered in the measurement, driven by the mathematical simplification of the constant volume of 3524 mm<sup>3</sup>.

The current dependency of the generated magnetic moment has been proven by this analysis, shown in the results of this report. In the main analysis, the generated magnetic moment has been compared to the relatively trivial equation  $m = NIA$ .

It needs to be emphasised that the errors of the generated magnetic moment are not mentioned in the charts given but described in the error analysis. The equation  $m = NIA$  can be used for further calculation aspects in the control loop for the satellite attitude control. The absolute error has been determined by applying the measurement principles described above and the results show a satisfactory error size with a maximum of 4.70 %. Nevertheless these relative errors describe a maximum range, i.e. all influencing factors need to be at maximum at the same time. This turns this error into an improbable error. A more probable occurrence of an error can be explained by a Gaussian distribution of the magnetic moment errors, shown in paragraph 9.1.6.

The Gaussian distribution is expressed with a relative error. This average error describes a relative constant size for different current flows referring to this measurement. It can be rounded off to 3 %.

Underlining the good measurement and the corresponding error analysis it must be emphasized that mass produced coils bear an absolute error range of  $\pm 15\%$ . The expected size and the real dependencies of the magnetic moment ( $m \approx 7.5 \text{ E-}02 \text{ Am}^2$ ) generated by the magnetorquer have been verified successfully by applying this extensive and phenomenon related oscillation test.

$$m_{average} = N \cdot I \cdot A \leq 3.00 \% \quad (7)$$

$$m_{max} = N \cdot I \cdot A \pm 4.70 \% \quad (8)$$

## 9.2 Demonstration Test

Besides the oscillation test have been used the Helmholtz coils for demonstration activities of the whole cube. The coils are mounted at the inside of the side panels. During the general development time of this project the structure team has built a prototype of the satellite. The cube was used for further set up and visualisation aspects, which was used also for this demonstration.

The main idea of this demonstration contains the verification of the coil driver placed on the ADCS PCB. Therefore the cube was suspended onto a frame in the centre of mass and was placed inside the Helmholtz coil pairs. Two coils with less than 400 turns, which fits into the coil holder, were produced with the not modified coil mould. At this stage the modified coil moulds was not produced. Except of the production of the two connected magnetorquer mounted at the side panels have been built and perform this demonstration by the ADCS supervisor.

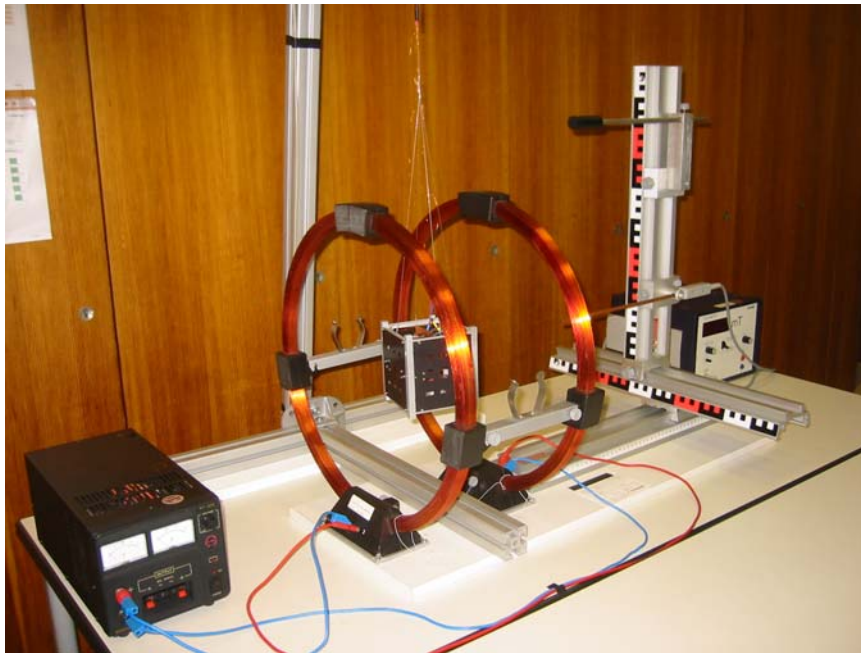


**Figure 9-17: Suspended cube place at the inside of the Helmholtz coils**

The demonstration have displayed the manoeuvre time of the cube with different drive scenarios, which was working very well. The driving software for the visualization was running on the laptop and was developed with Borland Delphi 7.0. The communication between the microchip module and the laptop was realized by RS232 serial interface. A lot of pictures exist and even a short video about this demonstration.

## 10 Control Unit Development

### 10.1 Cabling

After the production of the drive units the drive board has been cabled with the required sensors and the PC. The connection between the drive unit and the PC was established by using an extra PCB. At the small PCB all electric equipment are clipped where the connection to the drive board is made by RS232 connections. The particular boards will be placed in plastic housings so that the RS232 will allow a comfortable alliance of the electric equipment. The housings will be equipped with compatible fuses and the integrated RS 232 plug connector, a male plug for the stepping motors and a female plug for the incremental drivers. The different layouts of the plugs will avoid a permutation. For the first setup of the automated coil winder have been connected the electrical units directly without the using of the small PCB, which have considered an operation of the winder close to the PC.

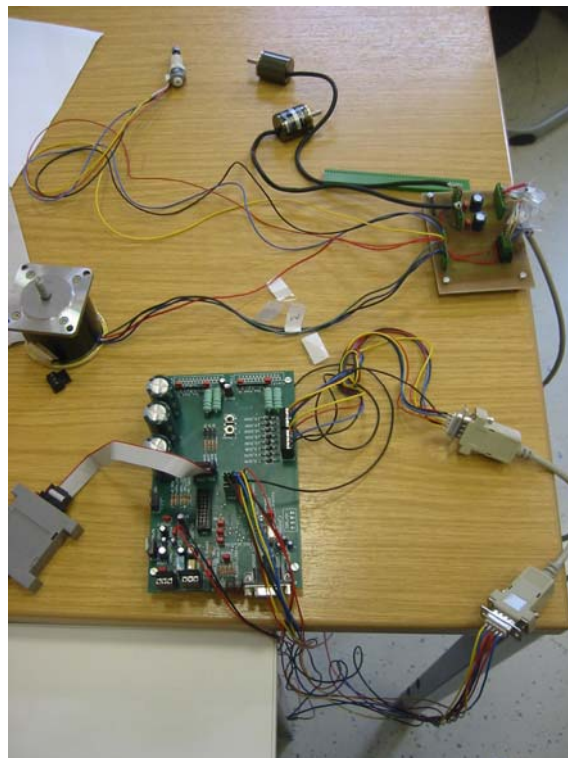


Figure 10-1: Cabling without board body

### 10.2 Software Result

The software is coded in the language C with the AVR Studio, whereas the configuration and the visualization software is processing on the PC and is developed with Borland Delphi 7.0.

Different challenges e.g. the correct adjustment of guidance steps or the final software coding and integrating of the incremental driver needed more attention as expected.

To realize the main task of automatic produced coils could be the software of the force measuring unit not finished in time. The decision was boosted additionally by considering the wire brake performances during the first automated drive tests. Nevertheless the software and visualization has resulted in a clear and satisfying user interface. The user interface contains the input of the following parameter: the wire diameter, the number of turns and the coil width.

The user interface is explained in detail in the Appendix-D. But before the automated winding can be started the coil winder must be calibrated..

### **10.3 Calibration**

First of all the vertical limiter at the wire carrier unit must be calibrated to a constant level for proper recoil of the wire. The diverse pulleys need to be oriented in a proper way so that the recoiling movements of the wire depot need to be balanced and pacified. As mentioned in the prototyping and development of the coil, the coils must be wined with the highest possible tension. The force measuring unit could not be finished in time so that the detection of the right brake tension is determined experimentally.

The first automated winding test extracted that the wire brakes just until the wire isolation gets ruff by a high tension. The surfaces of the guidance rolls at the guidance unit are very slick so that the rolls are getting in rotation after a certain tension. Hence the rolls help to find out a very good orientation for the setup of the brake tension. The guidance of the coil winder is adjustable very fine with the driver software where different tasks need to be fulfilled before.

### **10.4 Automatic Coil Winding**

The starting point for an automated winding is dependent on the wire mounting. The copper wire is integrated through the counter plate of the coil mould which appoints the maximum value as the starting point. The wire diameter, the number of turns and the coil width need to be entered at the next user surface

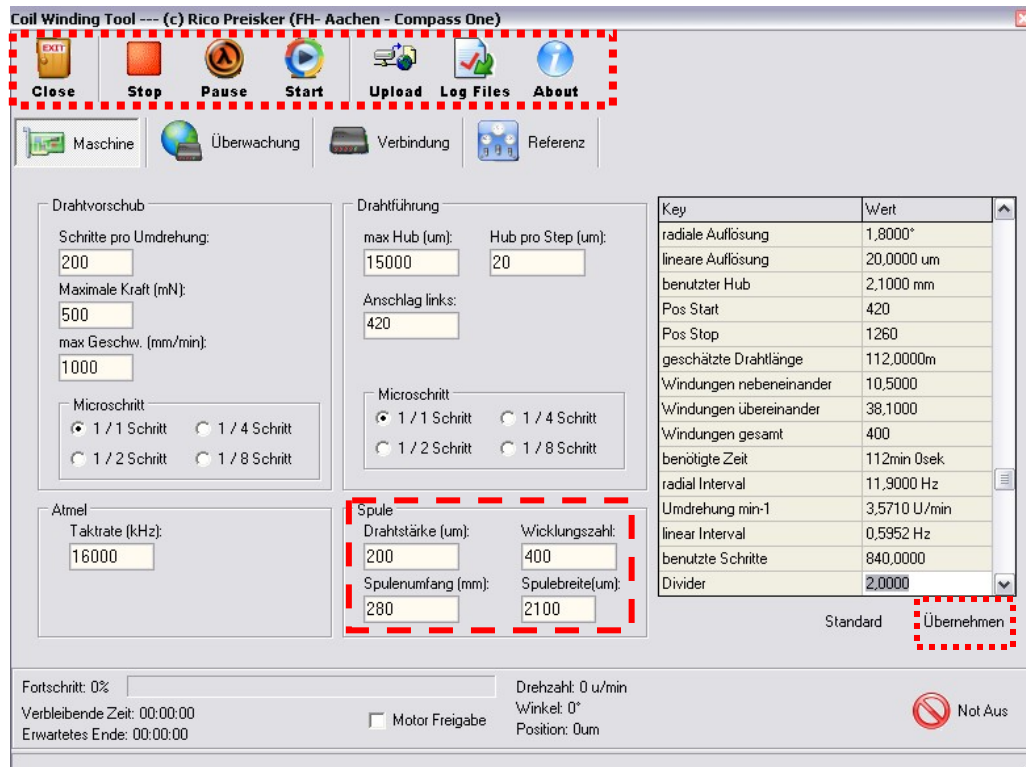


**Figure 10-2: Parameter input surface**

As displayed in the head figure the wire diameter and the coil width are entered in micrometers and not in millimetres. All set parameters need to be uploaded into the drive unit, by firstly overtaking and later uploading the parameter with using the overtake “Übernehmen” and “Upload” button. With this, upload finishes the calibration activities for the automated winding. The automated winding of the magnetorquer can be started and stopped by using the respective buttons also in the first line of the general user surface.

## 10.5 Results

The automated produced coils have been wound with the highest possible tension, resulting in a high quality of wound and bonded coil. The mechanical overload of total 2 mm after the prototyping have been erased with the proper guidance of the wire in combination with the high winding tension, so that the magnetorquer got the dimension of exact 74.20mm x 83.20 mm. The calculated mass had a size for one coil with nearly 20 gram as result. The produced magnetorquer have a mass of 17.5 gram including the cables and plug connection.

The ready crimped cable selected before is used for the cabling, where the respective lengths are depending from the position of the plug connection on the ADCS PCB.

These positions were defined in considering a correct assembly sequence of the mounted magnetorquer with the ADCS supervisor together. The automated production of the magnetorquer results in a much more accurate and stable coil as with manual winding. The guidance is working very well, so that the produced coils result in a much more homogenous mechanical body.



Figure 10-3: Ready produced coil

Parameter	Symbol	Value	Unit
max width	b	74.2	mm
max height	h	83.2	mm
max cross sectional width	d	2.1	mm
max cross sectional height	sh	5.7	mm
Mass of coils	Mc	17.5	g

Table 10-1: Automatic winded coil result

Parameter	Symbol	Manual	Automatic	Advancement
width	b [mm]	78	74.2	+ 4.87 %
height	h [mm]	87	83.2	+ 4.37 %
cross sectional width	d [mm]	2.1	2.1	0.00 %
cross sectional height	sh [mm]	7	5.7	+ 18.57 %
mass of coils	Mc [g]	17.6	17.5	+ 0.57 %

Table 10-2: Manual and automatic winded coil analogy

## 11 Outlook

During the development time of the magnetorquer it has been considered that for the Engineering Model (EM) and later Flight Model (FM) the magnetorquer need to be bonded under vacuum conditions. The reason for this decision is founded that air in normal environment could be caged between the windings during the bonding activities. This air could cause a inflation under space conditions which may end in worst case in a mechanical deformation of the coil. Therefore it has been decided that the only actuators on board of Compass-1 will be bonded in the vacuum chamber. The University of Applied Sciences offers a small high-vacuum chamber with a volume of about 50 litres which can generate a pressure of up to  $1 \cdot 10^{-5}$  mbar. The chamber has the mechanical inner diameter of 24 cm and a length of 58 cm, which will be used also for the general vacuum test of the satellite Compass-1.

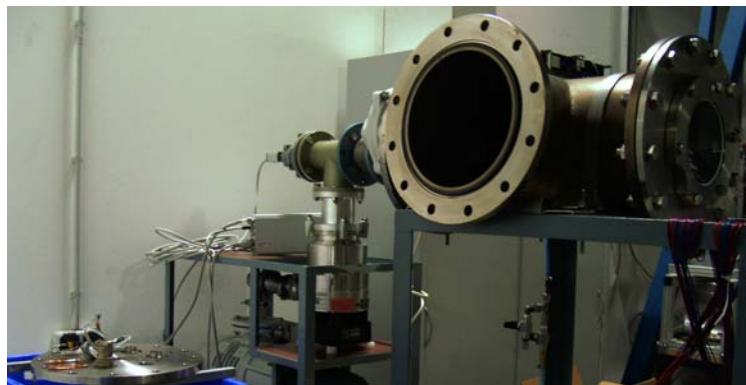


**Figure 11-1: Vacuum Chamber with cabling for the vacuum bonding**

The vacuum bonding activity has been scheduled with an integration of an automated thermal control loop. The vacuum bonding activities couldn't be finished with a automated thermal control in time but it is to point out, that the vacuum cabling for the bonding activity has been already set up. The bonding method will be the same as in the prototyping but with a difference that the bonding of the coil will accomplished under vacuum. The coil mould and the wire will therefore achieve faster the bonding temperature as under room conditions, previously from the less heat transfer through the environment under vacuum conditions.

Three Engineering Models of ready vacuum bonded and connected coils are required until February for following general qualification test of the whole satellite.

### **12 Conclusion**

The task of the design, development and production of three equal coils as magnetorquer was carried out successful. The existing overload of 0.2mm will be handled by the following production task. The whole laid software of the coil winder couldn't be finished at time, but considering the main functions, the winder is operating very well. The additional force measuring unit can be finished by implementing the software code into the main drive software. A LC-display and a keyboard can be also integrated for a "Stand-alone-function" by updating the software. As the past has shown, there is always a discrepancy between theory and reality.

Nevertheless the new coil production methods has resulted in a very good coil configuration.

It needs to be underlined that automated winded and bonded coils have a much higher density, stiffness and stability compared to not bonded coils.

A more secure cable connection of the magnetorquer could be established by using Teflon cables but as explained before ready crimped Teflon cables are not existing for a fair price. Diverse Teflon cables will be used in the Compass-1 satellite, so that the connection could be upgraded by ordering special crimp ends and the respective crimp nipper.

The primary goal of the main CubeSat program is to provide students the opportunity to develop complete mechanical or electrical satellite systems. This goal has been accomplished by gaining practical experience in realizing several magnetorquer as prototypes and nearly space qualified magnetorquer for the Attitude Control System.

## References

- [1] Jens Giesselmann, Ali Aydinlioglu, *Phase B Study of ADCS for COMPASS-1*, June 2004
- [2] W. Nolting, *Grundkurs Theoretische Physik 3 – Elektrodynamik*, 6. Auflage Springer Verlag, 2002, ISBN 3-540-42113-0
- [3] J.R. Wertz, W. J. Larson, *Space Mission Analysis and Design*, Third Edition, Space Technology Library, Kluwer Academic Publishers Group, the Netherlands, 1999 ISBN 1-881883-10-8
- [4] Torben Graveresen, Michael Kvist Frederisen, Soren Vejlgard Vedstesen, *Attitude Control System for AAU CubeSat*, June 2002, Aalborg University, Institute of Electronic Systems.
- [5] Sylwia Czernik, *Phase B Study of TCS for COMPASS-1*, June 2004
- [6] Elektrisola, Data specification: *Technical Data by size, IEC 317*
- [7] Elektrisola, Data specification: *Bonding wire types*
- [8] ISEL, Data specification: *Aluminium Profiles Overview*
- [9] Gede Hemer, Data specification: *Richttechnologien*
- [10] ISEL, Data specification: *Linearantriebe KG-Spindel*
- [11] A-drive, Data specification: *Linear Actuator LC-15*
- [12] Farnell, Data specification: *SMT Connections*
- [13] Wikipedia, *The free encyclopedia*, <http://www.wikipedia.org/>
- [14] Paul A. Tipler, *Physik, Das Torsionspendel*, 1. Auflage, Spektrum AkademischerVerlag, Heidelberg, Berlin, Oxford, 1995, ISBN 3-86025-122-8
- [15] Voltcraft VC 120; *Operation Instruction*; Version 05/03
- [16] Voltcraft VC 860; *Operation Instruction*; Version 11/04
- [17] PhyWE 2004/05, User manual: *Tesla Digital Multimeter 13610.930*
- [18] Paul A. Tipler, *Physik, Einheitssysteme*, 1. Auflage, Spektrum AkademischerVerlag, Heidelberg, Berlin, Oxford, 1995, ISBN 3-86025-122-8

## Abbreviations

ADCS	Attitude Determination and Control System
ACS	Attitude Control System
COTS	Commercial Of The Shelf
CNC	Computerized Numerically Controlled
DLR	German Aero Space Centre
EM	Engineering Model
ESA	European Space Agency
FM	Flight Model
GPS	Global Position System
IDE	Integrated Development Environment
LCD	Liquid Crystal Display
LEO	Low-Earth-Orbit
MCU	Microcontroller Unit
NRW	Nordrhein-Westfalen
PCB	Printed Circuit Board
PC	Personal Computer
PTFE	Polytetrafluoroethylene / Teflon
PWM	Pulse-width Modulation
Q	Quality
STR	Structure
VGA	Video Graphics Array

## Nomenclature

A	face area of coil [mm <sup>2</sup> ]
$a_w$	Wire cross sectional area [mm <sup>2</sup> ]
B	Geomagnetic field intensity [T]
b	Maximum coil width [mm]
C	amount of coil area [mm]
$d_w$	Bare wire diameter [mm]
F	magnetic force of a coil [N]
h	Maximum coil height [mm]
$h_{orbit}$	Orbit altitude [km]
I	Current through the coil [A]
$I_{x,y}$	Moment of inertia [kg m <sup>2</sup> ]
J	Current density [A/mm <sup>2</sup> ]
$k_p$	Wire stiffness “Direktionsmoment” [Nm]
l	Conductor length [mm]
$L_s$	Inductance [H]
M	mechanical torque [Nm]
$M_c$	Mass of the coil [g]
m	producible magnetic moment [Am <sup>2</sup> ]
N	number of turns
P	dissipated electrical power [W]
Q	Coil quality
R	total resistance [ $\Omega$ ]
$R_{earth}$	Earth radius [km]
T	Period time [s]
$U_c$	Coil Driver output voltage [V]
$v_d$	Average velocity [1/s]
$\mu$	Magnetic permeability [Vs/Am]
$\rho_\alpha$	Twist angle [ $^\circ$ ]
$\rho$	density of wire material [kg/m <sup>3</sup> ]
$\sigma(T)$	Material resistance with temperature coefficient $\alpha_0$ [ $\Omega mm$ ]
$\omega$	Angular acceleration [1/s <sup>2</sup> ]
$\Delta m$	Absolute error of the magnetic moment [Am <sup>2</sup> ]

## List of Figures

Figure 2-1	: ADCS hardware interface	3
Figure 3-1	: Lorentz force in a conductor	5
Figure 3-2	: Lorentz force on coil sides	6
Figure 3-3	: The second „Right-Hand-Rule“ used for a circular coil	6
Figure 3-4	: Power and mass diagram	13
Figure 3-5	: Design results	14
Figure 3-6	: Bonding wire type S180	16
Figure 4-1	: Winder architecture concept	18
Figure 4-2	: Coil mould sketch	18
Figure 4-3	: Catia V5 R13 screenshot of Compass-1 (EM)	19
Figure 4-4	: Different PT-aluminium-profiles	21
Figure 4-5	: PT 25 profile 3 D Catia model	21
Figure 4-6	: T groove screw nut M6 DIN 650	22
Figure 4-7	: Wire stock as 3 D model	22
Figure 4-8	: Wire carrier & wire brake mounted on the base plate	23
Figure 4-9	: Deflection pulleys with different offsets	24
Figure 4-10	: Deflection pulleys	25
Figure 4-11	: Pulleys placed on the base plate	25
Figure 4-12	: Redesigned guidance unit	26
Figure 4-13	: First design of the guidance	26
Figure 4-14	: Moved threat rod with interface	26
Figure 4-15	: Several spindles with different guide interfaces	27
Figure 4-16	: Base construction with guide rails	28
Figure 4-17	: Interface unit	28
Figure 4-18	: Guide rolls, Cam Followers, Roller Followers	29
Figure 4-19	: Roll board	29
Figure 4-20	: Linear Actuator LC 15	30
Figure 4-21	: Coil winder model with additional the guidance unit	30
Figure 4-22	: Winding unit mounted on a flat plate	31
Figure 4-23	: Design of the winding unit without the coil mould	32
Figure 4-24	: Coil mould	32

## List of Figures

---

Figure 4-25	: Design result of the coil winder	33
Figure 4-26	: Force measuring unit	34
Figure 4-27	: Tackle principia	35
Figure 4-28	: Coil winder with force measuring unit	35
Figure 4-29	: Bipolar stepping motor	37
Figure 4-30	: Incremental driver, rotary encoder	37
Figure 6-1	: Electrical interfaces of the Coil winder	41
Figure 6-2	: PCB layout without electrical parts	42
Figure 6-3	: PCB layout with electrical parts	43
Figure 6-4	: Soldered PCB	43
Figure 7-1	: Assembled coil winder without sensors	45
Figure 7-2	: Manual winded coil inside the coil mould	46
Figure 7-3	: Coil prototype Nr.I	46
Figure 7-4	: Cooling with MCU cooler	47
Figure 7-5	: Micro SMT multiway	48
Figure 7-6	: SMT crimp connector housing	48
Figure 7-7	: Produced coil Nr. VII	49
Figure 7-8	: LCR Meter Agilent 4284	50
Figure 8-1	: Modified coil mould and coil winder	53
Figure 9-1	: Dynamical test setup with current flow in the coil	55
Figure 9-2	: Suspension disposition of coils	57
Figure 9-3	: Schematic suspension test setup	58
Figure 9-4	: Electrical setup	58
Figure 9-5	: Frame position setup	59
Figure 9-6	: Suspended coil	59
Figure 9-7	: Oscillation dial gauge	59
Figure 9-8	: Test setup	60
Figure 9-9	: Excited coil during oscillation	61
Figure 9-10	: Magnetorquer	61
Figure 9-11	: Average exterior area	61
Figure 9-12	: Magnetic moment analogy of coil X	62
Figure 9-13	: Magnetic moment analogy of coil XI	63

## List of Figures

---

Figure 9-14	: Magnetic moment analogy of coil XII	64
Figure 9-15	: Magnetic moment analogy of coil XIII	65
Figure 9-16	: Magnetic moment depending on number of turns	66
Figure 9-17	: Suspended cube place at the inside of the Helmholtz coils	72
Figure 10-1	: Cabling without board body	73
Figure 10-2	: Parameter input surface	75
Figure 10-3	: Ready produced coil	76
Figure 11-1	: Vacuum chamber with cabling for vacuum bonding	77
Figure B-1	: Adjustment of work piece for mill aspects	95
Figure B-2	: Manufactured hardware parts at the FH workshop	95
Figure B-3	: Wire carrier, guidance block, pulleys and the winding unit in assembled configuration	95
Figure B-4	: Assembled coil winder without pulleys and coil mould	96
Figure C-1	: MCU circuit design	98
Figure C-2	: Stepping motor circuit design	99
Figure C-3	: Connector circuit design	100
Figure C-4	: Power unit circuit design	101
Figure D-1	: Connection surface	103
Figure D-2	: Guidance user surface	103

## List of Tables

Table 3-1	: Physical design dimensions	8
Table 3-2	: Defined operation temperatures	9
Table 3-3	: Wire data for copper and aluminium	9
Table 3-4	: Datasheet of available copper wire IEC317	12
Table 3-5	: Coil design result	14
Table 7-1	: Bonding test results with a low power supply	46
Table 7-2	: Bonding test results with high power supply	47
Table 7-3	: Inductance measurement results	50
Table 7-4	: Prototype Nr. VII dimension	51
Table 9-1	: Oscillation result of coil X	62
Table 9-2	: Oscillation result of coil XI	63
Table 9-3	: Oscillation result of coil XII	64
Table 9-4	: Oscillation result of coil XIII	65
Table 9-5	: Period time clock deviation	67
Table 9-6	: Angular velocity deviation	67
Table 9-7	: Stiffness deviation	68
Table 9-8	: Maximum absolute and relative error coil X	69
Table 9-9	: Maximum absolute and relative error coil XI	69
Table 9-10	: Maximum absolute and relative error coil XII	69
Table 9-11	: Maximum absolute and relative error coil XIII	69
Table 9-12	: Relative error ratio of term “a <sup>2</sup> ”	70
Table 9-13	: Relative error ratio of term “b <sup>2</sup> ”	70
Table 9-14	: Relative error of the coil X	70
Table 10-1	: Automatic winded coil result	76
Table 10-2	: Manual and automatic winded coil analogy	76

# Appendix

# **Appendix - A**

Coil Winder Drawings

# **Appendix - B**

## Coil Winder Manufacturing

The fabrication, total assembly and the control readings of the winder units were built at the mechanical workshop. The following pictures display one part during the milling at the CNC milling cutter, the produced unit parts and the assembled coil winder.



**Figure B-1: Adjustment of the work piece for mill aspects**



**Figure B-2: Manufactured hardware parts at the FH workshop**

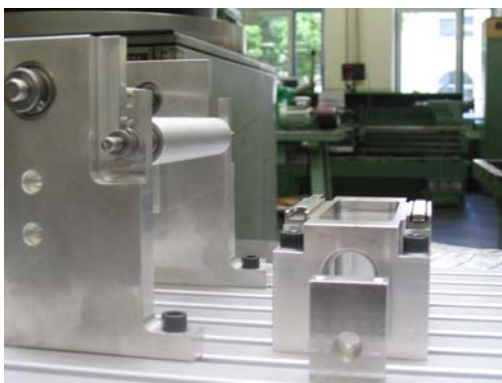


**Figure B-3: Wire carrier, guidance block, pulleys and the winding unit in an assembled configuration**

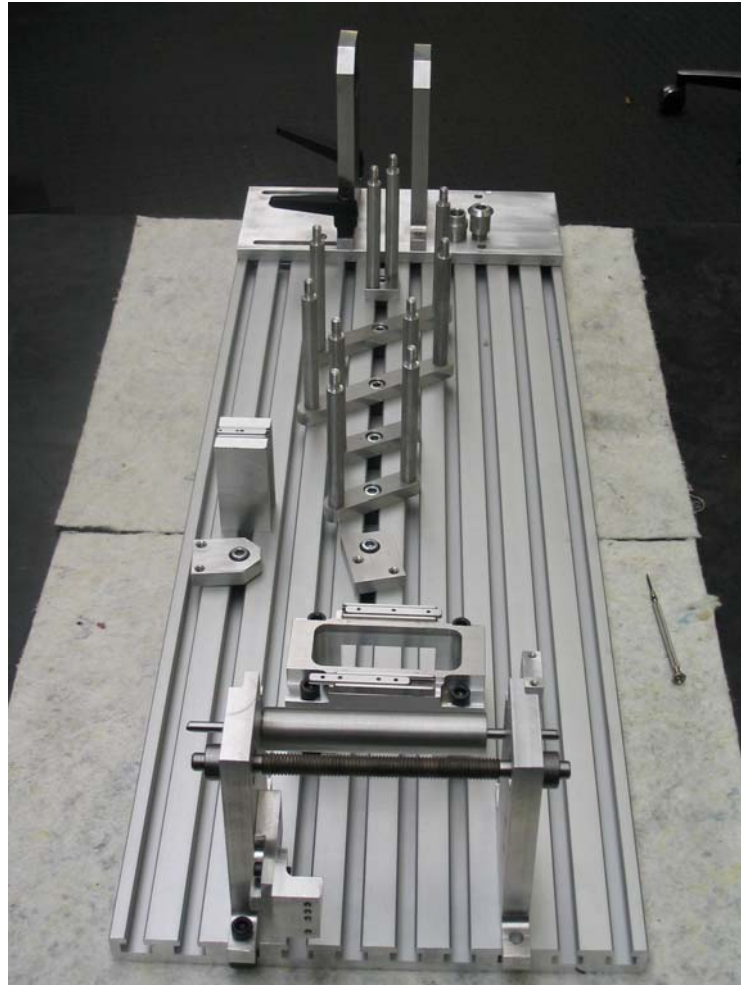


**Figure B-4: Assembled coil winder without pulleys and the coil mould**

# **Appendix - C**

## Coil Winder Circuit Design



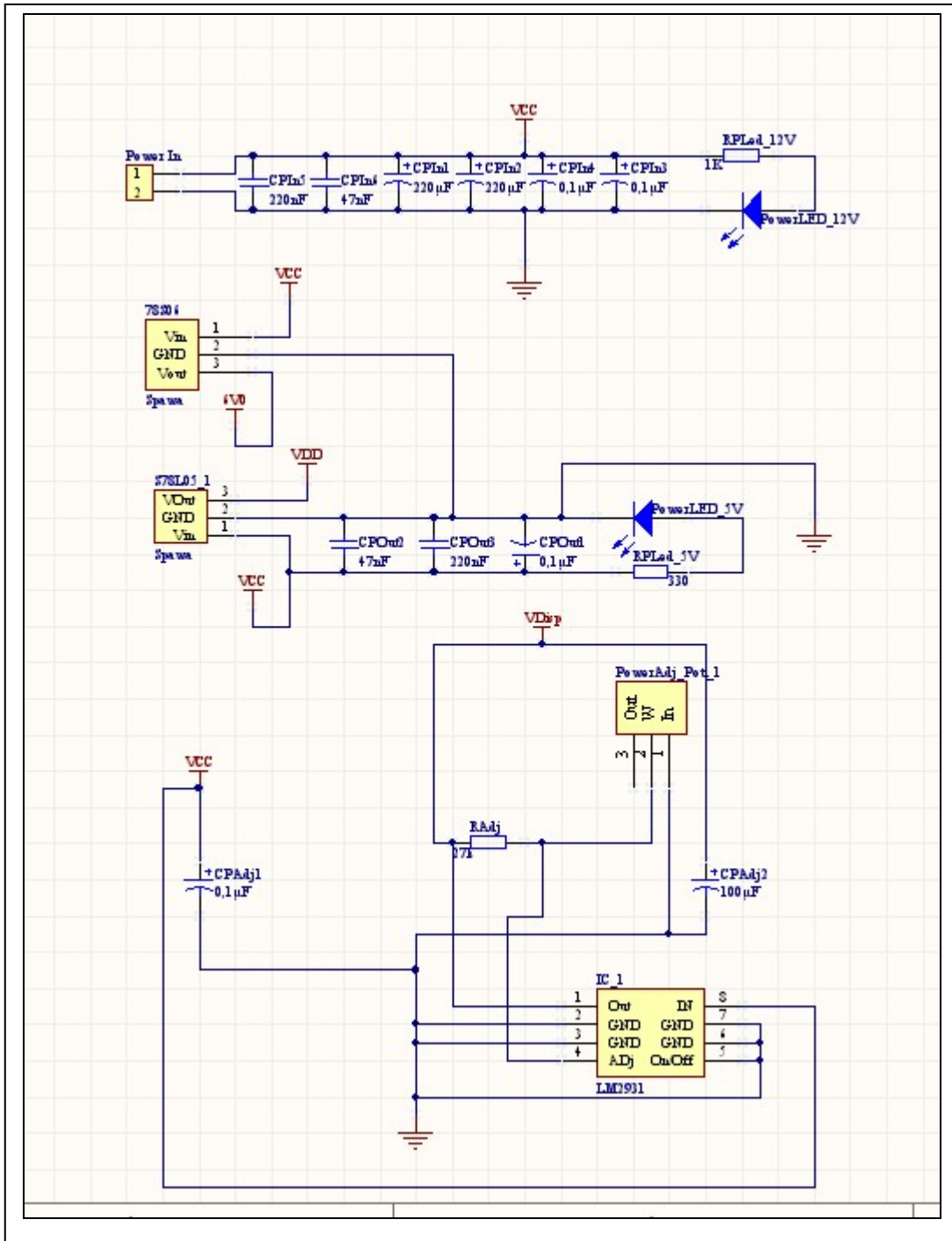


Figure C-2: Stepping motor circuit design



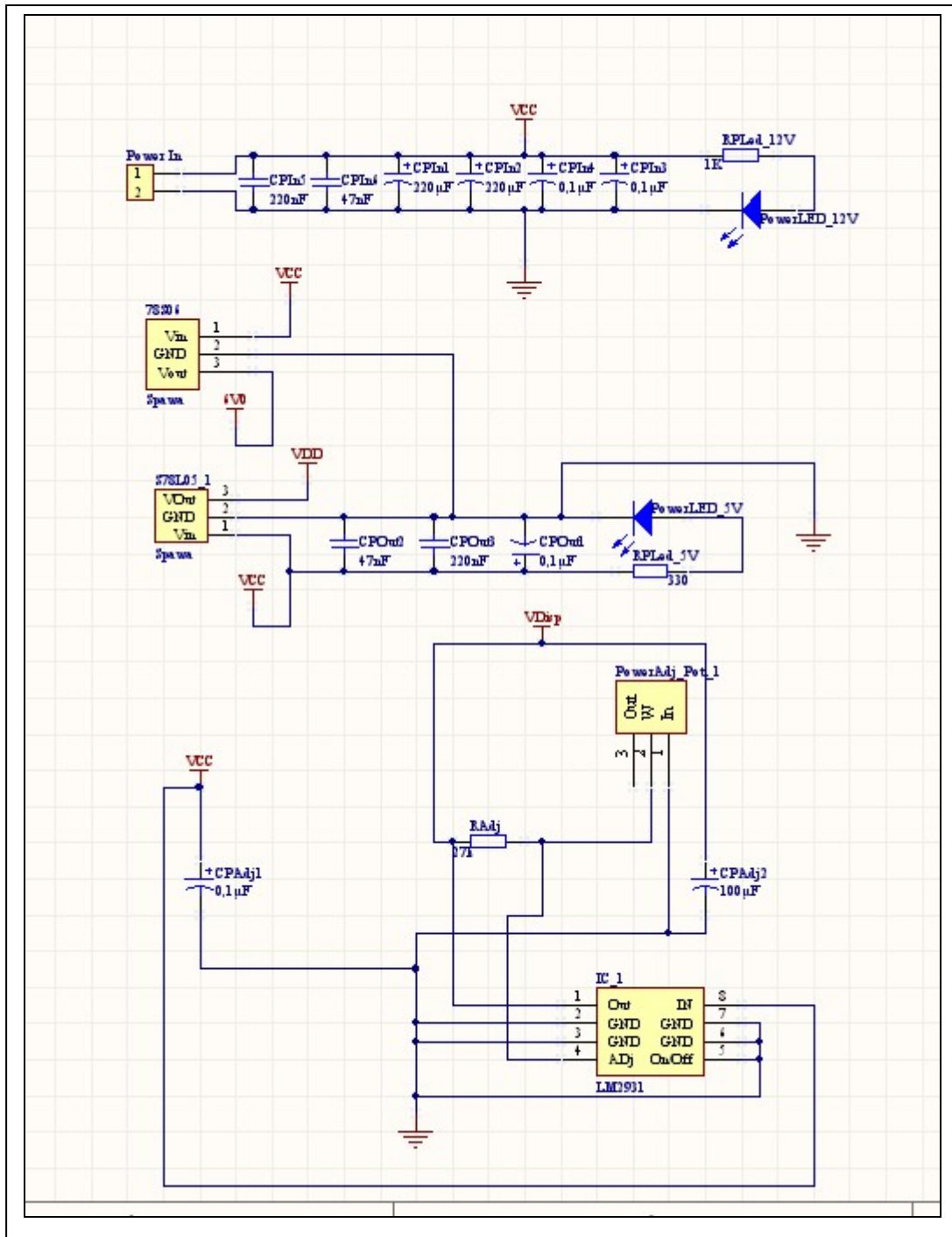
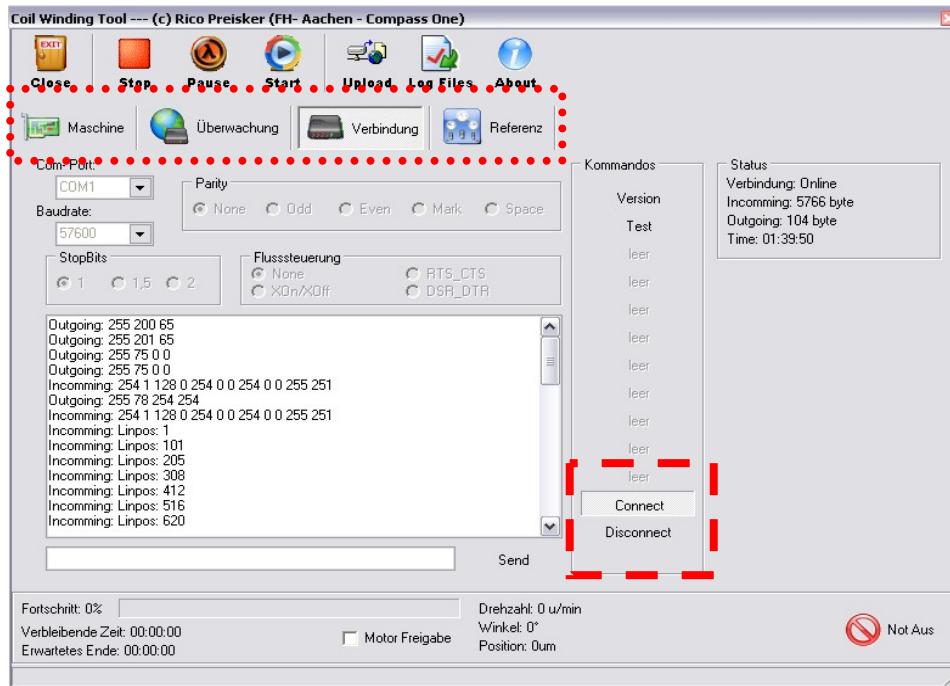


Figure C-4: Power unit circuit design

# **Appendix - D**

## Coil Winder Calibration Interface

The connection between the drive unit and the PC is established by pushing the “connect” button at the user surface shown in the next figure 10-3.



**Figure D-1: Connection surface**

The communication port and the baud rate are actually automated adjusted, but it is never a disadvantage to control the icons before the connection will be activated. The guidance is driven with the user surface as follows:

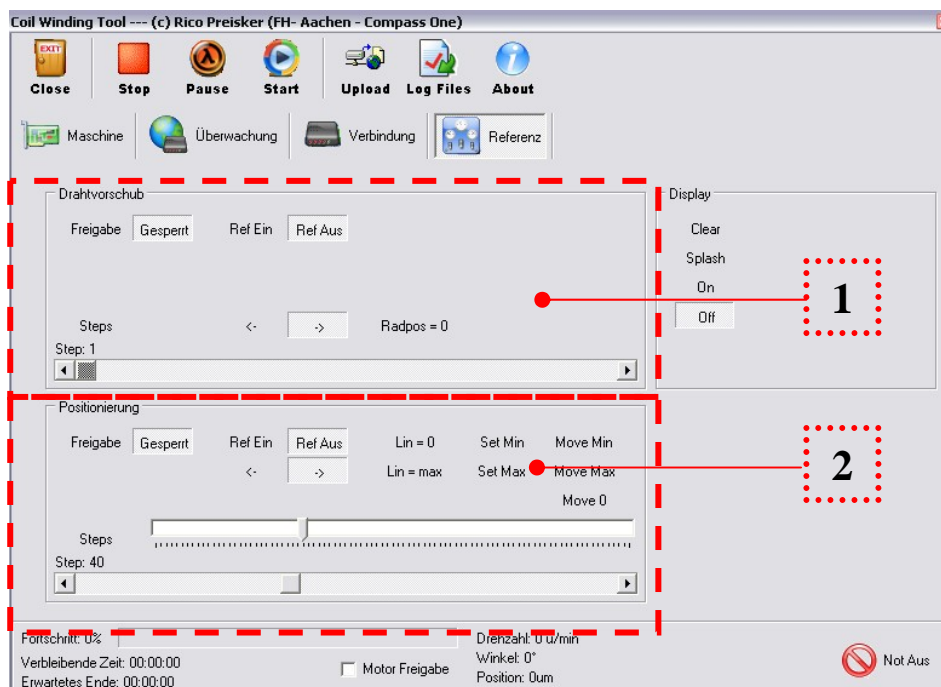


**Figure D-2: Guidance user surface**

The red marked window number one is supposed to drive the stepping motor of the winding unit. This section is actually able to drive the stepping motor in both rolling directions, but because of safety reasons only the winding direction is activated. The second section allows a very fine drive of the linear actuator of the guidance unit. The particular direction of motion is adjustable with (the) two arrows, whereby the step size of the motions is manually adjustable from one to 100 steps. For a proper guidance calibration run the linear actuator must be to his absolute zero point which need to be countersigned with pushing of the button “Lin=0”. The operation borders of the guidance are adjusted manually by the turning points of the traverse paths of the guidance unit. The lower reversal point must be tuned manually as a minimum value which is set by pushing the button “Set Min” at the user surface. The second reversal point can also be appointed manually but with the knowledge about the defined coil width, allows the software the definition of the maximum value by entering the size of the coil width which is displayed in figure 10-5. The minimum and maximum values can be checked by using the “Move Min” and “Move Max” buttons.